IMPROVED HYDROGEN PRODUCTION FROM BIOMASS GASIFICATION IN A DUAL FLUIDISED BED REACTOR

A thesis submitted in partial fulfilment of the requirements for the degree of Master of Engineering in Chemical and Process Engineering

University of Canterbury

2009

Hamish McKinnon

Supervisor: Prof. Shusheng Pang

Executive Summary

Biomass gasification is a technology under development that presents a means of generating hydrogen using renewable energy. While many forms of gasification have been investigated, steam gasification using a dual fluidised bed (DFB) reactor has been shown to efficiently produce high hydrogen content producer gas. The aims of this research were to increase the hydrogen yield from the 100kW DFB gasifier installed at the University of Canterbury, and thereby improve the current state of the art of gasifier operation.

In the first part of the project, the use of various catalytic bed materials was investigated as a means of enhancing the hydrogen-producing reactions that occur under steam gasification conditions. It was shown that iron-containing minerals such as olivine and magnetite catalyse hydrocarbon reforming reactions, increasing hydrogen production and reducing tar contamination in the producer gas. Calcium carbonate-based minerals such as calcite and dolomite were shown to be able to improve hydrogen production by absorbing carbon dioxide in the producer gas, promoting the water gas shift reaction. Bed material mixtures of olivine and calcite were the most effective at improving gasifier performance, increasing producer gas yield by 20%, increasing cold gas efficiency by 6% and increasing hydrogen yield by 85%. %. In addition, the carbon monoxide content was reduced and the ratio of hydrogen to carbon monoxide in the producer gas was ideal for Fisher-Tropsch synthesis of liquid fuels.

The second part of the project investigated the operating limits of the dual fluidised bed gasifier system and gasifier performance was improved considerably with gasifier modification. The modifications included siphon pipe improvement to increase freeboard height, addition of a bed material re-filling system to compensate for bad material loss, and biomass fuel feeding changes from above bed feeding to in-bed feeding. These modifications significantly improved the operability of the plant and increased the quality of the producer gas. In the project, digested sewage sludge was also used as an alternative fuel and results from these trials indicated that fuel quality is critical to gasifier performance. Analysis of the hydraulic properties of the bed materials tested showed that significant improvements could be made to the gasifier design which would further improve performance.

Finally, the cost of hydrogen produced by biomass gasification was investigated at a regional level. The analysis showed that 11,700 tonnes of hydrogen could be produced annually from the wood waste stocks around the Canterbury region in New Zealand, at a cost of

NZ$1.73/kg, a competitive price compared with current commodity prices of US$4.00/kg and US DOE targets of US$2.00-$3.00/kg. The amount of hydrogen produced would be sufficient to fuel approximately 31% of the current private vehicle fleet in Christchurch, the main city in the Canterbury region, assuming widespread adoption of fuel cell vehicles. Alternatively, 45 MW of electricity could be produced from the hydrogen-rich producer gas using molten carbonate fuel cells. The cost of electricity produced by this method was calculated to be 10.57 ¢/kWh.

Overall the research has improved performance of the gasifier, increased knowledge of the limits of the process and identified key technological opportunities for future research. It is hoped that this will increase the viability of biomass gasification as a clean, renewable alternative energy technology.

Acknowledgements

As with all large undertakings, there are many contributors to this project without whom none of this would have been possible. I hope this mere mention is enough.

Firstly, to my supervisor Professor Shusheng Pang, thank you for your leadership and guidance throughout my two years. I am very grateful for your continued support and understanding. Your enthusiasm is inspiring.

To the academic and technical staff working on the gasifier, you all have made fantastic contributions to the project and to my research in particular. The wisdom of Ian Gilmour and Chris Williamson was crucial to the success of many areas of my research and the technical expertise of Leigh Richardson, Bob Gordon and Tim Moore is unsurpassed. Special mention goes to Trevor Berry for his seemingly endless insight into all manner of complex problems and technical challenges; Trevor, your experience will be sorely missed. To Woei-Lean Saw, thank you especially for the guidance you've given me in the later stages of my research. I wish you all the best and continued success in your new role.

The contributions of the other past and present students working on the gasifier project were integral to all aspects of my research, and all of you deserve special thanks for your time and effort. To Chris Penniall, Doug Bull, Gershom Mwandila, Mook Tzeng Lim, Prasanth Gopalakrishnan and Xu Qixiang, for all those early mornings and late nights, my deepest thanks.

And finally, to Sarah, for all your love and support, my deepest thanks.

Contents

List of Figures

List of Tables

1. Introduction – The Case for Biomass Energy

1.1. Global Energy Outlook

International energy supply is currently undergoing dual crises: firstly, an ever-diminishing supply of fossil fuel resources, and secondly, an increased awareness of the harmful environmental effects of heavy fossil fuel consumption. Approximately 13TW of power is consumed worldwide, most of which is fossil-fuel based [Argonne National Laboratory, 2005]. By 2050 Energy demand is expected to increase 50% to 320% depending on the veracity of conservation of resources in that time [Begley, 2009].

"Peak Oil", as the supply crisis has come to be known, is the widely accepted view that the demand for crude oil now exceeds or will soon exceed economic supply capability, leading to higher prices and less availability, and in turn forcing reduced electricity generation and constraints on transport. To some extent that has been observed in recent history, with the price of oil tripling since 2001 [EECA, 2007]. This trend is also predicted over an extended timeframe (approaching 100 years) for natural gas. As the global population increases, the disparity between supply and demand is predicted to rise exponentially, leading to major societal restructuring, or more pessimistically, collapse.

The theory of anthropogenic climate change has become widely regarded and accepted, although less so than Peak Oil. Environmental evidence suggests that following the Industrial Revolution in the mid 19th century, emissions of greenhouse gases such as carbon dioxide, nitrogen dioxide, sulfur dioxide and methane have accumulated in Earth's atmosphere, exceeding concentrations that the natural ability of the global ecosystem is able to regulate and maintain at safe levels. This is held to be the direct result of over-utilisation of fossil fuels, which are now understood to be enormous geological carbon stores from the early development of the Earth. Consequently, climate models predict (with varying levels of certainty) that the global mean temperature will rise significantly in the coming century, with accompanying sea level rise and other environmental effects, including possible species extinctions. Whilst some pollutants such as nitrogen and sulfur dioxide are a direct consequence of combustion processes regardless of fuel source, increased concentrations of carbon dioxide in the atmosphere are undoubtedly the result of the release of the heretofore stored carbon.

Utilisation of renewable energy provides a solution to both problems. Renewable energy sources are raw materials used for energy generation, the stocks of which can be replenished within a reasonable time frame, measured on a generational rather than a geological scale. The migration of energy generation technologies away from fossil fuel combustion to other fuel sources and processing technologies would significantly reduce the level of greenhouse gases in the atmosphere, giving the geological carbon sequestration system a greater opportunity to remove the gases and store them as organic matter. The development of renewable energy has become a top priority for the leadership of the world's major economies, as they seek to distance their countries from the effects of diminishing fossil fuel supply.

1.2. RENEWABLE ENERGY SOURCES AND TECHNOLOGIES

The development of alternative energy sources and technologies is not a new phenomenon. In response to the perceived threats against global energy security however, recently a much more mainstream emphasis has been placed on development of non-fossil fuel energy generation.

Renewable energy sources can be broadly classified into two categories: continuous energy sources and Intermittent Energy sources. In general, public perception of renewable energy sources tends to focus on intermittent sources, such as solar and wind power, and consequently in many areas it is not held in high regard as a means for offsetting the dominance of fossil fuel energy generation. Considered below are a number of energy sources and their associated technologies.

1.2.1. Solar Energy

Solar radiation supplies approximately 1370±10 W/m² to the earth [NOAA, 2009], and at ground level on a clear day at noon approximately 1000 W/m² of incident radiation is recorded. The resource is considered intermittent, despite the ever-present nature of the sun, as the incident radiation can drop to around 100W/m² in overcast conditions. Even on a cloudy day, the total solar radiation reaching the Earth's land area exceeds global power demand one-thousand times [Pidwiny, 2006]. The biosphere has obtained its energy for growth from the sun for billions of years, and biomass still represents a viable solar collector. Other technologies have been developed to harness the solar flux, including solar photovoltaic

collectors which convert solar photons directly to electrical current and solar thermal systems which utilise solar energy to heat a working fluid.

1.2.2. Wind Energy

Energy generated from naturally occurring wind currents has been utilised for centuries for many applications, from pumping water and milling grain to modern electricity generation. Installed capacity of wind generation at the end of 2008 was 121.2 GW [World Wind Energy Association, 2009], but typically wind turbines operate at around 30% of installed capacity, as wind speed is intermittent in nature and varies over hourly, daily and seasonal cycles. Wind Energy currently accounts for 0.26% of total global power requirement.

1.2.3. Hydroelectric Energy

Hydroelectric energy is energy, usually electricity, generated by harnessing the gravitational potential energy of stored water as it flows. Hydroelectricity currently accounts for the largest proportion of renewable energy generated globally, and approximately 20% of global electricity generation. In New Zealand, the proportion of hydroelectric power generation is much higher, accounting for 59% of annual electricity generation [CAENZ, 2008]. It has a far lower degree of intermittency compared with wind and solar energy, but still relies on the essentially uncontrollable weather patterns to provide sufficient water to hydro storage lakes. The variability of the resource became painfully apparent to many New Zealanders in 2008 when low hydro storage lake inflows at the start of the year caused average power prices to rise 300% [M-Co, 2009].

1.2.4. Geothermal Energy

Geothermal energy has traditionally been considered a means of generating electricity, using superheated steam beneath the Earth's surface to power steam turbines. Recently however, the development of geothermal or ground-source heat pumps has given consumers a means of using the naturally temperate ground as a heat source or sink for space conditioning applications. At the end of 2007 geothermal energy provided 10GW of electrical power internationally with a further 28GW of thermal power.

1.2.5. Wave and Tidal Energy

Wave and Tidal generation both utilise the vertical cyclic nature of large bodies of water to generate electricity, either on short (wave) or long (tidal) frequencies. Wave energy conversion takes advantage of the wind's interaction with the ocean surface. Although many wave energy devices have been invented, only a small proportion have been tested and evaluated. Furthermore, only a few have been tested at sea, in ocean waves, rather than in artificial wave tanks [Electricity Innovation Institute, 2004]. Tidal energy is a development of hydroelectricity principles, whereby incoming tides can be dammed to be released through generators at a later stage. Ninety percent of today's worldwide ocean energy production is represented by a single site: the La Rance Tidal Power Plant (240 MW) that was commissioned in 1966. This type of installation has remained unique in the world and has only been reproduced at much smaller capacities in Canada (20 MW), China (5 MW) and Russia (0.4 MW) [CaEC, 2009]

1.2.6. Biomass Energy

'Biomass' is a term encompassing carbonaceous materials of vastly differing properties which are generated from trees, other plants, aquatic plants and algae. Biomass also includes agricultural and forestry wastes, organic wastes and organic municipal solid wastes. Energy from biomass is the oldest form of energy generation in human civilisation, beginning when Pleistocene man discovered fire and used it for warmth. Today, biomass supplies about 14% of global energy requirements [Sequeira, 2007], and represents the only base-load (i.e. continuous) renewable electricity source, accounting for 1% of fuel for electricity generation. Biomass also offers increased security of supply over most other renewable and non-renewable energy sources, with suitable crops able to be grown throughout most of the inhabited land area. Biomass is the world's oldest solar energy collector, utilising incident solar radiation for growth, predominately via photosynthesis. The overall solar-to-biomass thermodynamic efficiency is approximately 0.4%, compared with a theoretical maximum efficiency of 11% [US NRC, 2004] Several different conversion technologies exist or are under development, and these can be broadly categorised as either biochemical or thermochemical processes.

Biochemical processes utilise microorganisms to feed on the biomass substrate, and by processes such as fermentation or digestion, convert the biomass into useable fuels such as biogas or liquid biofuels. Unregulated biochemical conversion also takes place in certain

circumstances which is able to be harnessed, for instance in the plumbing of landfills for landfill gas, a high-methane content biogas.

Thermochemical conversion of biomass is usually defined according to the atmosphere in which the converting oxidation reactions take place. In an atmosphere of stoichiometric or greater oxygen requirement, the fuel is combusted releasing heat and non-reactive product gases. In less-than-stoichiometric air, or another oxidant such as steam, the fuel is gasified, forming a mixture of light reactive gases and small quantities of tars and char. In an inert atmosphere, the fuel is pyrolysed, forming mainly reactive liquids with some light gases and a solid component.

Gasification of woody biomass residues is the focus technology under development in this study. Log harvesting and wood processing generates two waste resource stocks. At the felling stage, trees are cut down leaving stumps, tops and branches stripped of the trunk. The trunks (logs, stems) are transported from the forest site, typically leaving the residues behind. At milling, the trunks are processed into wood products such as timber, veneer lumber or fibreboard. The various operations generate wood chips, sawdust, bark and black liquor which are together considered processing residues. In New Zealand, approximately 5.5 million m^3 of wood processing residues are generated annually [Pang, 2008].

1.2.7. Hydrogen

Although not an energy source, hydrogen is anticipated to play a dominant role as an energy carrier in the development of renewable energy worldwide [Muradov & Veziroglu, 2008]. This is discussed in detail in Section 1.4.

1.3. ENERGY RESOURCES IN NEW ZEALAND

1.3.1. New Zealand's Energy Supply

New Zealand's energy resources are characterised by high penetration of renewable sources, with 31.5% of total energy generation is classed as renewable (including hydro and geothermal). New Zealand is ranked third overall in OECD countries for magnitude of renewable energy sources. Fossil fuels continue to make up the bulk of energy generation at 68.4%.

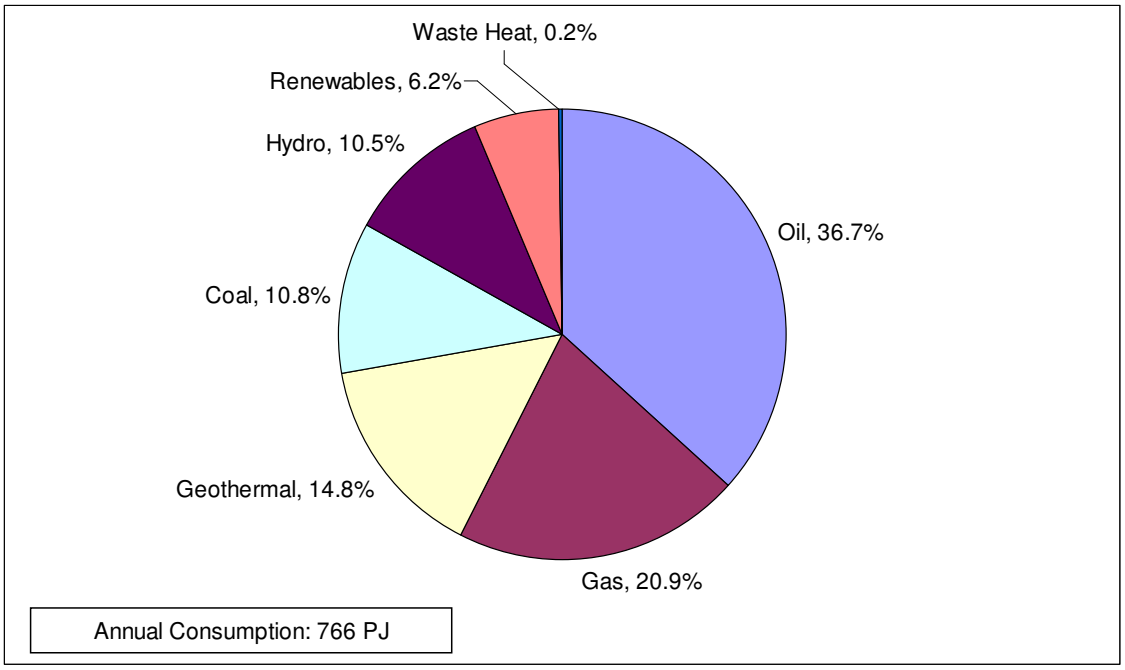

Figure 1.1 - New Zealand energy sources [CAENZ, 2008]

1.3.2. New Zealand's Energy Demand

New Zealand's energy demand is dominated by electricity and transport. Due to its geography and dispersed population, electricity is the dominant means of energy delivery, and transport is largely reliant on personal vehicles and road-going goods transport. Other large energy systems such as town heating and nationwide natural gas reticulation are rare for the same reasons. With large inefficiencies in electricity generation and faced with declining natural gas resources and increasing dependence on foreign oil, New Zealand's Energy Strategy to 2050 calls for increased distributed energy generation from domestically supplied fuels [MED, 2007].

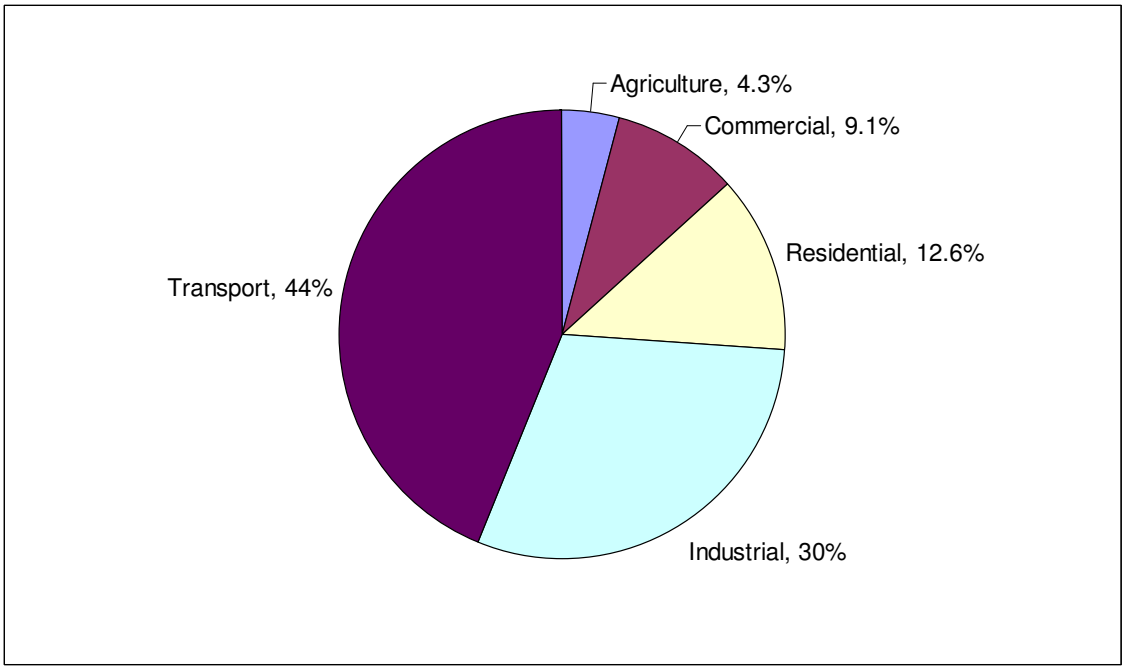

Figure 1.2 – New Zealand energy demand by sector [MED, 2007]

1.4. THE IMPORTANCE OF HYDROGEN

Hydrogen is widely tipped to replace fossil fuels as the primary energy carrier. The most abundant element in the universe, hydrogen can be produced by renewable methods, with water the sole product after conversion. Hydrogen can be applied to both stationary electricity generation and as an automotive fuel, making it very attractive if used in conjunction with alternative heating fuels.

1.4.1. Hydrogen Compared with Fossil Fuels

Hydrogen is the smallest of the elemental gases with a correspondingly low critical point of 33.2 K and 13 bar [NIST, 2008a]. Although hydrogen has a very high specific energy (120.1 MJ/kg), due to its low density the net calorific value (lower heating value) of a cubic metre of hydrogen at 288 K and 1 atm is only 10.1 MJ. Consequently as a thermal fuel, hydrogen is vastly different to the high energy density fossil fuels that modern society is built around. Figure 1.3 below compares the thermal energy quality of hydrogen with the fossil fuels and biofuels it stands to replace.

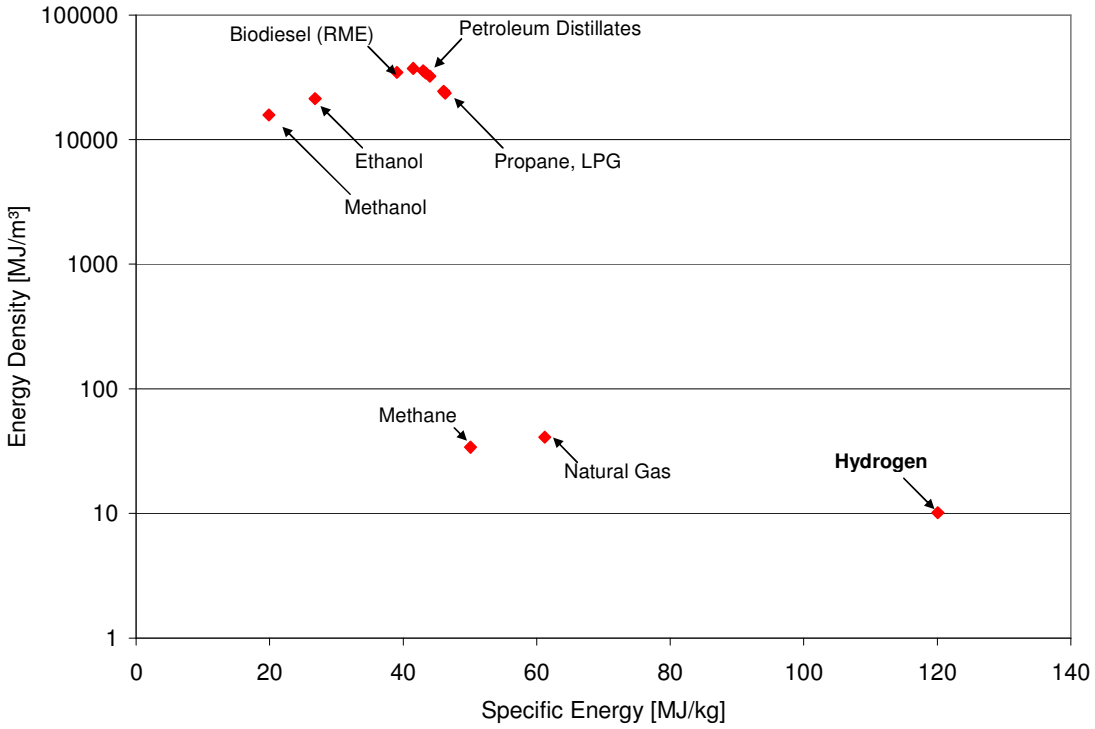

Figure 1.3 – Energy Density and Specific Energy of hydrogen compared with selected fossil fuels and biofuels. Energy Density is presented on a logarithmic scale.

1.4.2. Hydrogen Fuel Cells

Given its low energy density, hydrogen does not make an adequate alternative fuel in the existing infrastructure of liquid pipelines and tankers fuelling internal combustion engines. Hydrogen's key utility as fuel is for fuel cells. By extracting the electrical energy from the hydrogen molecule, the Carnot inefficiency of thermal engines is bypassed, allowing fuel cells to generate electricity at greater efficiency than has been achievable to date.

Discovered in 1838 by German scientist Christian Freidrich Schonbein, the first hydrogen fuel cell was demonstrated to work by Sir William Robert Grove in 1839 [Fuel Cell Today, 2009]. The technology lay largely dormant until the 1960s when American scientists began developing the technology as a fuel source for spacecraft [CaEC, 2003]. Fuel cells were considered ideal for this application as they were lightweight, easy to maintain and were fuelled by hydrogen, an abundant fuel aboard a spacecraft. Scientists from the General Electric Company developed a technique for depositing platinum onto a membrane, which served as a suitable electrolyte for a new generation of fuel cells. These polymer electrolyte membrane fuel cells (PEMFC) served aboard Project Gemini spacecraft. British scientist Francis Thomas Bacon went on to develop the potassium hydroxide electrolyte fuel cell later

in the decade, and by 1960 this new type of fuel cell was supplying electricity and drinking water as a by-product aboard Apollo missions.

Fuel cells work by catalytically disassociating the hydrogen molecule at the anode into its component protons and electrons. An electrolyte allows the positively charged particles to migrate to the cathode where it is oxidised, usually by oxygen. To arrive at the cathode the electrons must travel through an electric circuit. This process is represented diagrammatically in Figures 1.4 below. Newer fuel cell types such as the Molten Carbonate and Solid Oxide fuel cells also make use of hydrocarbons and carbon monoxide fuels by operating at such a temperature that hydrocarbons can be reformed directly at the anode, and that the electrolyte is not fouled by the carbon oxides.

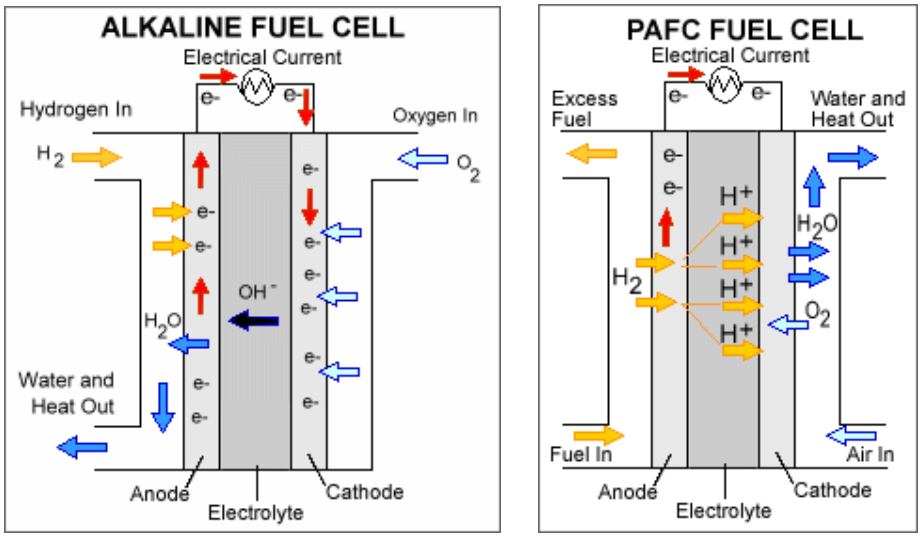

Figures 1.4 (a) and (b) – Basic operational schematic of alkaline and phosphoric acid (PAFC) fuel cells [US DOE Fuel Cells Technology Program, 2009]

Since the 1960s several types of fuel cells have been developed, categorised by their electrolyte, and with various operating parameters and requirements. Table 1.3 describes the operating parameters of each of the fuel cell types, with its level of technological advancement. As fuel cells typically use an ionic liquid or membrane to mediate the transfer of charged particles, they are particularly prone to contaminants in the fuel gas which may cause damage or poisoning.

Table 1.1 – Properties of various fuel cell types: Phosphoric Acid Fuel Cell (PAFC), Proton Exchange Membrane Fuel Cell (PEMFC), Molten Carbonate Fuel Cell (MCFC) and Solid Oxide Fuel Cell (SOFC) [CaEC, 2003]

	PAFC	PEMFC	MCFC	SOFC
Output power	100 - 200 kW	3 – 250 kW	250 – 10,000 kW	1 – 10,000 kW
Peak power density	~200 mW/cm²	~700 mW/cm²	~160 mW/cm²	150 – 500 mW/cm²
Operating Temperature	150 – 200°C	50 – 220°C	600 – 650°C	850 – 1100°C
Efficiency	36 – 42%	25 – 40%	45 – 55%	45 – 60%
Level of Commercialisation	Some available	Some available	Not yet commercialised	Not yet commercialised
Purchased Cost	$4,000/kW	$5,000/kW		
Applications	Spacecraft, Off-grid, emergency power generation	Automotive, Off-grid, emergency power generation	Stationary power generation	Stationary power generation, small-scale energy storage

1.4.3. Hydrogen Production Technologies

The advent of the hydrogen economy has seen increased interest in the development of hydrogen production technologies using renewable fuels. Ninety-six percent of commercially available hydrogen currently is produced by the steam reforming of fossil fuels. By combining methane reforming (R-1.1) with the water-gas shift reaction (R-1.2), four molecules of hydrogen can be produced from one molecule of methane, with carbon dioxide as a by-product (R-1.3).

$$CH_4 + H_2O \Leftrightarrow CO + 3H_2 \qquad \Delta H_{298K} = 206 \text{ kJ/mol} \qquad \text{R-1.1}$$

$$CO + H_2O \Leftrightarrow CO_2 + H_2 \qquad \Delta H_{298K} = -41 \text{ kJ/mol} \qquad \text{R-1.2}$$

$$CH_4 + 2H_2O \Leftrightarrow CO_2 + 4H_2 \qquad \Delta H_{298K} = 165 \text{ kJ/mol} \qquad \text{R-1.3}$$

This process is both energy-intensive and consumes fossil fuels, which negate the advantages of using hydrogen as an energy carrier. Consequently several other hydrogen production processes are in various stages of development. Two leading renewable energy technologies are catalytic electrolysis of water or hydrocarbons such as glycol, and reforming of biomass or biochemically produced feed stocks.

Electrolysis of water is essentially the fuel cell process in reverse. An electric current is applied to a body of water containing an electrolyte, which separates the water into its component elements, hydrogen and oxygen. Despite being thermodynamically reversible, electrical resistance limits the overall efficiency to at best 76% with current technology

[Marshall, 2008]. This is in excess of the threshold efficiency 75% that the California Energy Commission, the leading proponents of a hydrogen-based infrastructure, estimates to be economically viable. In spite of this, as solar energy is an intermittent energy source, large-scale hydrogen production will require coupling of this technology to a base-load generation system, in much the same way as solar-generated electricity requires a thermal (or otherwise) base-load generation capability for when solar energy is unavailable.

Reforming of biomass feed stocks to produce hydrogen is essentially similar to steam reforming of methane, but requires breaking down the biomass by gasification. Gasification combines pyrolysis, which is analogous to cracking of crude oil to produce lighter petroleum products, and the reforming reactions described above to produce a hydrogen-rich gaseous product stream. Gasification is the technology under investigation in this research.

1.5. BIOMASS GASIFICATION

Gasification has been applied to coal for almost 200 years for the production of town gas for municipal heating and lighting, with charcoal as a solid fuel by-product. During the Second World War, Germany, facing fuel supply shortages, applied gasification to its vast coal reserves to produce a syngas gas resource suitable for conversion to diesel by the Fischer-Tropsch process. This technology has been applied more recently in South Africa, where Sasol produces 150,000 bbl/day of synthetic fuels from coal gasification syngas [Sasol, 2005].

Biomass Gasification is one of the thermochemical conversion techniques that has recently been attracting great interests both from researchers and industry. This section describes the principles and application of gasification technology to biomass in its various forms. As New Zealand has a significant woody biomass resource base, there is particular interest in applying the technology within the forestry industry.

1.5.1. Principles of Gasification

As stated earlier, gasification is the process of heating a fuel to high temperatures in less-than stoichiometric quantities of air, or another oxidising medium such as steam. The primary product is a light reactive gas mixture called producer gas which consists of mostly hydrogen, nitrogen (in the case of air gasification), carbon oxides and light hydrocarbons. When the relative proportion of hydrogen in the gas is roughly double that of carbon monoxide, the gas is described as ‘syngas’.

Typically air-blown gasification yields a producer gas with a low calorific value around 4 - 8 MJ/Nm³, while oxygen- and steam-blown gasification yields a gas of medium calorific value, approximately 14 - 20 MJ/Nm³. The reason for the two different gas qualities is the presence of nitrogen in air-blown gasification producer gas, which effectively dilutes the reactive products. Secondary products produced in small quantities by gasification are tars, char and ash. Tars describe fluid products of gasification which condense below 300°C, and are typically aromatic hydrocarbons [Milne et. al., 1998]. Char is the solid remnant of the fuel, consisting almost completely of carbon. Non-reactive components of the fuel result in ash. For biomass, ash consists predominately of silicates, alkali metals and nitrogen and phosphorous compounds, with some heavy metals depending on local soil conditions.

1.5.2. Types of Gasification Reactor

Several reactor types have been applied for gasifying various fuels. Initially fixed bed reactors were used, in either an updraught (counter-current) or downdraught (co-current) configuration. These reactors are supplied with air or oxygen as a gasification agent.

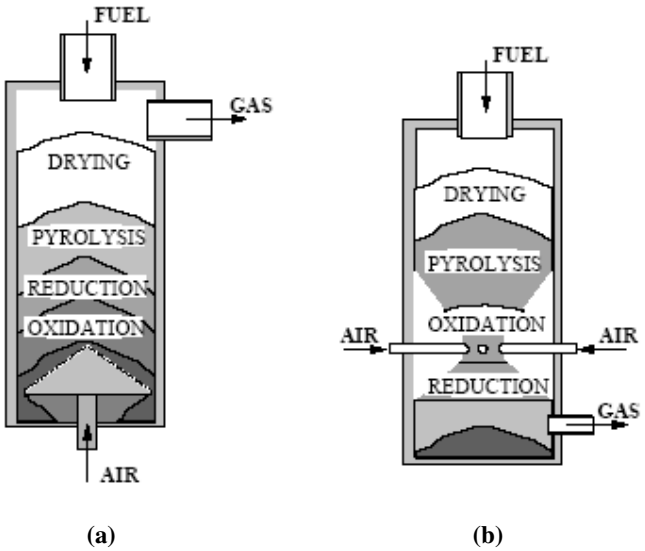

(a) **(b)**

Figures 1.5 (a) and (b) - Counter-current (a) and co-current (b) fixed bed gasifiers. In both cases, fuel enters at the top of the reactor and goes through reaction stages, culminating a low CV producer gas stream and an ash/biochar solid waste stream.

Most up-draught gasifiers have been decommissioned owing to high waste water loads from ash and char evacuation and gas cleaning. Down-draught gasifiers produce low-tar content gases as the tar is internally reformed at high temperature as the gas flows through the high temperature combustion zone in the gasifier.

Entrained-bed or slagging gasifiers (illustrated in Figure 1.6) are typically used in coal gasification processes or recently in black liquor gasification, and require a liquid or finely dispersed particle fuel. Pure oxygen is typically the gasification agent, resulting in medium calorific value producer gas. Because the fuel and oxygen enter the reactor at the same point, high heat and mass transfer result, leading to consistent producer gas quality. The high temperatures used in the process liquefy the ash compounds forming a slag which is collected at the bottom of the reactor, a design which necessitates large operating costs and is limited by economies of scale.

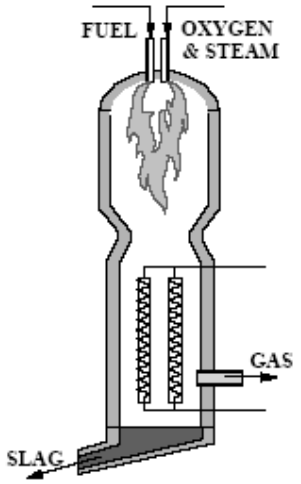

Figure 1.6 – Entrained bed gasifier

Fluidised bed gasifiers involve fluidising the fuel with the gasification agent, usually air or steam, in a bed material. This promotes heat and mass transfer between the biomass fuel and the bed material, hence increasing the reaction rates. Fluidised bed gasification is typically operated at lower temperatures (700-900°C) than fixed bed or entrained flow gasification, as above these temperatures the ash component of biomass can become sticky resulting in defluidisation. The use of steam requires a heat source, as the gasification is overall endothermic. One configuration is to use a dual fluidised bed reactor consisting of a combustion column and a gasification column. Heat is generated in the combustion column and carried by the circulating bed material which is then separated from the flue gas and provides heat in the gasification column for steam-gasification.

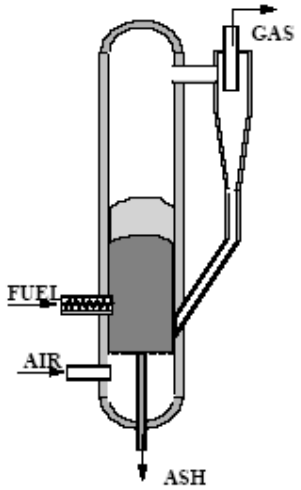

Figure 1.7 – Single fluidised bed gasifier

1.5.3. University of Canterbury Gasifier

A dual fluidised bed gasifier has been constructed at the University of Canterbury's Department of Chemical and Process Engineering ("the Department"), and has been operating as a pilot-scale experimental apparatus since 2005 [Brown, 2006]. It uses steam as a gasification agent and has a capacity of around 100 kW_{th} input, equivalent to 25 kg/h of wood pellet fuel. Figure 1.8 below shows the operational schematic of the gasifier. The gasifier is discussed in more detail in Chapter 4.

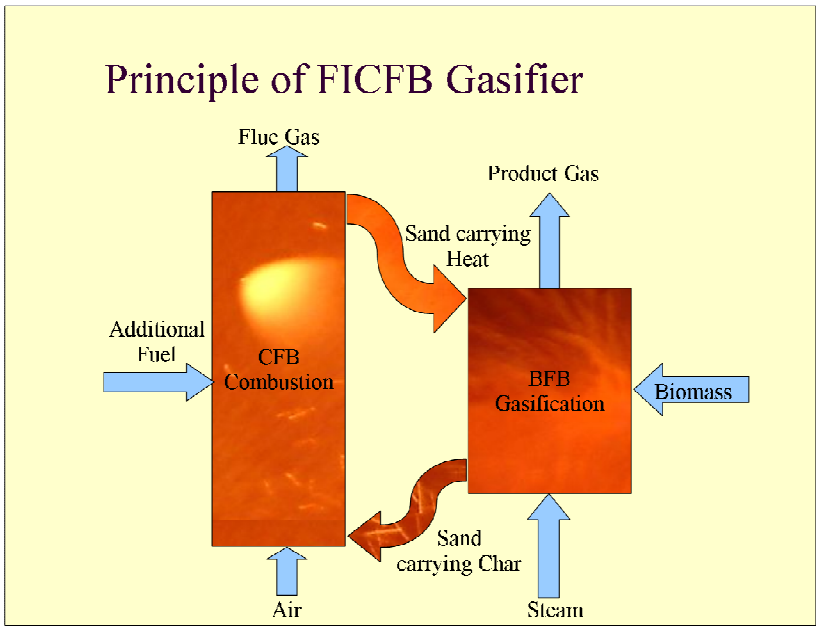

Figure 1.8 - Principle of operation of Dual Fluidised Bed gasifier

Since its construction the gasifier has acted as the test system for a number of experiments and operational trials, as part of the Biomass Integrated Gasification Combined Cycle (BIGCC) Programme at the University of Canterbury. Brown validated the choice of gasifier for the production of a medium calorific value gas, which potentially could be applied to the wood processing industries [Brown, 2006]. Rutherford used experimental results from the gasifier as validation for an equilibrium model of the gasification process that can be applied to similar processes universally [Rutherford, 2006]. More recently, Bull conducted an extensive analysis on gasifier operation resulting in a number of mechanical improvements [Bull, 2008], and Penniall combined experimental results with the equilibrium model to evaluate the feasibility of applying the technology to a number of wood-processing operations [Penniall, 2008].

From 2009 the focus of the biomass gasification programme at the University of Canterbury shifted to application of the technology to the production of liquid fuels. Investigations concurrent with this study included analysis of the potential of co-gasification of biomass with coal, development of a novel cold gas cleaning technology utilising scrubbing with biodiesel, a hydrological analysis of the dual fluidised bed system, and production of Fischer-Tropsch diesel from biomass syngas utilising microchannel reactor technology.

1.6. OBJECTIVES OF THE INVESTIGATION

1.6.1. Improve Yield and Quality of Producer Gas

A number of catalytic gasifier bed materials were to be used during the investigation, for the primary goal of increasing the yield of the producer gas and improving its quality, particularly in terms of hydrogen content. This effectively reduces the need for downstream processing to maintain product quality, thereby reducing cost. To give an adequate comparison between catalysed and non-catalysed gasification, a number of trials were conducted in the dual fluidised bed gasification using inert bed material. The parameters used as performance indicators include producer gas composition of hydrogen (H_2), carbon monoxide (CO), water content, and tar content. Hydrogen and carbon monoxide contents are important from the perspective of maintaining an optimum ration of H_2/CO at 2 for downstream F-T synthesis. Water content of the producer gas is used as a measure of fluid bed performance; and the tar content and composition remain the most significant hindrance to commercialisation of the gasification technology. The investigation considered only bed materials which are readily available and have low cost, relative to commercially developed catalysts.

1.6.2. Improve Understanding of Gasifier Operational Parameters

The Dual Fluidised Bed (DFB) gasifier has proven a complicated system to master with a number of interconnected variables affecting performance. A consequence of the testing of various bed materials of differing properties is gaining a more thorough understanding of the nature of the system. First-hand data will lead to better understanding of the reaction kinetics, hydraulics and heat and mass transfer within the system and will improve the design of the DFB gasification system, both as an energy plant and as a producer of hydrogen and liquid fuels.

1.6.3. Analyse the Effects of Different Bed Materials at the Systems Level

It was anticipated that the use of catalytic bed materials would increase the hydrogen content of the producer gas and overall producer gas quality. The increased hydrogen content and reduced tar content for the improved system can be related to cost saving, by considering the reduction in downstream processing equipment traditionally required for hydrogen purification.

With the development of fuel cells, hypothetical situations concerning the demand of the hydrogen in society can be evaluated. The integration of this demand with the supply potential of hydrogen from biomass gasification forms an economic evaluation for the ongoing development of biomass gasification systems.

2. Gasification Theory and Literature Review

2.1. Introduction to Gasification Theory

In the high temperature, low oxygen gasification environment a number of competing reactions take place which affect the composition of the exiting producer gas, regardless of the fuel being reacted. These reactions have a diverse range of thermodynamic and kinetic properties, and because many reactions are interlinked by consumption and generation of common chemical species, they are by no means independent. Any attempt to influence the final products of the gasification process requires consideration of the concurrent reactions individually, the reaction set as a whole, and their equilibrium and kinetic requirements.

The biomass gasification reactions can be classified according to the state of the reagents, and the extent of the passage of the fuel through the gasification system. Heterogeneous reactions describe the reactions of solids and fluids. As the fuel enters the gasification environment devolatilisation (pyrolysis) reactions occur first, which liberate the fuel of readily-forming light gas components, and breaks down some of the remaining solid fuel into lighter hydrocarbon components. The remaining solid fuel and char then undergo gasification reactions, consuming the oxidant and forming more light gases. In the dual fluidised bed gasifier system, some solid char flows to the combustion column to generate heat from combustion reactions. Finally, some of the heavier pyrolysis products (tars) are reacted further through thermal and catalytic cracking, and the Boudouard equilibrium reaction disproportionates carbon monoxide into carbon dioxide and graphite.

Secondarily, several homogeneous reactions between different gaseous species take place. The water gas shift equilibrium reaction balances the relative proportions of hydrogen, carbon monoxide, carbon dioxide and water. The steam reforming of light hydrocarbons such as methane and C2 hydrocarbons produces carbon monoxide and hydrogen. This also applies to the lighter tar components formed during devolatilisation.

2.1.1. Stage 1 – Devolatilisation (Pyrolysis) Reactions

For the sake of chemical balance, woody biomass in this investigation is given by the formula $CH_{1.5}O_{0.7}$, based on an ultimate analysis conducted by Hill Labs[*]. Nitrogen and sulfur are

[*] Analysis can be found in Appendix A.

considered only on the basis of formation of impurities for cleaning, and are not considered in the overall product reaction scheme. Other impurities in the wood such as minerals required for growth collectively form the ash component.

Subjected to heat, woody biomass undergoes various reactions producing a multitude of solid carbon and gaseous hydrocarbon products. These reactions are differentiated from gasification by the lack of an oxidant – although present in the reactor, the oxidant is excluded by the generation of inert gases from the wood particle. Between 200°C and 280°C the less thermally stable hemicellulose breaks down into light organic acids, xylans and furans, as well as carbon oxides and methanol [Grassi & Bridgewater, 1991]. At higher temperatures (up to 500°C) lignin breakdown is initiated with similar results to the hemicellulose. Lignin degradation produces phenolic compounds and other aromatics, collectively known as tars, which have boiling points higher than that of benzene. Both reaction sets are exothermic, but above 350°C an external heat source is required to maintain the increasingly endothermic process. Cellulose breaks down above this temperature producing water, carbon dioxide and char as final products.

The solid product of the devolatilisation process is char which is fundamentally solid carbon. With the gaseous pyrolysis products separated from the fuel pellet the char undergoes gasification. For the purpose of increasing production of hydrogen and minimising of tars, which are undesirable by-products, it is favourable to decrease the extent of devolatilisation reactions and increase gasification reactions. This is achieved in the reactor by reducing biomass moisture content, increasing heating rates and mechanically disengaging the gaseous products from the wood particles, easily achieved in fluidised beds.

2.1.2. Stage 2 – Gasification Reactions

The interaction between the biomass fuel particles and the oxidant is determined by the gasification reactions. For the gasification of woody biomass, typically wood is devolatilised before gasification reactions dominate, however in a fluidised bed reactor the reaction rates are sufficiently high that pyrolysis and gasification take place concurrently.

$$CH_xO_y + (1 - y)H_2O \rightarrow CO + (1 - y + \tfrac{1}{2}x)H_2 \qquad \text{R-2.1}$$

$$C + H_2O \rightarrow CO + H_2 \qquad \Delta H_{923K} = 135.8 \text{ kJ/mol} \qquad \text{R-2.2}$$

Gasification reactions are endothermic and consequently in a continuous process need to be sustained by a source of heat. In a single reactor where air or oxygen is the oxidising agent, this heat is supplied by combustion reactions occurring at the same time. Oxidising with steam requires an independent heat source, which in dual fluidised bed gasification is supplied by the separate combustion reactor and circulating hot bed material. As the main products of gasification are carbon monoxide and hydrogen, optimising the system for hydrogen production requires firstly considering how to maximise gasification over pyrolysis.

The gasification reactions are typically much slower than the solid circulation rates of dual fluidised beds. Consequently much of the residual char is transferred to the combustion column where reaction rates are much faster. Based on carbon balances typically one-third to one-fifth of the reacted char is gasified, and the rest is combusted [Bull, 2008].

2.1.3. Stage 3 – Gas Phase Reactions

The gases produced from pyrolysis and gasification of wood, char and intermediate hydrocarbons interact with other species in the reactor, setting up chemical equilibria. These reactions can be categorised as heterogeneous, where the gases react with the solid fuel and char components, or homogeneous, where the gases interact with each other.

The primary heterogeneous reactions in the gasification zone are methanation (R-2.3) and the Boudouard equilibrium (R-2.4). Methanation forms methane from the pyrolytic reaction of hydrogen and carbon. The Boudouard equilibrium is the disproportionation of two carbon monoxide molecules forming carbon and carbon dioxide. In the combustion zone, combustion reactions forming carbon dioxide dominate.

$C + 2H_2 \rightarrow CH_4$	ΔH_{923K} = -88.9 kJ/mol	R-2.3
$2CO \Leftrightarrow C + CO_2$	ΔH_{923K} = 171.4 kJ/mol	R-2.4

Several gas phase reactions determine the final gaseous reaction products. The water-gas shift equilibrium balances carbon monoxide and steam to form carbon dioxide and hydrogen, the extent of which is determined by equilibrium conditions at the operating temperature and pressure (R-2.5). Similarly, the steam reforming of methane is potentially active under gasification conditions, converting methane and steam to hydrogen and carbon monoxide (R-2.6). Other gas-phase reactions include the dry reforming of methane with carbon dioxide (R-

2.7), steam reforming of higher hydrocarbon gases (R-2.8), and cracking (hydrogenation) of tar compounds.

$CO + H_2O \Leftrightarrow CO_2 + H_2$	ΔH_{923K} = -35.6 kJ/mol	R-2.5
$CH_4 + H_2O \Leftrightarrow CO + 3H_2$	ΔH_{923K} = 224.8 kJ/mol	R-2.6
$CH_4 + CO_2 \Leftrightarrow 2CO + 2H_2O$	$\Delta H_{(298K)}$ = 247 kJ/mol	R-2.7
$C_aH_b + aH_2O \leftrightarrow aCO\ (a + ½b)H_2$		R-2.8

Each of the reactions in the above set has individual kinetic and equilibrium properties, making their relative extents at gasification conditions difficult to predict theoretically. The complex reaction set suggests multiple routes exist for attempting to enhance hydrogen production, either by selective removal of reaction products from the reactor or catalysing the reactions in the desired directions.

2.2. EQUILIBRIUM MODELLING

Several attempts have been made by various authors to model and predict the composition of producer gas formed by the gasification reaction set. Within this department Rutherford [Rutherford, 2006] and later Penniall [Penniall, 2008] developed a quasi-equilibrium model that predicted the producer gas composition and energy yield from the 100kW DFB gasifier to a reasonable accuracy. Internationally, several authors have analysed the biomass gasification system to determine the optimum conditions for high hydrogen content producer gas.

2.2.1. The Equilibrium Model of Rutherford and Penniall

Rutherford constructed and validated an equilibrium model using MS Excel and Aspen HYSYS software packages [Rutherford, 2006]. Validation was limited at the time due to operational difficulties with commissioning the gasifier. Initial predictions based on gasification temperature and steam/biomass ratio are given in Table 2.1, along with typical experimental results from the period. Penniall investigated the obvious discrepancies between the predicted and experimental gas compositions and was able to modify the model to give more accurate results [Penniall, 2008]. This was only achievable after modifications were made to the model which accounted for anticipated kinetic limitations intrinsic to the gasifier's design, which were mainly due to channelling in the bubbling fluidised bed causing effective reduction in the steam/biomass ratio. The success of the changes led Penniall to

conclude that at the gasifier's normal operating conditions an equilibrium producer gas composition was unable to be achieved.

Table 2.1 – Comparison of equilibrium model with the gasifier experimental results [Penniall, 2008]

	Experimental Results	Initial Modelling	Modified Modelling
Hydrogen	24.7%	49.4%	26.9%
Methane	14.6%	4.4%	18.5%
Carbon Monoxide	36.7%	40.3%	34.8%
Carbon Dioxide	18.7%	6.0%	15.1%
C_2 components	5.2%	--	4.8%

2.2.2. Other Thermodynamic Optimisation

Internationally several authors have focussed on optimising the gasification system for the generation of high hydrogen content producer gas, and maximum process efficiency. Shen and colleagues considered a steam-fluidised dual fluidised bed similar to the University of Canterbury DFB gasifier and applied a model developed using Aspen Plus [Shen et. al., 2008]. The study concluded that maximum hydrogen yield could be obtained with gasification temperature held between 750-800°C, combustion temperature of 920°C, and steam/biomass ratio between 0.6 and 0.7. Mahishi and Goswami considered a completely theoretical reactor and applied Gibbs energy minimisation principles to determine optimum hydrogen generation conditions [Mahishi & Goswami, 2007]. Their first law analysis concluded optimum hydrogen production was achieved at a gasification temperature of 1000K (727°C), steam/biomass ratio of 3 and equivalence ratio (ratio of supplied air to stoichiometric air) of 0.1. Murakami developed an Aspen model of gasification of dried coffee grounds, concluding that a cold gas efficiency in excess of 75% can be obtained with a gasification temperature of 800°C, provided fuel moisture content was less than 10% [Murakami et. al., 2007]. Sanz and Corella concluded fuel moisture content and equivalence ratio were the key parameters influencing producer gas calorific values and composition, in an air-blown reactor [Sanz & Corella, 2006]. Shuster considered a dual fluidised bed gasifier and concluded a 20% electrical efficiency can be obtained from biomass gasification, with gasification temperature and fuel oxygen content the most significant parameters [Schuster et. al., 2001].

2.2.3. Conclusions from Equilibrium Modelling

Results from the literature review show that a number of variables need to be considered when determining the theoretical outputs from the biomass gasification process. Gasification temperatures greater than 700°C are generally regarded as necessary, but reported optimum steam/biomass ratios are diverse, with the range covering half an order of magnitude from 0.6 to 3. Other factors such as equivalence ratio (not applicable to the dual fluidised bed system), fuel moisture content and ultimate composition and reaction time are other significant parameters influencing gasifier performance. Maximum hydrogen composition in the producer gas has been modelled up to 70%, but experimental verification suggests this is optimistic. Beyond the thermodynamic parameters of temperature, pressure and molecular composition, it is anticipated that the other influencing parameters are also dependent on gasifier reactor design influencing heat and mass transfer rates.

2.3. PREVIOUS CATALYSIS RESEARCH

The equilibrium conditions modelled for biomass gasification suggest clear boundaries with regard to producer gas composition, but do not consider the kinetic limitations of the system. Except for Murakami, the authors mentioned in Section 2.2 have not considered reaction time as a fundamentally limiting parameter. Rutherford and Penniall have both concluded from modelling studies that the discrepancies observed between the equilibrium model and experimental results can be related to the short time the biomass spends in the gasification reactor, prior to transfer to the combustion column where reaction rates are much faster [Rutherford, 2006; Penniall, 2008]. Influencing reaction rates by catalysis allows the producer gas composition to be closer to the equilibrium, which is a favourable outcome given the negative discrepancy between experimental results and the theoretical end-point.

In the ideal case most equilibrium models predict a hydrogen content of 50-60%. Applying biomass gasification to hydrogen production requires that the producer gas hydrogen content is as high as possible, to reduce the size and therefore cost of downstream purification equipment. Maximising hydrogen content therefore means shifting the equilibrium to completion, by influencing the relative concentrations of the hydrogen-producing reaction products.

Since its initial development catalytic promotion of the gasification reactions has been investigated by many authors. In the fluidised bed environment this is mainly accomplished

by substitution of the (inert) bed material with a catalytically-active alternative. These alternatives are discussed below.

2.3.1. Inert Materials - Greywacke

For biomass gasification tests in the University of Canterbury's DFB gasifier, greywacke river sand has been the primary bed material to date used and represents the inert material 'base case'. Its sole function is heat transfer medium, circulating heat from the combustion column to the gasification column and thereby supplying heat to endothermic gasification reactions. X-Ray Fluorescence (XRF) analysis concludes that the greywacke sand in use is predominately silica (SiO_2) and alumina (Al_2O_3), with small amounts of iron, alkali metals and alkali earths. Table 2.2 summarises the XRF analyses of six greywacke sands used in the UC gasifier programme with average values as considered in the forthcoming analysis.

Table 2.2 – Summary of XRF elemental results of six samples of greywacke river sand from around the Canterbury region [%]

%	SiO_2	TiO_2	Al_2O_3	Fe_2O_3	MnO	MgO	CaO	Na_2O	K_2O	P_2O_5
Washdyke	73.76	0.45	11.87	3.28	0.05	1.18	2.75	3.16	1.75	0.14
Rangitata	69.76	0.53	14.24	3.82	0.06	1.48	2.59	3.71	2.09	0.15
Wakanui	69.43	0.53	14.44	3.88	0.06	1.46	2.21	3.81	2.32	0.16
Rakaia	70.19	0.50	14.42	3.59	0.05	1.39	1.89	4.06	2.51	0.15
Ashburton	71.32	0.47	13.42	3.44	0.05	1.27	2.57	3.61	2.06	0.14
Kaitorete	73.76	0.41	12.57	2.98	0.05	1.12	2.52	3.38	1.79	0.13
AVERAGE	**71.37**	0.48	**13.49**	3.50	0.05	1.32	2.42	3.62	2.09	0.15

2.3.2. Olivine

Olivine is a magnesium-iron silicate with the generic formula $(FeMg)_2SiO_4$. Superficially it is greenish-grey sand, thought to be caused by the presence of traces of nickel, and can turn rust red after calcination. Olivine is characterised by the relative concentrations of magnesium and iron, which vary in geological deposits globally.

Olivine was one of the first catalytically active bed materials applied to biomass gasification in fluidised beds, and has been investigated by numerous authors. In 1998 Hofbauer and Rauch reported on the use of olivine in the Biomass Steam Gasification research funded under the non-nuclear renewable energies programme in the European Union. Under Task E2 of the project, a NiO-impregnated olivine catalyst was shown to be catalytically active leading to

reduced tar concentrations and 8% higher hydrogen concentration [Hofbauer & Rauch, 2001]. Pfeiffer's analysis of different olivines in the biomass gasification tests in a 100 kW-scale gasifier at TU Wein, Austria, concluded that catalytic activity increased with increasing relative proportion of iron [Pfeifer & Hofbauer, 2006]. Rapagnà compared the tar reduction potential using olivine and dolomite as bed materials in a laboratory-scale gasifier and found that olivine reduces tars in the producer gas at an extent comparable to dolomite, but the olivine has an additional advantage of having far greater resistance to attrition. The authors went on to conclude that temperatures of greater than 800°C were optimum when using olivine as a tar reducing catalyst, with steam/biomass ratio having little effect [Rapagnà et. al., 2000]. Devi showed that calcination (essentially 'baking') of olivine in air-blown gasification at 900°C improved the catalytic conversion of naphthalene, a major tar component [Devi et. al., 2005]. Table 2.3 below gives the elemental composition of the olivine sand used in the gasification trials in the current study.

Table 2.3 – XRF major elemental composition of olivine used in UC biomass gasification trials {%}.

%	SiO_2	TiO_2	Al_2O_3	Fe_2O_3	MnO	MgO	CaO	Na_2O	K_2O	P_2O_5
Olivine	41.12	0.02	0.24	11.04	0.16	46.64	0.25	<0.1	0.04	0.02

2.3.3. Nickel Compounds

Nickel has been used as a hydrogenation catalyst for many years in the petrochemical industry, and consequently was thought to have good potential as a tar reforming catalyst. Initially perovskite (lanthanum-nickel-iron calcite) was tried but in the fluidised bed environment showed extensive elutriation [Hofbauer & Rauch, 2001]. Consequently nickel oxide doping of olivine was used with great success, demonstrating the extensive tar reforming properties of the nickel mineral with the elutriation resistance of olivine. Nickel-doped aluminates and silicates such as NiO/Olivine have also shown to be deactivated by coking over time, which has led to the development of nickel-impregnated dolomite [Sato & Fujimoto, 2007]. The interaction between nickel and magnesium oxides present in olivine and dolomite was extensively characterised by Swierczynski, who concluded that following calcination at 1100°C a stable solid solution forms between the two compounds which acts effectively on the biomass-steam gasification reaction [Swierczynski, 2007]. Nickel catalysts have also been applied to downstream reforming processes to convert methane/CO_2 mixtures to hydrogen-rich syngas, which is essentially similar to the homogeneous gas phase reaction system present in the biomass gasification system. Hydrogen concentrations of greater than

60% have been measured in the product gas from these reactions at high steam/biomass ratios [Kolbitsch et. al., 2008].

Unfortunately the resources of nickel minerals are almost totally located in two regions globally, Western Australia and New Caledonia. Nickel-containing minerals are rare in New Zealand, and therefore, no investigation of nickel-containing bed materials was conducted in this research. In addition, nickel compounds have been used as reforming catalysts for a number of years, but because they are valuable and cannot be disposed of in an environmentally safe manner, their application to biomass gasification would be limited.

2.3.4. Iron

As a reforming catalyst Iron, though less reactive than nickel, is an abundant, inexpensive and harmless natural mineral. Iron is also used as a catalyst (with chromium) in high temperature water-gas shift reactors. Azhar Uddin and Nordgreen independently reported that iron and iron oxide catalysts were active at promoting biomass tar decomposition in steam- and air-blown gasifiers [Azhar Uddin et. al., 2008; Nordgreen, 2006]. Bleeker applied iron oxide reduction-oxidation cycling to pyrolysis oil, generating a high hydrogen content producer gas from a process similar in nature to the dual fluidised bed system [Bleeker & Kersten, 2007].

High concentration iron sands are available in New Zealand in two principle locations, near Raglan on the North Island west coast and on the South Island west coast at Barrytown, roughly 20km north of Greymouth. The North Island sand is predominately magnetite (Fe_3O_4), while South Island sand is ilmenite ($FeTiO_3$) which has higher concentrations of titanium. Ilmenite sand was applied to the UC gasifier in this research. In this report, 'magnetite' is used to describe the iron oxide component of the bed material regardless of mineral source, despite in some trials the iron oxide being sourced from ilmenite sands. Table 2.4 shows the major elemental composition of the ilmenite-containing sand sourced from the Barrytown beach.

Table 2.4 – XRF major elemental analysis of ilmenite-containing sand used in UC gasification experiments, sourced from Barrytown beach [%].

%	SiO_2	TiO_2	Al_2O_3	Fe_2O_3	MnO	MgO	CaO	Na_2O	K_2O	P_2O_5
Ilmenite	39.63	14.59	13.04	24.13	2.40	1.07	5.07	0.54	0.47	0.14

2.3.5. Calcium

The addition of calcium to the bed material used for fluidised bed gasification is perhaps the most important development of the technology since the inception of the dual fluidised bed design. Calcium forms an equilibrium between its carbonate and oxide species around 700°C, such that under gasification conditions carbon dioxide is absorbed by the incoming calcium oxide (CaO) in the bed material to form calcite ($CaCO_3$). After the bed material and the calcite flow to the combustion column, the calcium is regenerated under combustion conditions (heating). This is represented by Reaction (R-2.9) below. Calcium oxide has a theoretical maximum CO_2 absorption of 785g CO_2/kg CaO.

$$CaO + CO_2 \Leftrightarrow CaCO_3 \qquad \Delta H_{923K} = -170.5 \text{ kJ/mol} \qquad \text{R-2.9}$$

As a result of this reaction, a chemical carbon dioxide 'pump' is formed in the dual fluidised bed gasifier which transports CO_2 produced by the gasification reactions into the combustion column. This has a two-fold effect on producer gas composition. Firstly, removing inert CO_2 concentrates the other components in the producer gas, which is particularly advantageous from the perspective of hydrogen production. Secondly, carbon dioxide removal from the gasification column shifts the water-gas shift reaction to produce more hydrogen by Le Chatilier's principle. The subsequent drop in carbon monoxide concentration in turn stimulates the gasification and steam reforming reactions by the same method.

Calcium compounds have been an important addition to coal gasification processes for many years, used to prevent bed material and ash agglomeration at high temperatures [van Dyk et. al., 2008]. Florin and Harris reported that it is possible to enhance biomass gasification utilising carbon dioxide capture and using a thermodynamic model predicted a maximum hydrogen concentration of 83% [Florin & Harris, 2007]. Several other authors have also investigated the effects of CO_2 absorbing compounds on biomass gasification with generally favourable results. At TU Wein addition of limestone has increased hydrogen composition in producer gas by up to 20% [Pfeifer, 2008]. Mashishi and Goswami have reported increases in hydrogen concentration (48.6%), gas yield (62.2%) and carbon conversion efficiency (83.5%) compared with an inert bed material, in addition to an apparent reduction in overall tar yield [Mahishi & Goswami, 2007a]. Calcium has been utilised for enhancing steam reforming of methane in a catalysing nickel-alumina bed material, with analysis of the limiting effect of calcium hydroxide below 600°C [Hildenbrand et. al., 2006]. Contrary to the positive chemical effects that calcium-containing compounds have on the gasification process, the high attrition

of limestone and dolomite particles in circulating fluidised beds are also well reported in the literature.

Calcium compounds are readily available in nature as limestone (calcite, $CaCO_3$) and dolomite ($CaMg(CO_3)_2$), and calcium hydroxide. For the UC gasifier experiments both calcite and dolomite are tested. The dolomite tested was found to have very similar elemental composition to the calcite, but was shown to be physically more resistant to attrition. Table 2.5 gives the compositions of the calcite and dolomite used in the gasifier experiments.

Table 2.5 – XRF major elemental analysis of calcite and dolomite used in UC gasification experiments

%	SiO_2	TiO_2	Al_2O_3	Fe_2O_3	MnO	MgO	CaO	Na_2O	K_2O	P_2O_5	LOI[†]
Calcite	<0.2	<0.01	<0.2	0.04	0.02	0.33	55.47	<0.1	0.03	0.02	43.79
Dolomite	0.25	0.01	<0.2	0.06	<0.01	**0.25**	55.41	<0.1	<0.01	0.02	43.88

2.3.6. Noble Metals and Manufactured Catalysts

Various other heavy metals and commercially manufactured catalysts have been studied to determine their effects on biomass gasification reactions. Aluminosilicate zeolites such as ZSM-5 have been used for 35 years in the petroleum industry for hydrocarbon cracking, and have been applied to biomass gasification to reduce tar yields in producer gas. Asadullah considered gasification of many biomasses in a dual fluidised bed system using a rhodium-impregnated ceria (cerium oxide, CeO_2)/silica catalyst. The authors found that this catalyst completely prevented tar formation even at relatively low temperatures and in comparison to dolomite and nickel catalysts, substantially improved gasifier energy efficiency [Asadullah, 2004; Miyazawa, 2004]. The same authors also considered addition of very small amounts of platinum (0.01 wt%) which was much more effective than rhodium, ruthenium and palladium doped catalysts of the same base [Nishikawa, 2008]. The same combination of elements were considered independently by Haryanto in terms of hydrogen production via the water-gas shift and found again that platinum was most effective, giving a carbon monoxide to hydrogen conversion of 76.3% [Haryanto, 2007]. Tasaka studied the effects of cobalt-magnesite (MgO) for tar treatment of *Pinus radiata* gasification and found a 16% total tar conversion with 12 wt% cobalt in the catalyst [Tasaka, 2007].

Due to high costs for the noble metals and manufactured catalysts, these two types of catalytic bed materials were not considered during this research.

[†] Lost on ignition

2.4. CONCLUSIONS

Extensive research has been conducted on the thermodynamics of biomass gasification, with many authors showing that in-bed catalysis is viable method of improving producer gas quality. Numerous potentially catalytic bed materials have been studied, especially geological minerals such as calcite, dolomite and olivine and nickel-containing compounds. Tar reduction has been a major focus of previous research.

Calcium containing minerals such as limestone and dolomite appear to be most favourable for improving hydrogen composition in producer gas, by development of the carbon dioxide-'pumping' phenomenon when calcium is transferred from the gasification column to the combustion column in a dual fluidised bed gasifier. In general, the effects of catalytic bed materials have been studied with regard to an inert bed material base case. Also, combination of calcium compounds with other catalytic materials has not been extensively studied.

Despite a lack of geological minerals containing nickel and other catalytic metals in New Zealand, the literature review suggested upgrading of the biomass producer gas for the purpose of producing hydrogen can be accomplished with the resources at hand. Again, due to cost constraints for experimentation and in the interest of keeping biomass gasification economics favourable, noble metals and commercially constructed catalysts were not considered as part of this research.

3. Laboratory-scale Experiments

3.1. INTRODUCTION

Preliminary investigation of the potential for various bed materials to catalyse or otherwise influence the gasification process was conducted in a laboratory scale apparatus. At the smaller scale, less time and money was required to obtain the first indications of the effects of different materials. Based on similar experiments conducted by other authors, an apparatus was designed and constructed based on typical operating parameters in the Department's dual fluidised bed (DFB) gasifier. Experiments were undertaken on a variety of easily-obtained, naturally occurring geological materials, and mixtures of these materials were tested for combinatorial effects. Despite several technical problems hampering the experimental programme, results were obtained that show several bed materials are catalytically active not only at the gasifier operating conditions, but also during the heating period as the biomass fuel enters the gasifier. From the viewpoint that all of the materials appeared to have an effect on the producer gas composition, none were excluded from further testing in the larger-scale DFB gasifier. A secondary aim of the lab-scale tests was to determine if any of the materials were unsuitable for use in a fluidised bed gasifier based on their physical response to the conditions. The experiments were successful in this regard, identifying potential for agglomeration and elutriation that had been experienced in prior research.

3.2. EXPERIMENTAL AIMS AND JUSTIFICATION

3.2.1. Background of the Experiments

As described in Chapter 1, biomass gasification has been the focus of extensive research as a substitute energy source with the potential to displace fossil fuels in certain applications. Several large scale gasifiers haven been built around the world, all at considerable cost and with varying degrees of success. The scaling of fixed and fluidised bed reactors is well understood, which allow specific areas of the gasification process to be investigated at the laboratory scale.

In Chapter 2, the results of many investigations into the equilibrium composition of producer gas from steam gasification were discussed. The key implication from the literature review is that at the equilibrium conditions, the maximum proportion of hydrogen in biomass gasification producer gas is 50-60% where catalytic bed materials are not utilised. For fuel

cell applications which require a very pure hydrogen fuel gas, the cost of downstream purification operations based on a biomass gasification production system would be prohibitive. To reduce the purification requirement, the gasification reactions can be kinetically enhanced by using the catalytic bed materials to give an increased hydrogen composition exiting the gasifier.

3.2.2. Objectives

The primary aim of the laboratory-scale project was to simulate the DFB gasifier developed in this department. Specifically the objectives for this part of the work are:

- Designing a lab-scale reactor with similar physical properties to the DFB gasifier
- Testing the compatibility of various individual bed materials and combinations of the materials with the hydraulic properties of the reactor at reaction conditions
- Testing the catalytic effects of the bed materials on an ideal producer gas mixture in the reaction environment

Prior research has suggested that some geological compounds are unsuitable for use in high temperature fluidised beds due to their low melting points and subsequent potential for agglomeration. Other materials are too soft to endure long periods in high velocity gas flows without attrition. Additionally some catalytic materials are thought to lose their kinetics-enhancing abilities over time, whether by the physical degradation of the material or by chemical deactivation. Based on these observations, the secondary aims of the experiments are:

- Observing the agglomeration and elutriation effects of the reaction environment on the bed materials
- Determining the catalyst lifetime in the pure gas environment

3.3. EXPERIMENTAL DESIGN AND METHOD

3.3.1. Prior Work

Cusumano gives an excellent description of several types of reactor available to the researcher for lab-scale investigation [Cusumano et. al.., 1978]. Small scale reactors operate predominately in the fixed bed domain either under batch conditions or where gas velocity does not exceed the fluidisation velocity. An exception is the fluidised bed reactor which uses the reactant gas as a fluidising medium. The major restriction of this reactor set-up is the

inability to control residence time in the reactor as an experimental variable, which can be corrected to a certain extent by the addition of a recycle loop. The experiment was not designed to accommodate the input of solid fuel, hence only homogeneous gas-phase reactions are investigated.

3.3.2. System Design

Figure 3.1 gives a schematic of the reactor design. An ideal producer gas mixture is fed to a mixing tee where it is diluted to a measured nitrogen concentration in order to prevent possible ignition. The gas mixture is piped to a dual-column tube furnace where the pipe is coiled through the first tube to preheat the gas to reaction temperature. The gas then enters the base of the reactor and is diffused through a 500µm mesh into the bed material, which is then fluidised. To simulate steam a peristaltic pump injects water into the base of the bed which flashes, generating steam and reacting with the incoming gas. The bed is fluidised to around half the height of the reactor tube (depending on the fluidisability of the bed material) with the remaining height acting as a freeboard. Gas exits the reactor at the top of the column and passes through a water/ice cooler which quenches the gas and condenses out water vapour thus the gas samples can be safely taken from the exhaust tube. The gas is sampled from the exhaust tube. The system was constructed primarily from 316-grade stainless steel to cope with extremes of temperature and sealed Swagelok fittings were used throughout.

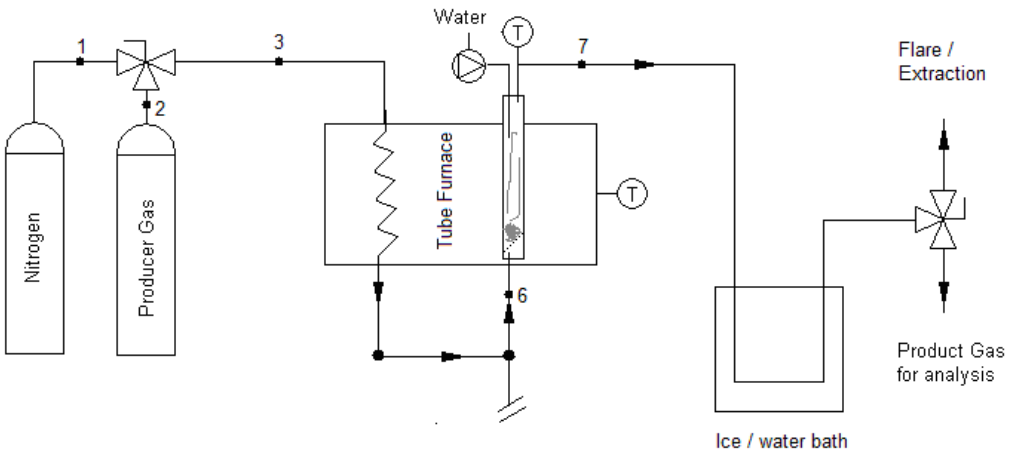

Figure 3.1 – Flow schematic of the laboratory scale reactor used for bed material catalysis testing

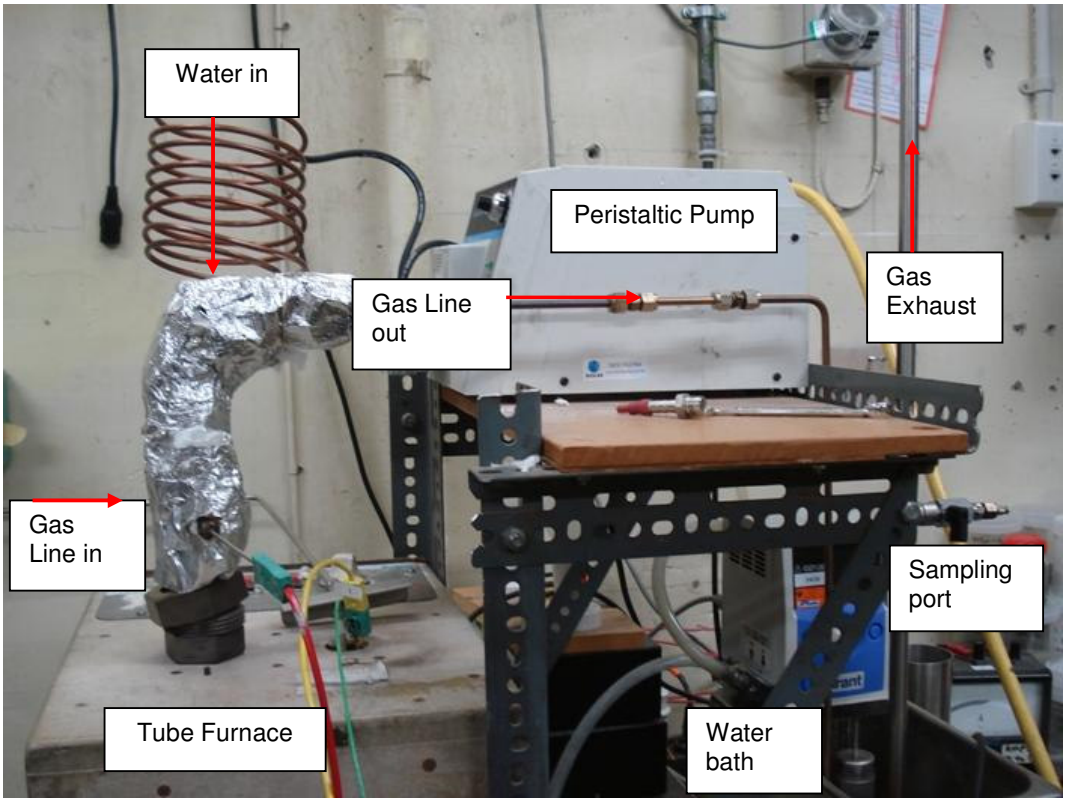

Figure 3.2 – Photograph of the as-built lab scale reactor

3.3.3. Reactor Design and Construction

The reactor itself consisted of two concentric steel tubes, a housing and a reactor tube. The housing was fixed inside the tube furnace and sized to maximum 25mm diameter to present a large surface area to the heating coil and reduce heat losses by convection through the top of the furnace. The gas line was welded into the base of the housing and jetted vertically upwards. The top of the housing was expanded to a 50mm diameter to accommodate a similarly sized mac union arrangement with a 5mm copper gasket which sealed the reactor chamber. The expanded top provided a ledge to seat the reactor tube as shown in Figure 3.3.

The reactor tube diameter was sized to sit flush within the reactor housing to improve heat transfer between the two coils. Its height was slightly shorter than the housing to accommodate a 500µm mesh arranged in a cone. As the mesh cone proved to be prone to developing small cracks where bed material could leak out, this was changed to a half-sphere shape. The mesh acted as a diffuser through which the gas could flow and fluidise the bed material. Temperatures were measured with K-type thermocouples (maximum temperature 1200°C) at the base of the reactor column and at the gas outlet of the reactor for the gas.

Figure 3.3 – Photograph of the dual-column reactor tube showing the expanded top ledge. To the right is the incoming gas line coiling into the second tube furnace for preheating.

The downcomer for the water supply was welded into the centre of the top reactor flange to allow it to drop vertically through the centre of the reactor tube and into the base of the bed. The water flashes within the tube and is forced out by the positive displacement pump through six small, evenly-spaced holes arranged around the base of the downcomer.

To prevent contamination of the gas samples a water cooler and particle trap was installed. The exterior of the producer gas pipe was exposed to air to allow the producer gas to cool prior to water cooling. The pipe entered an expansion chamber consisting of a flat spheroidal chamber, with a steel impact plate in the centre. The gas entering the chamber struck the plate and any entrained particulates dropped out. The gas was forced around the plate into the exhaust tube. The chamber and pipework were immersed in a room-temperature water bath to cool the gas to a manageable temperature, and quench any ongoing reactions.

Figures 3.4 (a) and (b) – Photographs of the gas cooling chamber with steel impact plate mounted (a) and removed (b) to show accumulation of bed material.

The gas was exhausted via vertical 12mm diameter pipe with a three way valve at half-height. For sampling, a 50mL syringe was locked to a receptacle on one leg of the three way valve, and during sampling the valve was slowly switched from the exhaust line to the sample port. The gas pressure allowed the syringe plunger to expand until the required volume was collected, at which point the valve was returned to the exhaust leg, and the sample was isolated before disconnecting from the apparatus. An Agilent 3000C Micro-GC Gas Chromatograph was used to analyse the samples for the concentrations of the key gaseous species.

3.3.4. Bed Materials

A range of commonly available geological minerals were selected for catalyst testing, in line with the aim of identifying low-cost, easily-obtainable materials for potential use in biomass gasification. This was to ensure that the economics of biomass gasification remained favourable [Penniall, 2008]. Calcite was sourced from the Canterbury region, olivine from Otago and magnetite from Taranaki, all in New Zealand. Pure iron oxide and calcium oxide were also tested, and obtained through Merck. Table 3 gives photos and data of the three geological minerals tested.

Table 3.1 – Geological minerals tested using laboratory-scale fluidised bed reactor

			
Common name	Calcite	Olivine	Magnetite
Chemical formula	$CaCO_3$	$(FeMg)_2SiO_4$	Fe_3O_4
Particle size	500µm	500µm	180µm
Bulk density	1360 kg/m³	1760 kg/m³	2400 kg/m³
Mohs hardness	3	6.5	5.5

The 500µm mesh size, while convenient for acting as a diffuser for the fluidising gas stream, was much larger than the pure chemical particle size. A smaller mesh however would have greatly impacted on the efficiency of the fluidisation of the bed. Subsequently while the calcite and olivine required no particle size modification, the magnetite and pure chemicals required some forced agglomeration to allow them to be used in the fluid bed over the 500µm mesh. Pellets were made using a pellet press, whereby approximately 10g of material was compressed at 6000kPa into a solid mass. The pellet was then commuted to an average particle size of less than 1mm. This method also allowed testing of simple combinations of materials.

3.3.5. Gases

As genuine producer gas was unable to be collected from the DFB gasifier due to the complexity and safety issues of collecting and storing flammable gases, two idealised gas mixtures were used in the testing. These mixtures were based on gases originally obtained for calibration of the micro GC analysis equipment, and were modelled on theoretical equilibrium concentrations of the gases.

Table 3.2 – Composition of idealised gas mixtures compared with typical experimental results from the 100 kW DFB gasifier (mol %)

	Gas 1	Gas 2	Gasifier Results
Hydrogen	43.5%	46%	21.2%
Methane	11%	13%	14.2%
Carbon monoxide	11%	13%	36.9%
Carbon dioxide	27.5%	28%	21.5%
Ethene	3.5%	--	5.2%
Ethane	0.5%	--	1.0%

Because of the safety implications of experimenting with a flammable and poisonous gas mixture, the experimental gas stream was diluted up to 50% by volume with nitrogen. This limited the concentration of flammable components to below the lower explosive limit. Care was required in designing the apparatus that no oxygen would be present in the gas stream between the reactor vessel and the water bath, as temperatures in this region were by design in excess of pure gases autoignition temperature.

3.3.6. Method

In each case it was necessary to determine the influence of the catalytic materials on the producer gas composition. Due to the design of the apparatus and fluidisation requirements, many of the typical experimental variables were fixed, so temperature became the independent variable in the analysis. Influence of steam-to-biomass ratio (SBR) was not tested due to the minimum observable flow of the peristaltic water pump being in excess of the producer gas feed, and minimum gas flow through the reactor to fluidise the bed material. Table 3.3 describes the minimum fluidisation requirements in terms of Archimedes number and superficial velocity for the idealised producer gas/nitrogen mixture in the reaction vessel. Appendix E details the calculations performed in determining these parameters.

The minimum water flow applied to the experiments was in excess of stoichiometric requirements. These were calculated by assuming that all of the supplied reactive components (carbon monoxide, methane, ethane and ethane) were reacted either by water-gas shift in the case of carbon monoxide, or steam reforming in the case of the organic compounds.

Table 3.3 – Fluidisation parameters of the five bed material combinations tested with calculated minimum fluidisation velocities and gas flow rates. Assumptions for calculations are listed below.

	Olivine	Magnetite	25% Calcite + 75% Olivine	Calcite	25% Magnetite + 75% Calcite
Particle Size [μm]	500	500	500	500	500
Bulk density [kg/m³]	1760	2400	1660	1360	1620
Minimum fluidisation velocity [m/s][1]	0.12	0.17	0.13	0.14	0.15
Required gas flow rate [mL/s][2]	20.7	28.1	21.2	23.6	25.1

Note:
1 Minimum fluidisation velocity is calculated based on gas density = 0.301 kg/m³ and gas viscosity = 3.56×10^{-5} Pa.s
2 Gas flow rate is calculated based on pipe diameter = 6mm and bubbling fluidisation velocity = 6x min. fluidisation velocity

The apparatus was prepared by charging the reactor column with 30-40g of bed material and mounting it in the tube housing. Gas flow was calibrated by increasing nitrogen flow until bubbling fluidisation was observed in the open column. No producer gas was used until sampling was required. While fluidising the bed, the water inlet tube and top reactor flange were lowered into place and the reactor sealed. Heating commenced and the experiment run timer started.

Initially samples were taken only at temperatures greater than 600°C, which is the lower limit of the operational range of the pilot-scale DFB gasifier. Once the apparatus was heated to 600°C water was introduced by starting the peristaltic water pump and nitrogen flow was halved to accommodate the producer gas flow. The gas pressures were tuned to give a mixed flow equal to that of the initial nitrogen flow which gave bubbling fluidisation. Samples were taken periodically up to a temperature of 700°C. The maximum temperature obtained by the apparatus was 700°C, which is slightly lower than the typical operating temperature of the pilot-scale gasifier of 720°C.

Maintaining operation of the apparatus for long periods of time was restricted by a number of factors. The producer gas mixtures were expensive and in limited supply, hence runs were limited by the amount of gas available. Physically, the apparatus was well equipped to handle

the high temperatures for a short period, but condensation of water in the exhaust tube limited gas flow, as did elutriation of some of the bed materials tested. Soon after reaching maximum temperature this combination of moisture and fine bed material formed a cake around the impact plate in the cooling chamber, limiting the running time. Experimentation was delayed further by various mechanical failures and damage to the quartz furnace tubes from repeated heating and cooling. The system's instability meant further trials were run with producer gas flowing at the start of the run, and samples from these runs were taken at lower temperatures.

3.4. RESULTS

3.4.1. Effects on Relative Gas Concentrations

Testing required the use of different producer gas mixtures. In order to quantify the effects of the bed materials on producer gas, four components were identified and analysed: hydrogen, methane, carbon monoxide and carbon dioxide. These components were selected based on their activity in the water gas shift and steam methane reforming reactions, which are thought to strongly influence the final producer gas composition. As different ideal gas mixtures were used in the tests, the results have been normalised to show changes in component molar concentrations from initial values. Figures 3.5 (a)-(d) below show the relative changes in component concentration across the analysed temperature range for each bed material tested.

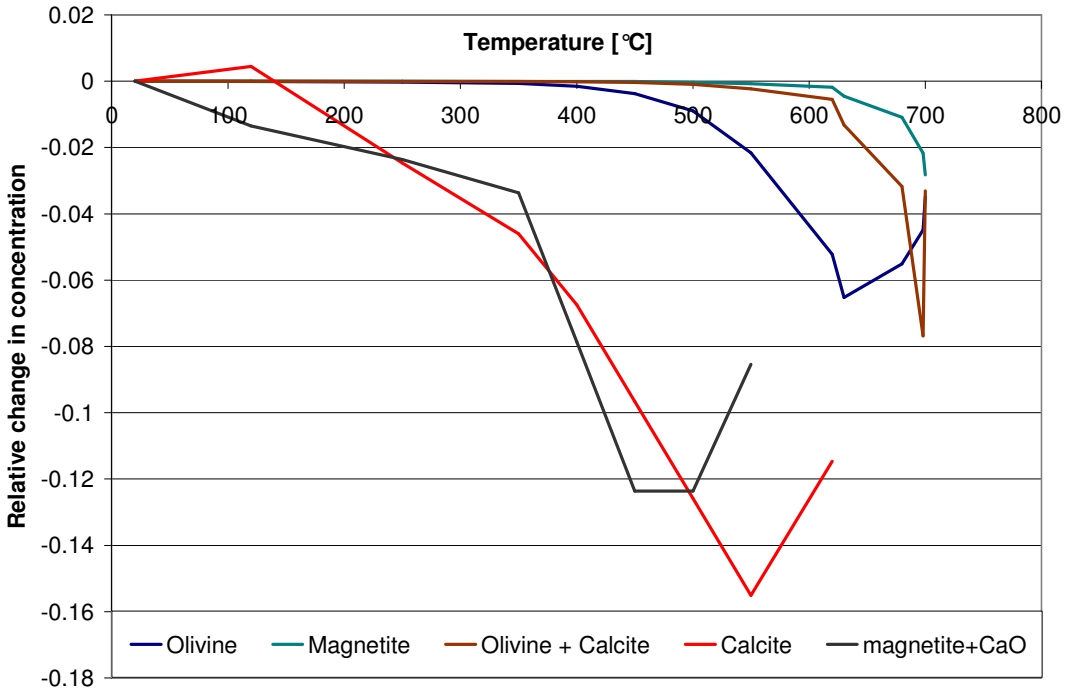

(a) - Hydrogen

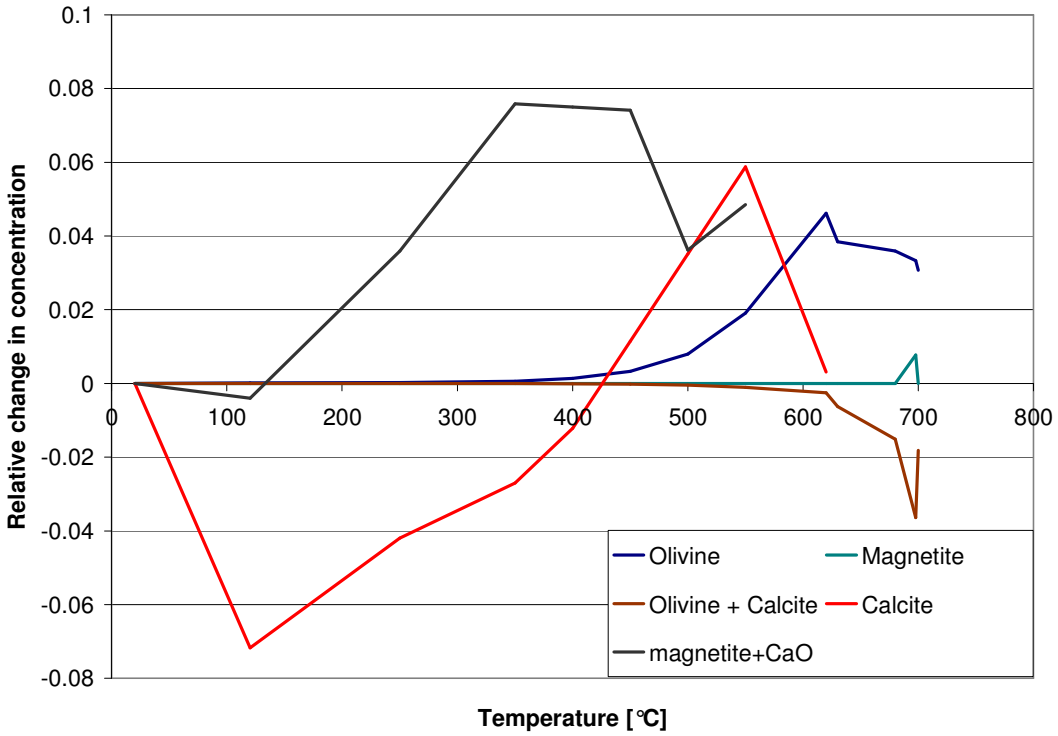

(b) – Methane

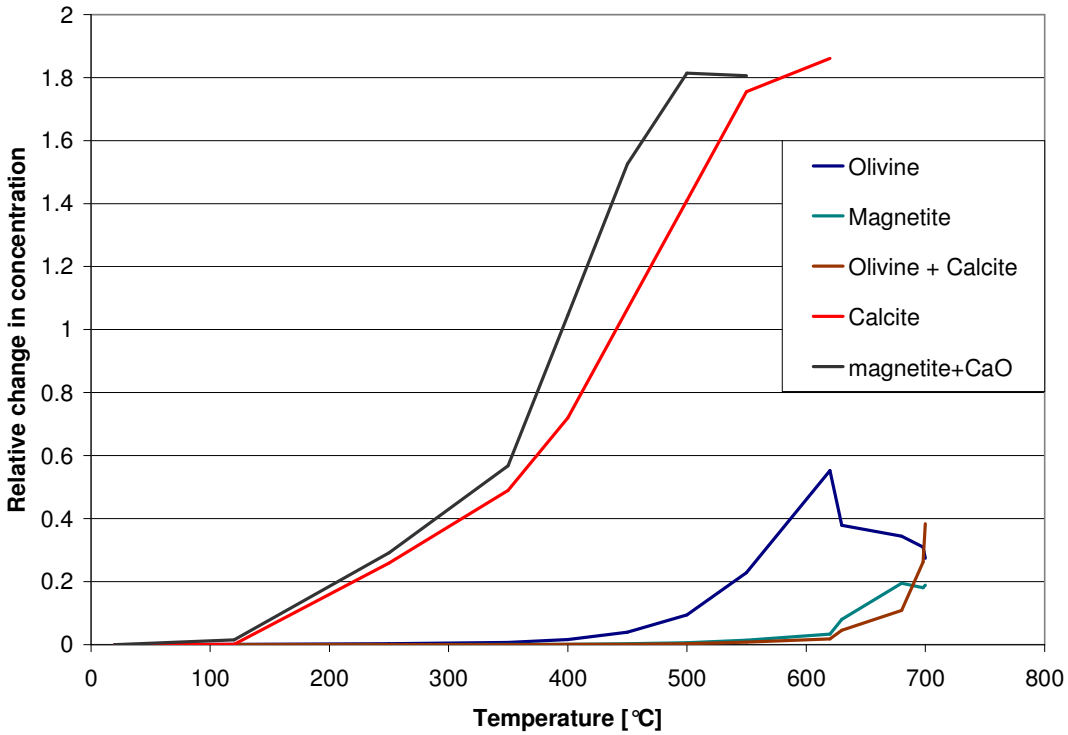

(c) – Carbon monoxide

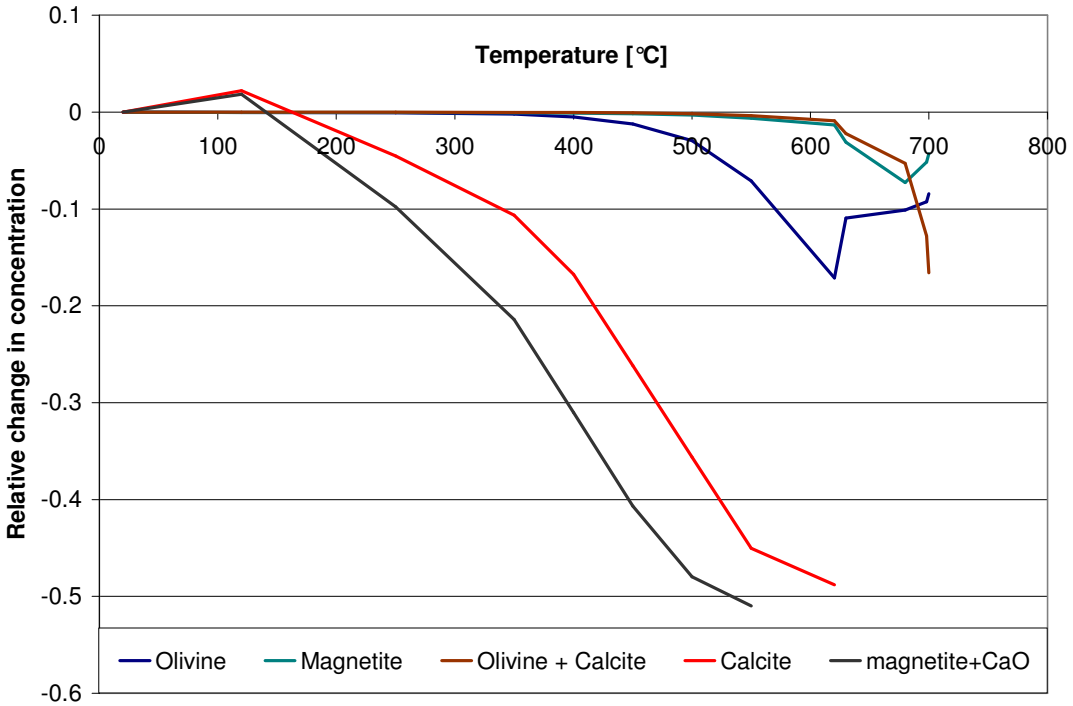

(d) – Carbon dioxide

Figures 3.5 (a) – (d) – Relative changes in concentration (mol %) of four major producer gas components for the five tested bed materials.

A maximum temperature of 700°C was achieved in the trials. While this is less than the typical gasification temperature required for high hydrogen production from biomass gasification, catalysis would effectively lower the temperature at which the homogeneous gas-phase reactions would occur. It was anticipated that in spite of the relatively low temperatures tested, indications of improved reaction activation energies (i.e. lower temperatures) would be present.

The results from Figure 3.5 (a) show that none of the bed materials tested increased the concentration of hydrogen in the producer gas. This indicates that either hydrogen is being consumed by low temperature reactions such as the reverse water gas shift reaction, or the quantity of the other components increases over the course of the trial, perhaps by devolatilisation of some bed material components. While concentration changes of methane are relatively minor, suggesting a lack of methane reforming or methanation reactions, carbon oxide levels change significantly. As no free (gaseous) oxygen was present in the reaction chamber during the experiments it is unlikely that carbon oxides were formed as a result of combustion reactions.

Of the bed materials tested, calcite (calcium carbonate, $CaCO_3$) and the calcium oxide/magnetite mixture were shown to have the greatest effects on the four components analysed. Figure 3.6 below shows the relative composition changes of hydrogen, methane, carbon monoxide and carbon dioxide for the two materials tested, with solid lines representing the calcite tests and dashed lines representing the calcium oxide/magnetite tests. In general the main effect of the magnetite was to lower the temperatures at which the relevant reactions occurred, resulting in component composition changes more quickly. In a continuous process, this would suggest a quicker reaction rate and more product formation under the appropriate conditions.

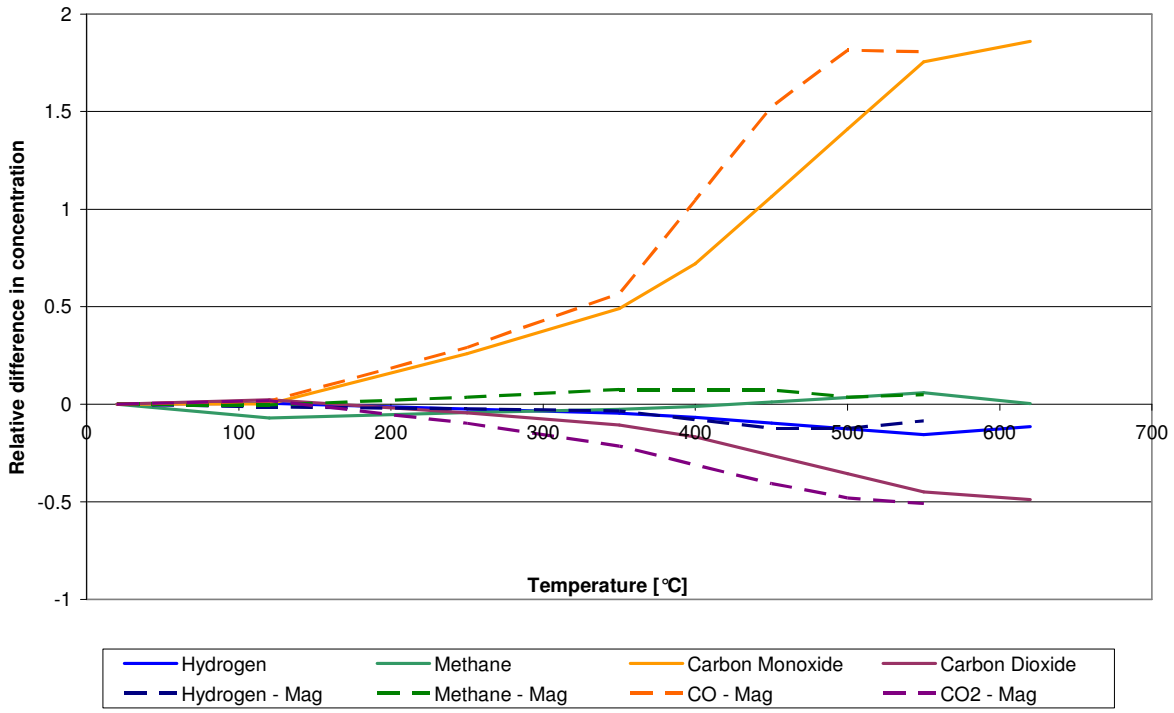

Figure 3.6 - Relative changes in molar composition of hydrogen, methane, carbon monoxide and carbon dioxide in calcite and Ca/Fe Oxide bed materials. Labels appended with '- Mag' signify the latter tests.

3.4.2. Effects on Bed Materials

A secondary aim of the initial laboratory-scale tests was to establish the potential for the bed materials selected to agglomerate or elutriate under fluid-bed gasification conditions. The agglomeration process was thought to depend on the presence of alkali metals and alkali earth elements, usually present in biomass ash. Prior work on the 100 kW DFB gasifier has shown that greywacke and olivine sands can agglomerate under certain gasification conditions, usually when insufficient fluidisation leads to extreme localised heating. It was unknown

whether alkali components were present at the time of agglomeration. At the conclusion of the laboratory scale tests the recovered bed material was examined visually for signs of agglomeration.

Figure 3.7 - Photograph of agglomerated bed material extracted from the 100 kW DFB gasifier following an experimental run.

During normal runs in the 100 kW DFB gasifier particle elutriation was not generally observed. It was expected however that due to the relative softness of calcite, some of the calcite samples tested would be worn down. It was unknown whether the smaller particles resulting from the elutriation would remain in the bed and perhaps contribute to agglomeration, or be carried out with the gas stream.

Initial commissioning trials with the lab-scale apparatus using greywacke sand showed little agglomeration or elutriation of the bed material. Table 3.hh below gives the greywacke bed material weights before and after trials, and any observations noted on recovery of the material. Some losses due to imperfect screening of the bed material to >500μm were expected. Results from the commissioning trials indicated that greywacke was a robust sand for fluid-bed gasification, and no agglomeration was observed in the test temperature range below 700°C.

Table 3.4 - Greywacke bed material sample weights before and after fluidisation/gasification trials

Trial	Initial weight [g]	Final weight [g]	Comments
Commissioning 1	20.0	16.3	Fluidisation trial, losses due to spill-over from unsealed column
Commissioning 2	20.2	20.0	Sealed column, losses due to imperfect BM screening prior to test
Commissioning 3	30.0	29.6	As above

Olivine and magnetite similarly gave little indication of particle wear over the course of the experiments, which typically lasted between 100 and 120 minutes. Some small agglomeration of olivine particles was observed in some trials, where small clumps of olivine grains lightly fused together. Given that these particles were easily were broken up (manually, following the run) it was deemed likely that the mechanism causing this agglomeration was similar to that in the larger-scale gasifier. Based on the experience of running the small-scale apparatus, it is thought this mechanism is dependent on localised heating at the base of the bed, with a relatively high concentration of steam present.

Tests using calcite and calcium oxide bed materials are described together in terms of physical properties as, in the presence of carbon dioxide, an equilibrium is established between the two compounds, in spite of the original form of the bed material. These two materials exhibited significant elutriation over the course of the run, in many cases limiting runtime and fouling the equipment, as shown in Figure 3.8.

Figure 3.8 - Photograph showing interior of water bath contacting chamber fouled with calcium compound.

3.5. DISCUSSION OF SMALL-SCALE EXPERIMENTS

3.5.1. The Reverse Water Gas Shift

The experimental results from the lab-scale apparatus indicate bed materials, even common minerals, can have a significant effect on producer gas composition. Despite this, the expected increase in hydrogen composition with temperature did not eventuate; conversely, hydrogen production decreased up to 16% over the temperature profile. Carbon dioxide concentrations also decreased significantly, but carbon monoxide increased almost two-fold. This set of circumstances is best explained by catalysis of the reverse water gas shift reaction. Increasing temperature appears to increase the extent of the reaction which correlates with the endothermic nature of the reaction. However, based on the curve of hydrogen composition with temperature the reverse water-gas shift appears to peak around 600°C. For large-scale gasifier experiments this should represent the minimum gasification temperature.

Magnetite and calcite minerals have the greatest effect on this reaction, although the 25% calcite present in the olivine-calcite mixture showed that the calcite was not sufficient to significantly affect the reaction. Magnetite alone had little effect, but appeared to shift the reaction temperature forward. This was demonstrated clearly in Figure 3.6 above.

3.5.2. Steam Reforming of Methane

Prior to the experiments it was suggested that iron would act as a catalyst for steam reforming of methane. The steam reforming reaction (R-2.6) is highly endothermic and so is expected to have greater extent at high temperatures. Analysis of the results indicated that methane concentration varied ±8% from initial concentration (approximately ±0.8% of total producer gas content) and that all three minerals tested had an effect on methane yield. Calcite apparently had a negative effect on methane yield at low temperatures, but methane concentration increased with temperature between 100°C and 550°C. Beyond 550°C methane concentration began dropping off rapidly, perhaps indicating the beginning of the steam reforming reaction. As with the reverse water-gas shift, magnetite was shown to reduce the temperature at which this effect occurred. Olivine was also shown to increase methane concentration slightly up to around 600°C, whereby the concentration began to drop. Again, this suggests that large scale gasification should be conducted at temperatures greater than 600°C.

3.5.3. Reactor Design

Overall the small-scale reactor was able to adequately perform its primary objective, to test small quantities of bed materials for their catalytic ability. The design was well verified and used by numerous authors [Raju et. al., 2009; di Felice et. al., 2009; Wiltowski et. al., 2008], although commonly the catalyst is tested as a fixed bed. As a fluidised bed reactor, the gas flow required to maintain fluidisation limits the residence time of gas in the reactor. At minimum gas flow rate for all of the bed materials trialled, gas residence time is 3.7s. Since the gasification reactions on the whole are slow, maximising residence times is important to obtain maximum yield. As discussed previously, reaction times greater than 160s are recommended for gasification reactions. In a dual fluidised bed gasifier, residence times are maximised by the constant recirculation of the fuel through the gasification reactor.

3.5.4. Reactor Performance

Reactor operation and results measurement were plagued by many difficulties. Temperature control and measurement were hindered by use of thermocouple probes approximately 3mm in diameter, or 15% reactor column diameter. It has been shown in previous works that thermocouple size relative to reactor size influences temperature measurement, and it has

been recommended that thermocouples used should have been of the thin-wire type to eliminate errors in measurement caused by proximity to the reactor walls [Saw, 2009].

Fluidising gas was supplied by two gas bottles with independent flow measurement and valve control. Initially experimental procedure was implemented for low-flow nitrogen during heat up to fluidise the bed and ensure no hot spots formed in the reactor which could lead to bed material agglomeration. However, due to density changes gas flow progressively dropped over the course of heating up to the point where is was difficult to estimate whether the initial flow was maintained. Changing over to a 50%/50% nitrogen/producer gas mixture while at high temperature was also difficult for this reason. As initial gas concentrations were measured without water added, changes in composition were independent of gas flow rate, but gas residence time could not be accurately verified.

3.6. CONCLUSIONS

In general the laboratory-scale experiments were able to overcome significant technical difficulties to yield limited results. Calcite and calcium-containing compounds were shown to have significant effect on the composition of a typical producer gas mixture when reacted with steam at high temperature, as compared to olivine sand which showed less of an effect. The addition of iron-containing compounds was shown to slightly lower the temperature at which the water-gas shift and steam methane reforming reactions occurred. Olivine sand tended to agglomerate to a small degree at gasification conditions, a result that agreed with prior observations from tests in the 100 kW DFB gasifier.

The results from this testing showed that combination of minerals in the bed material can positively influence producer gas composition to a greater extent than would otherwise have occurred by testing single minerals alone. This suggests that experiments on the 100 kW DFB gasifier should include analysis of mixed-mineral bed materials in an effort to promote as many of the hydrogen producing reactions as possible, to the optimal extent. Also, as the effects of the various minerals on the heterogeneous reactions were not tested, applying the minerals to the 100 kW DFB gasifier will provide a greater knowledge of their effects overall.

4. Gasifier Experiments: Bed Material Tests and Results

4.1. BACKGROUND

While thermal gasification technology has been applied in various forms for 200 years, biomass gasification in fluidised beds is a relatively recent conjunction of the two technologies of gasification and material fluidisation. As discussed earlier in this thesis, initial gasification processes were generally operated in fixed bed reactors. The application of fluid bed reactors to the gasification and other thermal processes allowed more uniform heat transfer at higher rates, resulting in more consistent producer gas quality. When applied to gasification however, single bed designs either produced a low calorific value producer gas from air gasification, or required expensive oxygen separation plant for a pure oxygen-blown gasifier. The development of the dual fluidised bed design improves the gasification process, generating a medium calorific value producer gas without the pure oxygen requirement.

4.1.1. Overview of the University of Canterbury BIGCC and BEFL programmes

In 2004, the Department of Chemical and Process Engineering at the University of Canterbury began research on a Biomass Integrated Gasification - Combined Cycle (BIGCC) process for conversion of unused wood wastes to energy. The programme consisted of four distinct objectives [Pang, 2008]:

Objective 1:	Evaluation of BIGCC technologies developed overseas
Objective 2:	Transfer and development of BIGCC system to suit NZ conditions
Objective 3:	Modelling of feedstock supply and energy demand
Objective 4:	Design and modelling of BIGCC systems

The first objective identified the dual fluidised bed gasification method being developed by Technical University of Vienna in Austria ('TU Wien', 'TUV') as being most suitable for application to New Zealand's biomass availability. The Austrian development consisted of a 100 kW scale test bed, installed at TUV. This design was later scaled-up to 8 MW size and used for a combined heat and power application in the town of Güssing in south east Austria. This installation has been operating successfully since 2002 [Pfeifer, 2008].

The gasifier technology demonstrated on the 100 kW input scale reactor was transferred back to New Zealand and under Objective 2, a similar system was designed and built at the

University of Canterbury. The gasifier has been commissioned and operating at the Department of Chemical and Process Engineering since 2005.

In 2008 the BIGCC programme ended, with several important developments completed. The gasifier design was validated and shown to be effective at converting wood fuel to a medium calorific value gas [Brown, 2006; Bull, 2008]. A chemical equilibrium model was developed which with subsequent modification was able to predict to reasonable accuracy the producer gas yield and composition [Rutherford, 2006; Penniall, 2008]. Various economic models showed however that the gasifier operating in its present state would fail to be feasible in many of the industries proposed for its use. Further development was required to improve gasifier efficiency and to increase the plant scale.

While the combined heat and power application of gasification technology is a suitable end goal, high process efficiency requires a low-grade heat sink. In Austria, such a sink is provided by the district heating schemes typically found in European towns, however, no such end use exists in New Zealand. Several other options exist for utilisation of the producer gas. With high hydrogen and carbon monoxide concentrations, the producer gas is ideal for the downstream production of liquid fuels and hydrogen from renewable resources. Currently syngas is generated primarily by the gasification of coal and the steam reforming of methane, both of which are fossil-fuel consuming and environmentally unsustainable. The use of syngas generated from biomass gasification would reinvigorate these processes in today's environmentally-conscious age. With the rising cost of liquid fuels, synthetic transport fuels produced from the Fischer-Tropsch and Mobil processes are becoming more attractive. As discussed previously, use of hydrogen as an energy carrier for both stationary and automotive power generation is a future option for replacement of the status quo. Thus, in 2008 the Biomass to Energy and Liquid Fuels (BEFL) programme was instituted at the Department to investigate biomass gasification as a suitable production process for hydrogen and liquid fuels.

4.1.2. Gasifier Design and Operation

The Chemical and Process Engineering Department's gasifier is built based on a Dual Fluidised Bed design, with independent fluidised beds for combustion and gasification, as shown in Figure 4.1 below. In addition to the description given below, other excellent descriptions of the gasifier's design and construction can be found in Brown [Brown, 2006] and Bull [Bull, 2008].

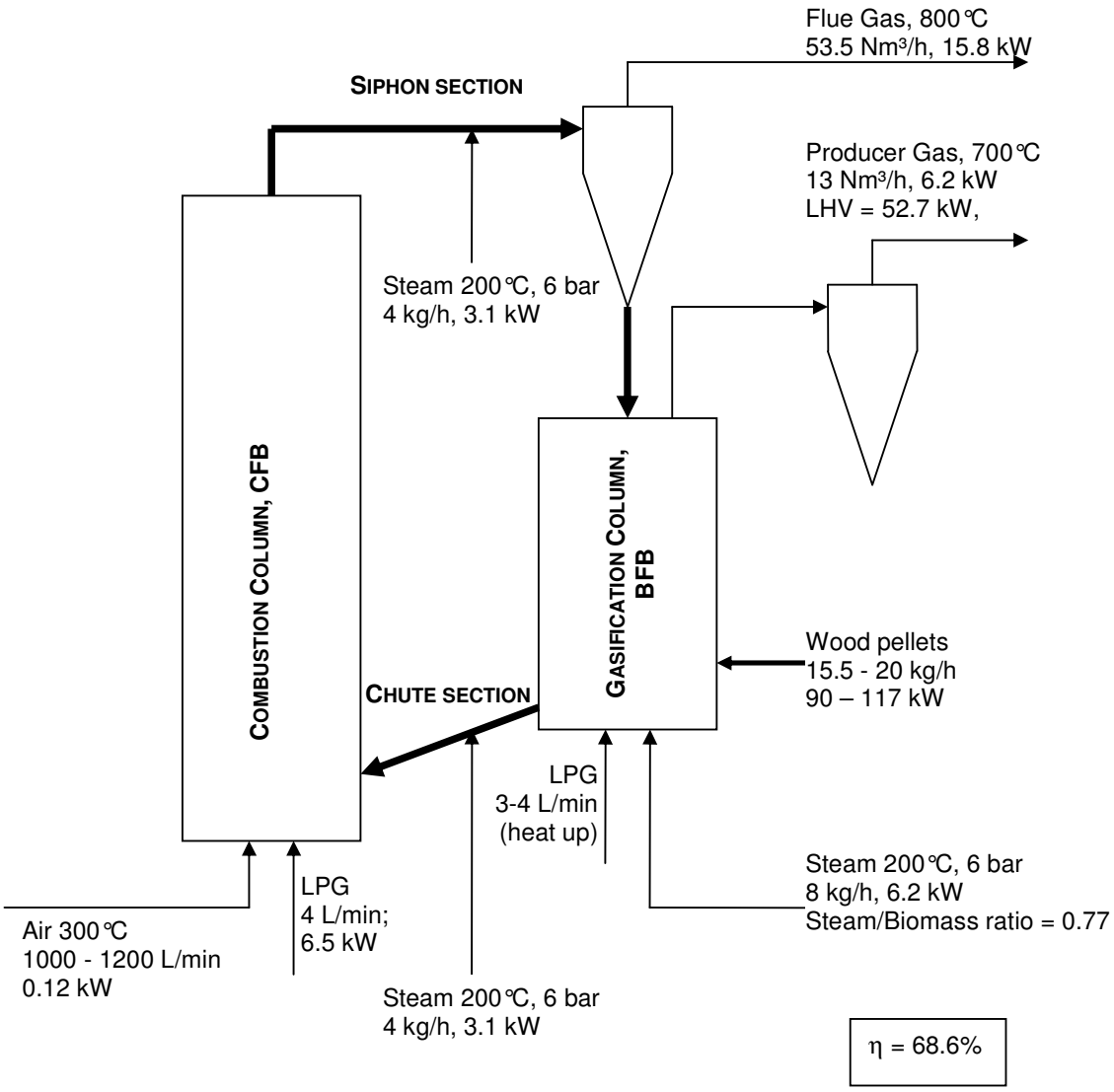

Figure 4.1 - Schematic diagram for CAPE Dual Fluidised Bed gasifier

The gasifier is constructed using refractory material for the columns, afterburner and chute and 253 MA grade stainless steel for the cyclones and siphon section. The 253 steel was chosen due to its high thermal capability, being rated to a temperature of 1200°C. Air is supplied to the gasifier from a 50 HP Rootes blower and air compressor, and steam from the departmental boiler. LPG is piped from an LPG bottle store at 1 bar gauge pressure. Pressure measurements from the CFB and BFB reactors and siphon using electronic transducers and K-type thermocouples (max reading 1200°C) are situated throughout the reactors and ancillary components.

The dual fluidised bed design allows gasification of biomass using steam, which is an endothermic process according to reaction R-2.1 below.

$$CH_xO_y + (1 - y)H_2O \rightarrow CO + (1 - y + ½x)H_2 \qquad \text{R-2.1}$$

In the experiments, the reactor must be preheated to 770°C in the start-up phase of operation to achieve gasification. At start-up, air is introduced to the CFB and BFB columns at 1000–1100 L/min and 80-100 L/min respectively, in order to fluidise between 12 and 15 kg of bed material in the appropriate fluidisation régime. The lower BFB fluidising rate represents a bubbling fluidised bed velocity, while the high CFB fluidising rate allows the bed material to be pneumatically transferred to the BFB, and circulate through the system. Fluidising air is also injected into the chute and siphon transition regions to maintain bed material circulation. LPG is fed to the CFB at 40 L/min and to the BFB at 4 L/min, heating the bed material and reactor.

Typically the start-up period lasts 4-5 hours, during which time bed material circulation, temperatures and reactor oxygen content are monitored in order to minimise the likelihood of 'hot spots' developing within the reactor which could lead to bed material agglomeration. LPG injection is gradually increased in small proportions to maximum levels once circulation is observed to be consistent, usually between 30 and 45 minutes into the run. Heat-up is generally constant once circulation and LPG flows are stable, with a slight increase in heating rate usually observed around 650°C. The reason for this is unknown, and will be investigated in future studies.

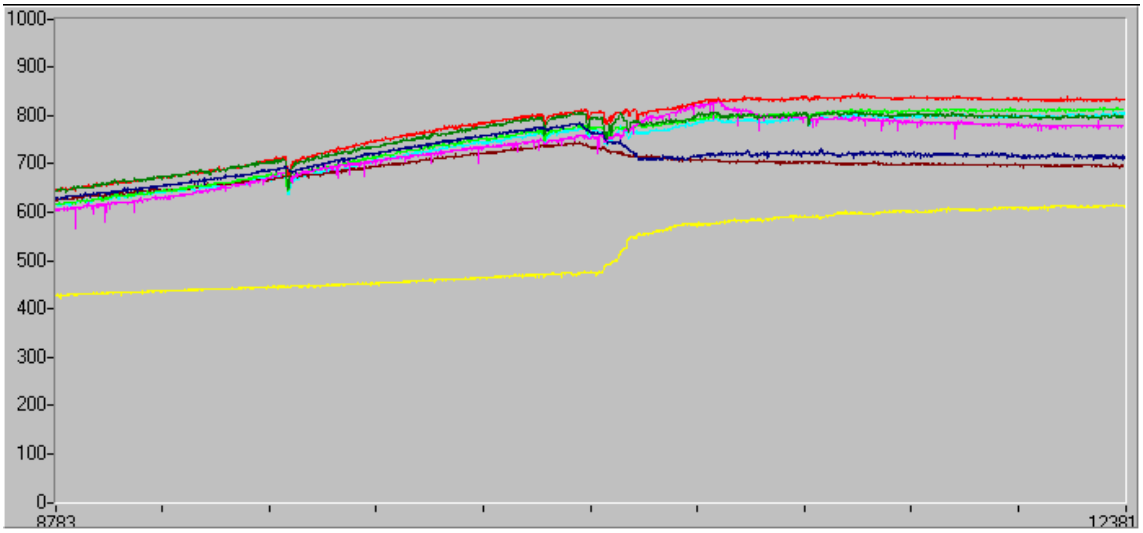

Figure 4.2 – Start-up temperature profile showing initialisation and ramping up around 650°C

At a reactor temperature of 770°C or higher, the fluidising air to the bubbling fluidised bed (BFB) gasification column is switched to steam and wood feed is started, usually with an accompanying change in pitch in the afterburner and reactor temperature drop of around 50°C. Steam is applied to the BFB at around 8 kg/h. *Pinus radiata* pellets are fed to the BFB, entering 300mm from the base of the gasification column, where it devolatilises and begins endothermic gasification reactions. The fuel mixes intimately with the bed material in the gasifier, and having undergone gasification the residual char travels pneumatically with the bed material through the chute section to the circulating fluidised bed (CFB) combustion column, where it is oxidised, releasing heat to the circulating bed material. After combustion, the remaining char and ashes are carried up with the heated bed material by the flue gas through the full height of the CFB, where the solid particles are separated from the flue gas. Finally the bed material and ash are transferred pneumatically to the BFB to complete the cycle. Pneumatic seals are formed at the chute and siphon connections between the two columns, allowing for independent operation and separation of producer gas from flue gas. Maintaining these gas seals through applying minimum effective fluidisation steam is critical to the efficient operation of the gasifier. Without these seals being maintained, flue gas is able to travel against the flow of bed material through the chute or out of the siphon, diluting the producer gas with flue gas and defeating the primary advantage of the dual fluidised bed design.

Steady-state operation of the gasifier is maintained with careful control of LPG flow to the combustion column during gasification. At the start of gasifying, the LPG flow rate is reduced to around 20-25 L/min to maintain reactor temperatures and ensure that sufficient heat is being supplied to fuel the endothermic gasification reactions. Over the period of operation a quantity of char builds up in the system, which gradually displaces the need to supplement heating with LPG. Depending on the extent of the gasification reactions, steady-state operation typically requires supplementary firing with 4-20 L/min of LPG. Normal biomass gasifier operations are usually limited to around four hours of gasifying due to a number of factors, such as bed material elutriation or agglomeration, discussed further in Chapter 6. During that four hour period, steady-state operation is usually reached and a number of gas samples are taken, as described in §4.1.4. The samples are taken around the same time as a complete set of gasifier operating parameters are logged. These parameters include temperatures from 19 locations, CFB and BFB column pressures, air flows to the CFB and steam flows to the BFB as well as to the chute and siphon, along with other ancillary measurements.

Shutdown is initiated by cutting fuel flow to the gasifier and allowing the residual char circulating in the system to burn out for 15-20 minutes. After that time fluidisation is stopped and the system is allowed to cool for 24 to 36 hours prior to dismantling the gasifier and examining the bed material and char particle residues. This requires removing the CFB and BFB gas distributor sections which are bolted onto the bases of the reactor columns, sieving out the remaining char particles from the bed material and weighing the bed material to determine losses from the run. For a typical greywacke or olivine sand 25%-30% of the bed material can be lost through bed material attrition, resulting in some of the smaller particles escaping via the flue gas and producer gas streams. Most of these particles are entrained by the BFB cyclone separator and CFB particle trap. For softer bed materials such as calcite and dolomite, almost all the bed material is lost due to the rapid attrition and elutriation of the mineral particles in the system.

4.1.3. Biomass Feedstock

Pinus radiata pellets are used as the fuel for the gasifier. The pellets are formed by compression of pine sawdust through a ring-die pelletiser, and are typically 5mm in diameter and 10-20mm in length. Pine pellets are used because they are readily available and are of consistent quality and moisture content, which cannot be achieved with other wood waste feed stocks such as unpelletised sawdust or wood chips. The consistent fuel quality allows accurate experimental investigation of the process without considering fuel quality as a variable. The ultimate analysis for the wood pellets is provided in Appendix A. Table 4.1 below gives the wood pellet's proximate analysis.

Table 4.1 – Proximate analysis of wood pellet fuel used, on as received and dry bases.

Item	Method		As rec'd	Dry
Moisture	ISO 5068	%	8.0	--
Ash	ASTM D1102	%	0.4	0.4
Volatiles	ISO 562	%	77.4	84.1
Fixed Carbon	By difference	%	14.2	15.4
Gross Calorific Value	ISO 1928	MJ/kg	18.63	20.25
Carbon	micro analytical	%	47.2	51.3
Hydrogen	micro analytical	%	5.35	5.81
Nitrogen	micro analytical	%	<0.2	<0.2
Sulfur	ASTM D4239	%	0.01	0.01
Oxygen	By difference	%	38.7	42.4

4.1.4. Gas Sampling Method

The sampling method is a combination of two syringes and a tar trapping column that concurrently extract a 50mL sample of producer gas and tar. It is an unmodified method developed by Bull [Bull, 2008] in reaction to the unsuitability of the on-line gas chromatography system for analysing producer gas samples. Prior to use of the current sampling procedure, on-line gas chromatography was used to sample producer gas. This was prone to error due to the long length of sampling tube from the producer gas sampling port at the gasifier to the analysing instrument, a micro GC. It was decided that manual acquisition of a producer gas sample using a double-syringe device would provide more accurate readings of producer gas composition for a specific set of gasifier operating conditions.

Producer gas samples are extracted in two 50mL aliquots through a 3mL Bakerbond amino normal phase SPE column, which traps the tar components in the producer gas for later extraction and analysis. The first 50mL aliquot is extracted from the producer gas line and injected into a 50mL plastic sample syringe to condition the syringe, then expelled. The second 50mL aliquot is extracted the same way and stored in the sample syringe, which is then sealed, removed from the sampling device and transported to the GC for analysis. Figure 4.3 below shows the gas sampling device and its important components.

An Agilent 3000C micro gas chromatograph (‘Micro GC’) is used for the gas sample analysis. Using a specified mixture of producer gas components as a calibration standard, the Micro GC is calibrated to analyse the components in Table 4.2 below. In addition to the eight major producer gas components, helium is also analysed. The injection of a known flow of helium into the producer gas stream and subsequent analysis of helium concentration in the producer gas allows the determination of producer gas flow rate.

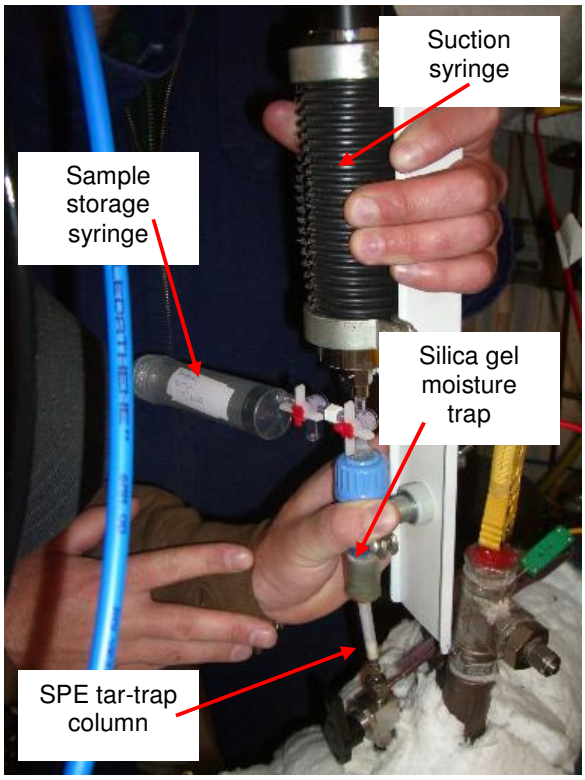

Figure 4.3 - Manual producer gas sampling device. Indicated are the suction syringe used for drawing the gas sample, the sample storage syringe, the silica gel moisture trap and the SPE tar-trap column

Table 4.2 – Micro GC calibration gas mixture and composition

Component	Concentration
Helium	1.0%
Hydrogen	24.5%
Oxygen	--
Nitrogen	3.0%
Methane	13.1%
Carbon Monoxide	7.3%
Carbon Dioxide	19.1%
Ethene	4.0%
Ethane	1.0%

4.2. EXPERIMENTAL JUSTIFICATION AND AIMS

4.2.1. Prior Research

As discussed in Chapter 2, many authors worldwide have investigated the effects of different be materials on producer gas composition. In general the research has focussed on tar

reduction, increasing hydrogen production and improving carbon conversion efficiency. Many of the materials tested in literature studies are geologically rare minerals in New Zealand, such as nickel compounds, or are manufactured catalysts based on noble metals. Both of these med material groups have been discounted for this research in the interest of maintaining the economic feasibility of the introduction of gasification technology in New Zealand. Additionally, few researchers have investigated the feasibility of simple mixtures of dissimilar minerals being used together as bed material. Therefore all bed materials tested in this research were easily available to the author, and were environmentally benign.

4.2.2. Objectives of the Experiments

The results of the bed material tests will be evaluated with regard to a three-tier analysis, based on the overall objectives of the BIGCC and BEFL projects discussed above. The primary objective is investigating the ability of the bed materials to improve the hydrogen yield from biomass gasification, for the purposes of using the hydrogen either as a commercial raw material or in fuel cell technology. Necessarily the extraordinarily high purity hydrogen required for these applications represents the highest level of downstream processing difficulty, and the maximum extent to which the catalyst can be effective. This objective can be analysed in two parts, firstly by hydrogen composition as much of the difficulty with hydrogen purification is removing the other components from the gas, and secondly in terms of hydrogen yield, as it makes little economic sense to intensify hydrogen concentration at the expense of limiting the amount of hydrogen produced overall.

The secondary objective of this project is to improve the producer gas quality sufficiently for use as a syngas for liquid fuel production. This is supplementary to the first objective in that it represents a (slightly) lower standard of producer gas quality than that required for pure hydrogen production. The main requirement for syngas utilisation for Fischer-Tropsch or Mobil synthesis of liquid fuels is a 2:1 ratio of hydrogen to carbon monoxide. Using the Fischer-Tropsch process, synthetic long-chain hydrocarbons may be formed by reaction 4.1 below.

$$2nH_2 + nCO \rightarrow (-CH_2-)_n + nH_2O \qquad \text{R-4.1}$$

Prior to this research the typical gas composition of producer gas exiting the gasifier was 20-25% hydrogen and 35-40% carbon monoxide, almost the inverse of the required composition

for liquid fuels synthesis. The most direct method of improving gas composition to generate more hydrogen and less carbon monoxide is catalysing the water gas shift reaction, and shifting the equilibrium to the right to increase hydrogen and carbon dioxide. Alternatively, catalysing the steam reforming of methane and higher hydrocarbons will increase hydrogen content, without reducing carbon monoxide yield.

Thirdly, a fundamental goal of the project is to improve the overall energy efficiency of the process. Previously the University of Canterbury gasifier operated with a cold gas efficiency of approximately 35% mainly due to poor producer gas yield, high auxiliary fuel usage and limited opportunity for process heat recovery. It was anticipated that higher gas yields and efficiencies could be achieved through the use of catalytic bed materials, particularly materials that positively influence the gasification reactions and improve fuel conversion. It was also likely that increased experience in operating the gasifier would reveal changes to operating conditions that would improve the process yields. The results of this objective not associated with use of specific bed materials are given in Chapter 5, while modifications and other improvements that have been made to enhance gasifier operation are discussed in Chapter 6.

Finally, an ancillary objective of trialling different bed materials was reducing tar yield in the producer gas. All downstream processes require minimisation of tars whether they have rigorous gas quality requirements, or simply to reduce maintenance of downstream equipment. The original incentive for investigating the catalytic effects of various bed materials on biomass gasification was the potential to reduce tar loading, as demonstrated by comparisons of olivine and nickel oxide-doped olivine at the Technical University of Wein (TUV) [Pfeifer, no date]. Despite no firm quantitative method being developed for tar analysis, it is hoped that the experimental investigation would at least contribute to the overall understanding of the tar reduction process.

4.3. Experimental Materials and Conditions

4.3.1. Bed Material Selection

Selection of the bed materials to be tested in the gasifier was based on availability, physical parameters and the experiences of prior researchers as discussed in Chapter 2, as well as the results of testing in the small-scale fluid bed reactor as described in Chapter 3. The successful

gasification runs and the bed materials that were tested on each run are detailed in Table 4.3 below.

Table 4.3 – Gasifier run dates and bed material combinations analysed.

Date	Greywacke	Olivine	Magnetite	Calcite	Dolomite
25/9/08	100%				
20/1/09	100%				
03/2/09		100%			
16/2/09		100%			
02/3/09		75%		25%	
13/3/09		50%		50%	
19/3/09 – 05/5/09: Five biosolids runs (discussed in Chapter 5)					
29/5/09		50%		50%	
26/6/09		50%		50%	
24/7/09	50%				50%
31/7/09	75%				25%
14/8/09[1]	75% 60%		25% 20%		 20%
28/8/09	75% 60% 50%		25% 40% 33%	 17%	

Note:

1 After this date, modifications to the gasifier allowed addition of bed material in-run, so many combinations were able to be tested each run.

Physical suitability was an important consideration in gasifier material selection, especially with regard to fluidisability. The gasifier operates with relatively constant fluid flows based on using superficial velocities as design criteria. Superficial velocity is defined as the velocity of the fluid through the empty column. Together with particle diameter and density, these flows determine the fluidising régime for the two columns which can be calculated from Archimedes number. Geldart [Geldart, 1986] identified four specific particle groups that exhibited certain fluidisation behaviours. The four Geldart Groups are discussed below and represented diagrammatically in Figure 4.4.

Group A: Particle diameter = 20 – 100 μm; particle density up to 1400 kg/m³. Prior to the initiation of a bubbling bed phase, a bed of these particles will expand by a factor of 2 to 3 at incipient fluidization, due to a decreased bulk density.

Group B: Particle diameter = 40 – 500 μm; density between 1400 – 4500 kg/m³. Particles (such as sands) enter the bubbling fluidisation régime at incipient fluidisation.

Group C: Particle diameter = 20 – 30 μm; Particles are like fine powders and are very difficult to fluidise due to strong cohesive forces.

Group D: Particle diameter > 600 μm; high particle densities. Such particles require high fluid energies for fluidisation normally resulting in high abrasion and spouting régime fluidisation.

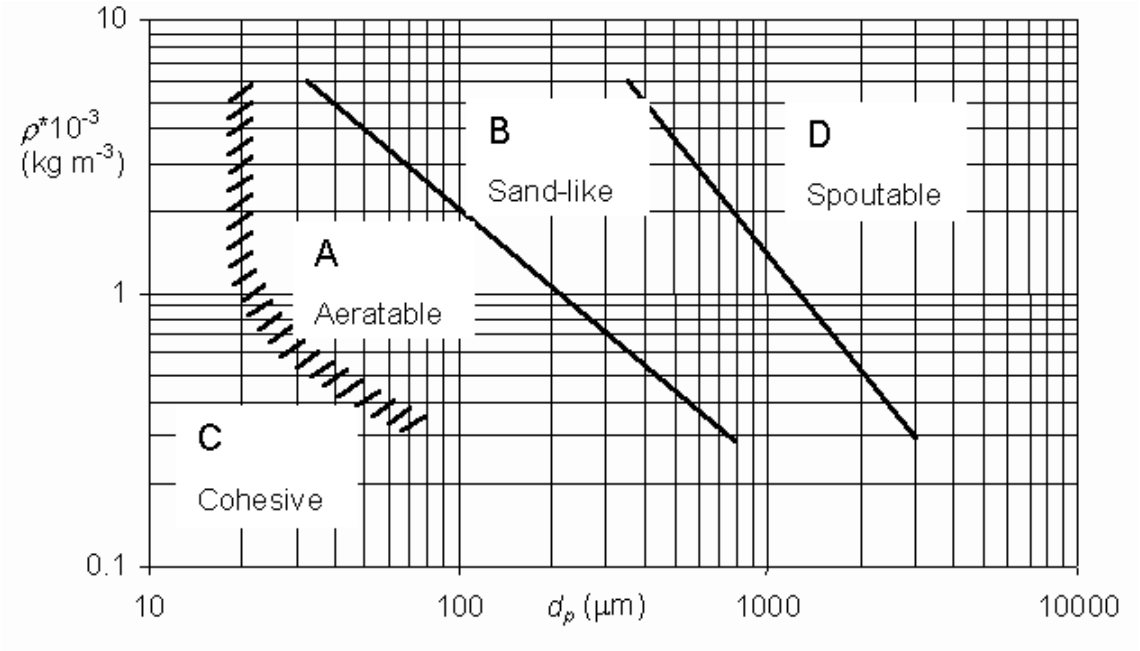

Figure 4.4 – Geldart groups displayed on chart of particle density vs. diameter

While greywacke, olivine and magnetite bed materials sit comfortably in the Geldart Group B range, calcite and dolomite are classified as Group D particles. The fluidisability of the particles are extensively analysed in §6.4.1. The particle size distributions for each of the bed materials are given in Figure 4.5 below. Other parameters affecting material suitability for the gasifier included hardness, or resistance to attrition and elutriation. Little testing of particle attrition potential was completed prior to gasifier operation.

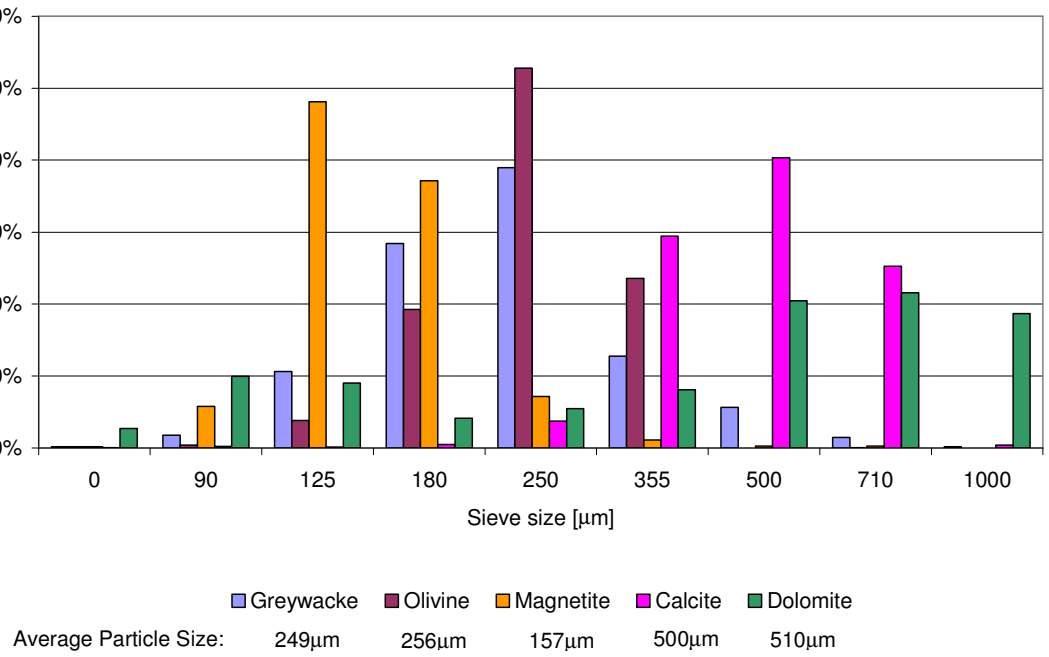

Figure 4.5 - Particle size distributions of the five materials tested

4.3.2. Combined Material Testing

Prior research suggests that different materials may function in two distinct ways. Firstly, catalytically active materials influence the *rate* at which reactions occur without affecting the overall equilibrium composition; a gasification catalyst will improve the producer gas by bringing it closer to the equilibrium composition. Examples of catalytic materials used in prior research include nickel, which has been shown to reduce tar yield, and iron, which is known to catalyse the water gas shift reaction.

Secondly, introducing a reactive material into the fluidised bed can alter the producer gas composition by absorbing or reducing an undesired component. For example, calcium oxide has been shown to absorb carbon dioxide from a gas stream at temperatures around 650°C. The absorption of carbon dioxide promotes the formation of hydrogen by 'encouraging' the water gas shift reaction to generate more products, according to reaction R-2.5. The subsequent reduced concentration of carbon monoxide stimulates the gasification and reforming reactions to increase reaction products, further increasing hydrogen generation.

To date, little research has been focused on the use of simple mixtures of bed materials taking advantage of both these modes of action. Several researchers have attempted to upgrade geological materials by chemical doping with catalytic elements, however this represents an

expensive option to a commercial-scale gasifier installation. It was expected that simple mixtures of two or three minerals would enhance the gasification reactions additively. Table 4.3 above shows the material combinations tested and overall chemical composition. For the sake of comparing the cumulative effects of mixtures of bed materials, materials used in combination with greywacke, an inert sand, are considered as single components.

4.3.3. Experimental Conditions

For consistency all experiments were performed with similar experimental parameters, within the limits of that achievable by the plant. The notable plant parameters are documented in Figure 4.1. These operational parameters were well established by previous work with the gasifier, and due to the time investment required to attain gasification temperature and concern about causing irreparable consequences to the experiments or damage to the plant, sensitivity tests on the plant operation conditions were not conducted although the plant failed a number of times through the course of this project.

4.4. EXPERIMENTAL RESULTS

The results generated from the test runs performed during the experimentation (Table 4.3) are considered from two perspectives. Fundamentally, the gasifier is intended as an energy plant. Traditional measures for the gasifier performance consider producer gas yield, producer gas calorific value, and overall energy efficiency. Secondly, the gasifier is considered as a chemical plant for the downstream purification of hydrogen or production of liquid fuels. For this target application, the gasifier performance is measured based on the yields of individual gas components and the relative concentrations of the components. A more rigorous systems analysis considering energy input for hydrogen output, and economic values for both, is given in Chapter 7. Note that all relative compositions are given as molar fractions.

4.4.1. Sampling Calibration and Results Normalisation

During analysis of the experimental results from the commissioning trials conducted in 2008, it was apparent that producer gas compositions changed over the course of a run, independent of sampling time or conditions being tested. Generally the results indicated rapidly increasing carbon dioxide concentration over the number of samples taken, with corresponding modification to the relative concentrations of the other components. Further investigation concluded that the silica gel used in the sampling apparatus for reducing the sample moisture

content was inadvertently absorbing carbon dioxide and desorbing pre-absorbed nitrogen and oxygen. This effect appeared to become less significant over time, suggesting that the silica gel could be equilibrated to a gas stream containing a certain composition of carbon dioxide.

Based on the above observation, a trial was set up to measure the absorption of carbon dioxide by silica gel. Calibration gas, a dry producer gas mixture prepared by BOC used for GC calibration, was used as the sample gas. This gas was drawn through the sampling apparatus containing 7g of silica gel in 100mL aliquots, as would typically occur for results sampling during a gasifier run. The gas composition was analysed by GC and compared to the standard composition. Figure 4.6 below shows the variation in gas composition with subsequent sampling of the calibration gas. Actual calibration gas composition is given by dashed lines, while the sample results are shown as markers.

Using these results it was possible to establish the relative error in sampling producer gas through silica gel, proportional to the sample number. This error was accounted for in all results obtained from gasifier experiments. Figure 4.7 shows the relative error applied to producer gas composition readings.

In addition to the sampling error, in later runs it was suspected that flue gas was infiltrating into the gasification column and contaminating the producer gas. This was thought to be caused by damage to the chute leading to defluidisation and channelling through the bed material. In order to make adequate comparisons between the runs, all results were normalised to exclude nitrogen and account for contamination by flue gas. The calculation procedure for making these adjustments is detailed in Appendix D.

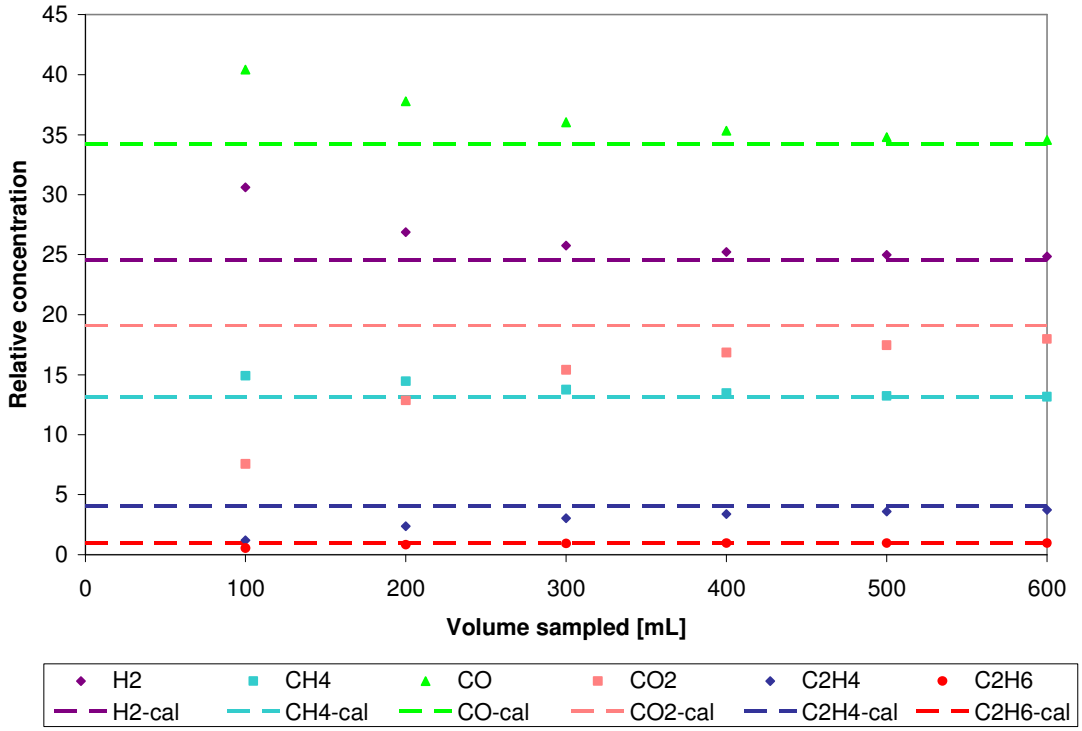

Figure 4.6 - Variation of composition of calibration gas with subsequent sampling through 7g silica gel

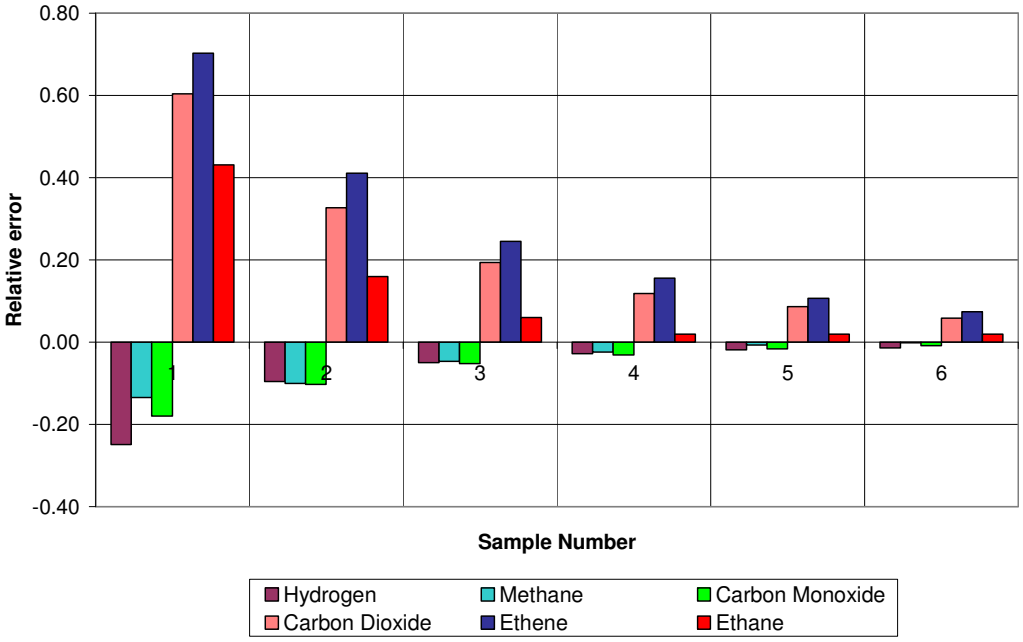

Figure 4.7 - Relative error in sampling producer gas components through silica gel. Sample number assumes each sample has a volume of 100mL, which is standard practice during gasifier operations.

4.4.2. Greywacke

Prior to this investigation all gasifier commissioning and operational trials were conducted by this research team using inert greywacke river sand as bed material. The results from these runs are used as a comparison set for subsequent runs using catalytically active bed materials.

Following installation of a new fuel feed auger, four runs using greywacke as bed material were conducted between 2 September 2008 and 20 January 2009. The new feeder system allowed wood pellets to be fed into the lower third of the bubbling bed, replacing the previous arrangement by which the wood pellets were onto the top of the bed. Initial indications were that the new feeder improved producer gas generation by around 20% compared with the previous system, with higher cold gas efficiencies observed and high hydrogen content appearing in the producer gas composition. A complete analysis of the effect of the new feed system is given in the Masters of Engineering thesis by Bull [Bull, 2008].

Typical performance values for greywacke bed material along with calculated hydrogen yield are given in Table 4.4. Yields are given as flow per unit mass of wood fed, while producer gas lower heating value (net calorific value) is given per unit volume of producer gas at 1 atmosphere pressure and 0°C temperature. Energy efficiency is given as cold gas efficiency, which is the ratio of the available chemical energy of the producer gas mixture to the energy input to the system, but does not account for sensible heat available from cooling the hot gas streams.

Table 4.4 – Average gasifier performance measurements using greywacke as bed material

Producer gas yield [Nm^3/kg]	0.729
Lower Heating Value [MJ/Nm^3]	16.2
Energy efficiency	45.3%
Hydrogen yield [kg/kg]	0.170

Representative producer gas component concentrations are shown in Table 4.5. In addition to being recalibrated based on sample number due to the influence of silica gel on the composition measurement, the composition has also been normalised to exclude nitrogen. Nitrogen is typically present in producer gas on the order of 3-5%, as a result of purging the wood feed system to prevent producer gas escaping up the screw conveyor. Given that nitrogen is present artificially and is not produced by the gasification reactions, it has been discounted from the analysis to give a better comparison of the different bed materials.

Hydrogen to carbon monoxide ratio is given as an indication of the suitability of the producer gas for liquid fuels synthesis.

Table 4.5 – Average producer gas composition using greywacke as bed material

Hydrogen	21.2%
Methane	14.2%
Carbon Monoxide	36.9%
Carbon Dioxide	21.5%
Ethene	5.2%
Ethane	1.0%
H_2:CO ratio	0.57

Compared with equilibrium predictions as given in Table 2.1, this composition is close to that with effective steam/biomass ratio of approximately 0.35. In the current experiments however the steam/biomass ratio applied to the gasifier is 0.77, which is calculated based on the steam flow into the gasification reactor and the chute section divided by wood flow. The discrepancy is thought to be the result of steam channelling within the fluidised bed, causing much of the steam to pass through unreacted. The consequences of this effect are discussed further in Chapter 6.

4.4.3. Olivine

Olivine ($(FeMg)_2SiO_4$) is a naturally occurring mineral mixture of magnesium and iron silicates. Its appearance is a crystalline solid with a greenish hue before calcination, changing to a rust red colour following calcination due to iron oxidation. The relative proportions of magnesium and iron vary with geological location; the olivine sourced for the gasifier runs generally contained 41-46% silica, 10-11% iron oxide and 42-47% magnesium oxide. As discussed in Chapter 2, previous researchers have discussed olivine fundamentally as a catalytic bed material for tar reforming, with little attention given to improving producer gas composition and yield.

It was shown that olivine had a beneficial effect on producer gas yield, in particular returning considerably higher hydrogen yield without compromising the overall efficiency of the system. Producer gas yield increased by 7%, but with a slightly lower heating value the overall energy efficiency dropped 2.5%. Tables 4.6 and 4.7 below give the average performance results for olivine bed material.

Table 4.6 – Average gasifier performance measurements using olivine as bed material, compared with values for greywacke.

	Greywacke	Olivine
Producer gas yield [Nm³/kg]	0.729	0.782
Lower Heating Value [MJ/Nm³]	16.2	15.2
Energy efficiency	45.3%	42.8%
Hydrogen yield [kg/kg]	0.170	0.225

Table 4.7 – Average producer gas composition using olivine as bed material, compared with values for greywacke.

	Greywacke	Olivine
Hydrogen	21.2%	26.1%
Methane	14.2%	13.0%
Carbon Monoxide	36.9%	32.6%
Carbon Dioxide	21.5%	22.8%
Ethene	5.2%	4.5%
Ethane	1.0%	0.9%
H_2:CO ratio	0.57	0.80

The relatively lower cold gas energy efficiency using olivine compared with greywacke can be inferred from the known cracking properties of olivine. In the olivine tests reduced hydrocarbon concentration and subsequently elevated hydrogen concentration in the producer gas as shown in Table 4.7 leads to lower overall energy density. The carbon monoxide / carbon dioxide proportionality remains relatively unchanged, indicating a consistent degree of oxidation compared with greywacke sand and little influence on the gasification and water gas-shift reactions.

4.4.4. Olivine / Calcite Mixtures

The incorporation of calcite into an olivine-based bed material attempted to utilise the combined effects of a catalytic material (olivine) which does not undergo reactions itself, and a CO_2 absorbent (calcite, $CaCO_3$). Initially, calcite was not able to be tested solely as a bed material due to its negative elutriation characteristics and poor fluidisability, which are discussed in detail in Chapters 3 and 5 respectively. Modifications to the gasifier discussed in Chapter 5 allowed more effective investigation of the effects of calcite on the gasification process as it enabled on-the-run addition of fresh calcite, and later removal of calcite fines.

It was hoped that the positive hydrogen production effect observed with olivine could be enhanced with absorption of carbon dioxide, thereby promoting the water gas-shift reaction and increasing hydrogen production further. Several trials using olivine and calcite mixtures were attempted, but success was limited to a maximum 50% calcite in olivine bed material. Additionally, many runs were abandoned due to loss of the calcite component of the bed material, and subsequent cyclone and afterburner fouling by calcite fines. The results presented in this chapter are those of the successful runs, but due to the elutriation of the calcite during runs it is likely that on the commercial scale, with a constant feeding of calcite, the observed effects would be much greater.

Table 4.8 – Average gasifier performance measurements using olivine/calcite mixtures as bed materials, compared with values for greywacke and pure olivine.

	Greywacke	Olivine	Olivine + 25% Calcite	Olivine + 50% Calcite
Producer gas yield [Nm^3/kg]	0.729	0.782	0.877	0.720
Lower Heating Value [MJ/Nm^3]	16.2	15.2	14.2	14.0
Energy efficiency	45.3%	42.8%	51.4%	38.8%
Hydrogen yield [kg/kg]	0.170	0.225	0.286	0.317

Clearly calcite affects gasifier performance to varying degrees depending on the relative proportion of calcite added. A 20% higher producer gas yield was produced with the mixture of olivine/calcite bed material compared with greywacke which suggests addition of one quarter calcite improves the reactivity of the initial gasification reactions. When this proportion of calcite is increased to 50%, overall producer gas yield drops while hydrogen yield increases. The drop in overall producer gas yield contributes to the reduction in energy efficiency. It is suggested that olivine improves the extent of gasification reactions, which peak with a relative olivine proportion between 50% and 75%, whereas increase to the extent of the water gas-shift reactions appears boundless based on the continued increase in hydrogen composition in the producer gas with increasing the calcite proportion.

The much higher hydrogen proportion and lower carbon monoxide proportion in the producer gas confirms that the water gas shift is enhanced by addition of calcite. The expected increase in carbon dioxide concentration does not eventuate due to the increased absorption of carbon dioxide by the calcite. The higher proportion of hydrogen also appears to enhance the hydrogenation of ethene to ethane, which may be catalysed by one or more of the bed material

components. In the industrial context, the relative proportions of hydrogen to carbon monoxide observed are very close to the optimum ratio for Fischer-Tropsch synthesis of liquid fuels.

Table 4.9 – Average producer gas composition using olivine/calcite mixtures as bed materials, compared with values for greywacke and pure olivine.

	Greywacke	Olivine	Olivine + 25% Calcite	Olivine + 50% Calcite
Hydrogen	21.2%	26.1%	29.5%	40.0%
Methane	14.2%	13.0%	11.6%	12.0%
Carbon Monoxide	36.9%	32.6%	28.1%	20.2%
Carbon Dioxide	21.5%	22.8%	25.9%	23.4%
Ethene	5.2%	4.5%	4.1%	3.3%
Ethane	1.0%	0.9%	0.9%	0.9%
H_2:CO ratio	0.57	0.80	1.05	1.98

4.4.5. Dolomite

Due to the constraint of testing higher proportions of calcite (more than 50%) as bed material, it was decided to attempt dolomite as an alternative, to quantify the effects of a pure calcium carbonate mineral. The dolomite as sourced was atypical dolomite in that the concentration of magnesium oxide was very low, almost as low as that observed with the calcite. However, it was an improvement over calcite as physically the mineral was harder, more amorphous and more resistant to elutriation. While 100% dolomite was not able to be tested due to fluidisation problems, 25% and 50% mixtures of dolomite with inert greywacke were tested. Table 4.10 shows the gasifier performance measurements of the two dolomite proportions, while Table 4.11 shows average producer gas compositions obtained from these trials.

Table 4.10 – Average gasifier performance measurements using dolomite/greywacke mixtures as bed materials, compared with values for greywacke.

	Greywacke	25% Dolomite in Greywacke	50% Dolomite in Greywacke
Producer gas yield [Nm^3/kg]	0.729	0.571	0.534
Lower Heating Value [MJ/Nm^3]	16.2	14.9	15.1
Energy efficiency	45.3%	29.3%	26.4%
Hydrogen yield [kg/kg]	0.170	0.233	0.235

Table 4.11 – Average producer gas composition using dolomite/greywacke mixtures as bed materials, compared with values for greywacke.

	Greywacke	25% Dolomite in Greywacke	50% Dolomite in Greywacke
Hydrogen	21.2%	37.1%	39.6%
Methane	14.2%	11.9%	12.1%
Carbon Monoxide	36.9%	25.7%	23.4%
Carbon Dioxide	21.5%	20.0%	19.5%
Ethene	5.2%	4.2%	4.4%
Ethane	1.0%	1.0%	1.0%
H_2:CO ratio	0.57	1.45	1.70

The above results suggest that the dolomite has an inhibitory effect on gasifier performance. Producer gas yields observed with greywacke and olivine were not obtained, either due to a chemical inhibition of the gasification reactions, or poorer heat and mass transfer. It is suggested that the larger particle size of the dolomite combined with reduced particle fragmentation decreased the heat transfer area of the bed material, resulting in slower reaction rates of the fuel pellets. Lower producer gas yield leads to lower energy efficiency, caused by relatively higher concentrations of hydrogen reducing the producer gas energy density.

Analysis of the producer gas composition shows the expected increase in hydrogen concentration, with evidence that the water gas-shift proceeded to a lesser extent than that observed for calcite. This is possibly further indication that the larger particle size and greater resistance to attrition of the dolomite compared to the calcite presented less surface area to the gas mixture, and hence less reactive sites for the absorption of carbon dioxide and reduced promotion of the water gas-shift. Alternatively, the reduced catalytic activity of the greywacke compared to olivine could have limited the available carbon monoxide for reaction, reducing overall hydrogen concentration.

4.4.6. Magnetite (Ilmenite)

Iron-containing minerals are known as cheap and effective catalysts of the water gas shift reaction. As has been shown previously, focusing on catalysing this reaction is of fundamental importance in improving overall gasifier conversion. Iron oxide has also been reported as a steam reforming catalyst. In New Zealand few natural minerals contain significant amounts of iron, but some natural deposit of ‘black sand’ on west coast beaches

present ideal iron sources. The sand used in the gasifier was approximately 24% iron or iron oxide (magnetite), as determined by XRF analysis (see Appendix C).

Due to the fine particle size and high density of the magnetite it was anticipated that retention of magnetite in the gasifier would be difficult, hence the magnetite was mixed in greywacke sand, at ratios of 25% and 40%. This resulted in bed materials with iron concentrations of 9% and 12% respectively. Lab-scale trials indicated that the magnetite/greywacke mixture was difficult to fluidise with cold air so the magnetite portion was added at the end of the start up period, into the high temperature air flow.

Table 4.12 shows the average performance measurements for the two bed material mixtures described above. A numerical assessment concludes that once again, addition of the catalytic material has initially hindered the process, with lower producer gas yields and energy efficiency.

Table 4.12 – Performance measurements of 25% and 40% magnetite/greywacke bed material mixtures, compared with values for greywacke

	Greywacke	25% Magnetite in Greywacke	40% Magnetite in Greywacke
Producer gas yield [Nm^3/kg]	0.729	0.544	0.707
Lower Heating Value [MJ/Nm^3]	16.2	14.8	14.2
Energy efficiency	45.3%	27.6%	36.1%
Hydrogen yield [kg/kg]	0.170	0.266	0.294

Table 4.13 – Average producer gas composition using 25% and 40% magnetite/greywacke mixtures as bed materials, compared with values for greywacke

	Greywacke	25% Magnetite in Greywacke	40% Magnetite in Greywacke
Hydrogen	21.2%	26.6%	29.4%
Methane	14.2%	12.2%	11.9%
Carbon Monoxide	36.9%	34.5%	31.9%
Carbon Dioxide	21.5%	22.1%	22.8%
Ethene	5.2%	3.7%	3.2%
Ethane	1.0%	0.9%	0.8%
H_2:CO ratio	0.57	0.77	0.92

Clearly from Table 4.13, magnetite (iron oxide) has a positive influence on the water gas-shift and steam reforming reactions, indicated by reduced relative concentrations of carbon monoxide and hydrocarbon gases, and increased concentration of carbon dioxide. From these experiments it is unclear whether the increased hydrocarbon reforming is a result of catalysis or an equilibrium shift caused by enhanced water gas-shift, leading to reduced overall carbon monoxide concentrations. The increase in hydrogen concentration however is not sufficient to allow the producer gas to be used for downstream conversion for liquid fuels.

4.4.7. Magnetite / $CaCO_3$ / Greywacke mixtures

Following the positive results from the magnetite trials it was decided that combination of magnetite with a calcium carbonate-containing compound such as calcite or dolomite would likely yield significant improvements to producer gas composition. Again, due to the difficulty of fluidising both magnetite and the calcium carbonate minerals, these were added just prior to the start of gasification to the hot air stream, to minimise the possibility of bed material defluidisation and accumulation in the plant.

Table 4.14 shows the performance measurements of the gasifier running with three different combinations of the proposed bed materials, consisting of 20% magnetite and 20% dolomite in a greywacke base. From the XRF analysis the total composition of calcium in the bed material amounts to approximately 12% and iron approximately 5%. Comparatively, in the 25% dolomite results calcium concentration was around 14%, and in the 25% magnetite results iron was approximately 6%.

Table 4.14 – Performance measurements of gasifier operating with bed material consisting of 20% magnetite and 20% dolomite in greywacke, compared with each of the individual minerals

	Greywacke	25% Dolomite in Greywacke	25% Magnetite in Greywacke	20% Magnetite + 20% Dolomite in Greywacke
Producer gas yield [Nm^3/kg]	0.729	0.571	0.544	0.663
Lower Heating Value [MJ/Nm^3]	16.2	14.9	14.8	13.7
Energy efficiency	45.3%	29.3%	27.6%	34.3%
Hydrogen yield [kg/kg]	0.170	0.233	0.266	0.296

The results above indicate that the combination of magnetite and dolomite in the bed material positively influence in the gasification reaction and improve the composition of the producer

gas. Despite the lower LHV of the resultant gas, producer gas generation is increased leading to higher cold gas efficiency.

Table 4.15 compares the producer gas compositions of the four bed material combinations considered above. Again, it is clear that the combined effects of magnetite and dolomite in the bed material positively influence the gasification reactions, with high hydrogen composition and lower hydrocarbons and carbon monoxide, suggesting improved water gas-shift and steam methane reforming reactions. The slightly higher carbon dioxide concentration is an indication of the increased extent of the water gas-shift. The CO_2 concentration would be much higher were it not for the calcium-controlled pumping of CO_2 to the flue gas.

Table 4.15 – Producer gas compositions of 20% magnetite and 20% dolomite in greywacke bed material, compared with results from each of the components individually

	Greywacke	25% Dolomite in Greywacke	25% Magnetite in Greywacke	20% Magnetite + 20% Dolomite in Greywacke
Hydrogen	21.2%	37.1%	26.6%	40.4%
Methane	14.2%	11.9%	12.2%	10.7%
Carbon Monoxide	36.9%	25.7%	34.5%	21.8%
Carbon Dioxide	21.5%	20.0%	22.1%	22.8%
Ethene	5.2%	4.2%	3.7%	3.3%
Ethane	1.0%	1.0%	0.9%	0.9%
H_2:CO ratio	0.57	1.45	0.77	1.85

Following this trial, a similar experiment was conducted utilising a higher proportion of magnetite, and calcite instead of dolomite. By this stage in the experimental campaign the supply of dolomite had been exhausted, and with in-run bed material loading capability calcite was less of a risk to use, with less run-time available for it to elutriate and foul the gasifier components. It was expected the addition of extra magnetite to the bed material, effectively increasing iron concentration to around 10%, would stimulate further reforming of the hydrocarbon gases. In order to guarantee at least 50% of the bed material would remain fluidised, the amount of calcite was limited to 17%, giving an effective calcium concentration of 9% compared with 11% for the previous trials. Table 4.16 compares the performance measurements for the two combinations of bed materials. Despite a slightly lower LHV and reduced hydrogen yield, gasifier cold gas efficiency has been improved markedly, suggesting less auxiliary fuel and steam was required to yield the results of the previous trial.

Table 4.16 – Performance measurements for two complex mixtures of bed material containing magnetite and calcium-containing minerals

	Greywacke	20% Magnetite + 20% Dolomite in Greywacke	33% Magnetite + 17% Calcite in Greywacke
Producer gas yield [Nm^3/kg]	0.729	0.663	0.673
Lower Heating Value [MJ/Nm^3]	16.2	13.7	13.6
Energy efficiency	45.3%	34.3%	40.1%
Hydrogen yield [kg/kg]	0.170	0.296	0.283

Table 4.17 – Producer gas component concentrations for two complex mixtures of bed material containing magnetite and calcium-containing minerals

	Greywacke	20% Magnetite + 20% Dolomite in Greywacke	33% Magnetite + 17% Calcite in Greywacke
Hydrogen	21.2%	40.4%	38.0%
Methane	14.2%	10.7%	11.3%
Carbon Monoxide	36.9%	21.8%	23.3%
Carbon Dioxide	21.5%	22.8%	23.6%
Ethene	5.2%	3.3%	3.0%
Ethane	1.0%	0.9%	0.8%
H_2:CO ratio	0.57	1.85	1.63

The results from producer gas analysis indicate that the increased concentration of magnetite may have had a positive effect on reforming higher hydrocarbon gases, but the expected increase in reforming of methane has not occurred. Conversely, both carbon dioxide and carbon monoxide concentrations have increased, suggesting a reduction in CO_2 pumping and subsequent reduction in water gas-shift. This was anticipated with reduced calcium present in the bed material.

4.5. DISCUSSION

Gasifier performance in general did not vary as significantly as producer gas composition with different bed materials, however the effect of the catalytic bed materials has been more profound compared with past attempts at changing gasifier operating conditions to stimulate performance improvements. Increasing hydrogen yield generally resulted in reduction in overall producer gas yield and cold gas efficiency. As a consequence of CO_2 transfer from gasification column to combustion column, the overall producer gas output from the

gasification column is reduced and the energy density from a high-hydrogen gas mixture is decreased.

Figure 4.8 demonstrates graphically how the bed material mixtures trialled during this project have affected producer gas composition. The addition of calcium-containing compounds into the mixture have clearly had the most prominent effect on hydrogen and carbon monoxide concentrations, while catalytic materials such as olivine and magnetite have a small but positive effect on producer gas composition by reforming hydrocarbon gases.

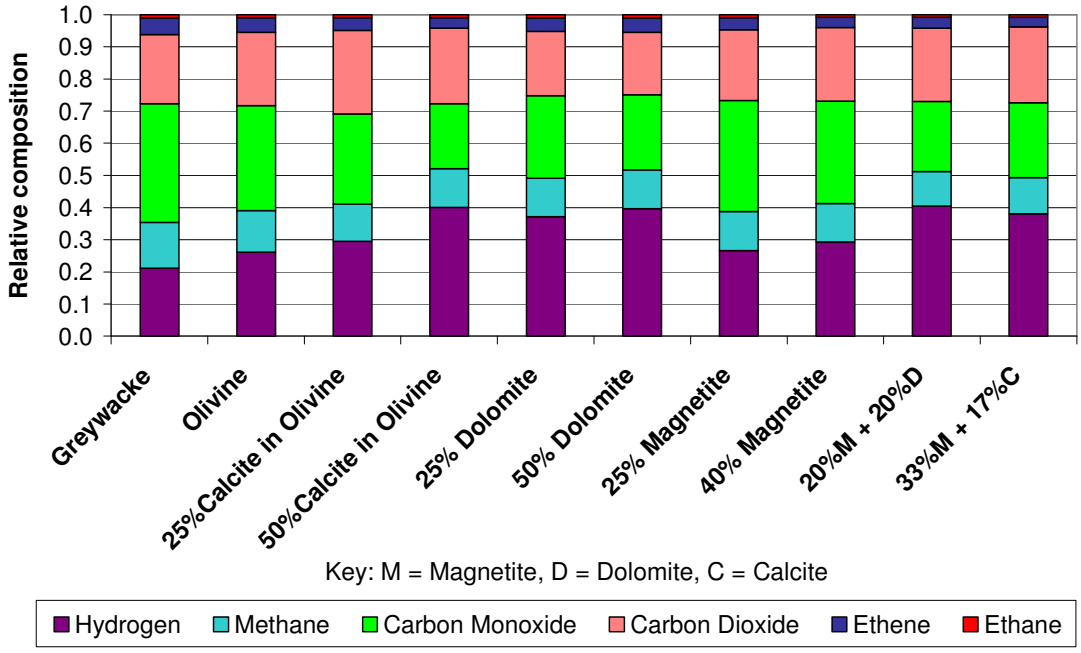

Figure 4.8 – Graphical representation of effects of bed materials on producer gas composition

Figure 4.9 demonstrates that as calcium content in the bed material increases, hydrogen concentration and hydrogen yield per unit mass wood fed increase proportionally. It is suggested that the presence of magnesium may influence this relationship as magnesium will establish a similar equilibrium reaction between magnesium oxide and carbonate. Given that there may be other factors influencing the results, no firm mathematical relationship has been established between the concentrations of calcium and magnesium in the bed material, and the hydrogen concentration in producer gas.

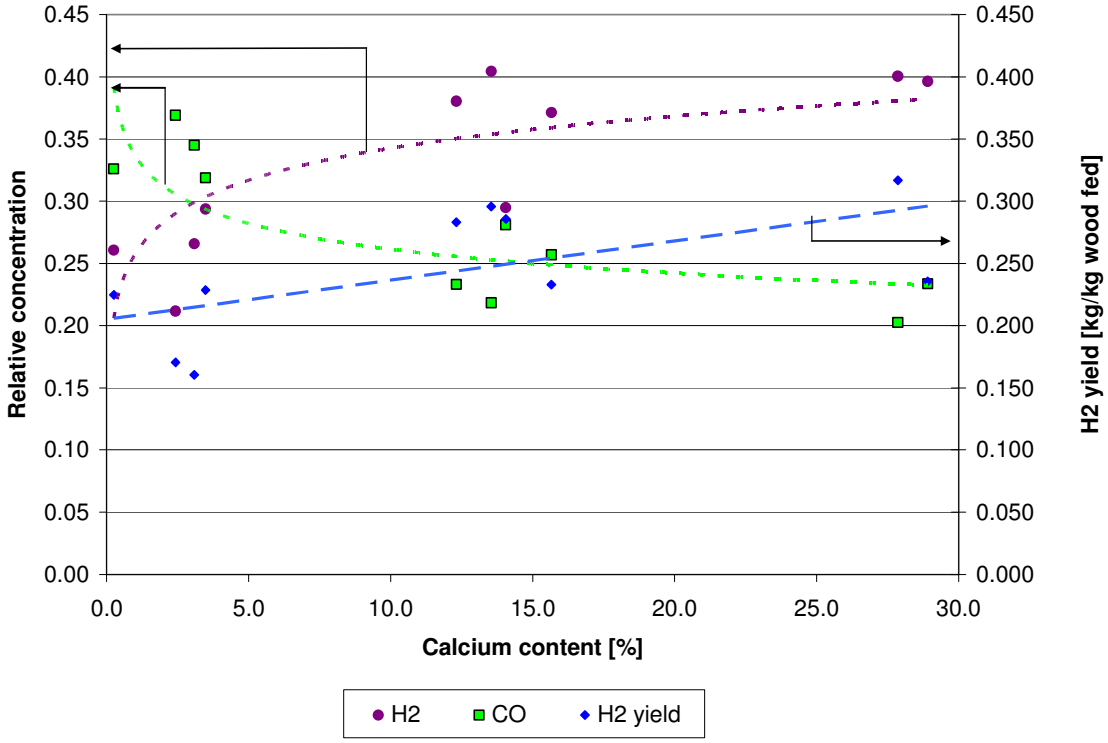

Figure 4.9 – Relative concentrations of hydrogen and carbon monoxide in producer gas and change in hydrogen yield compared with concentration of calcium in bed material.

Conversely, a clear linear relationship exists between the amount of iron in the bed material, and the relative concentrations of methane and C2 hydrocarbon gases in the producer gas. Figure 4.10 shows that as iron concentration increases, the relative concentration of methane, ethane and ethene in the producer gas decrease.

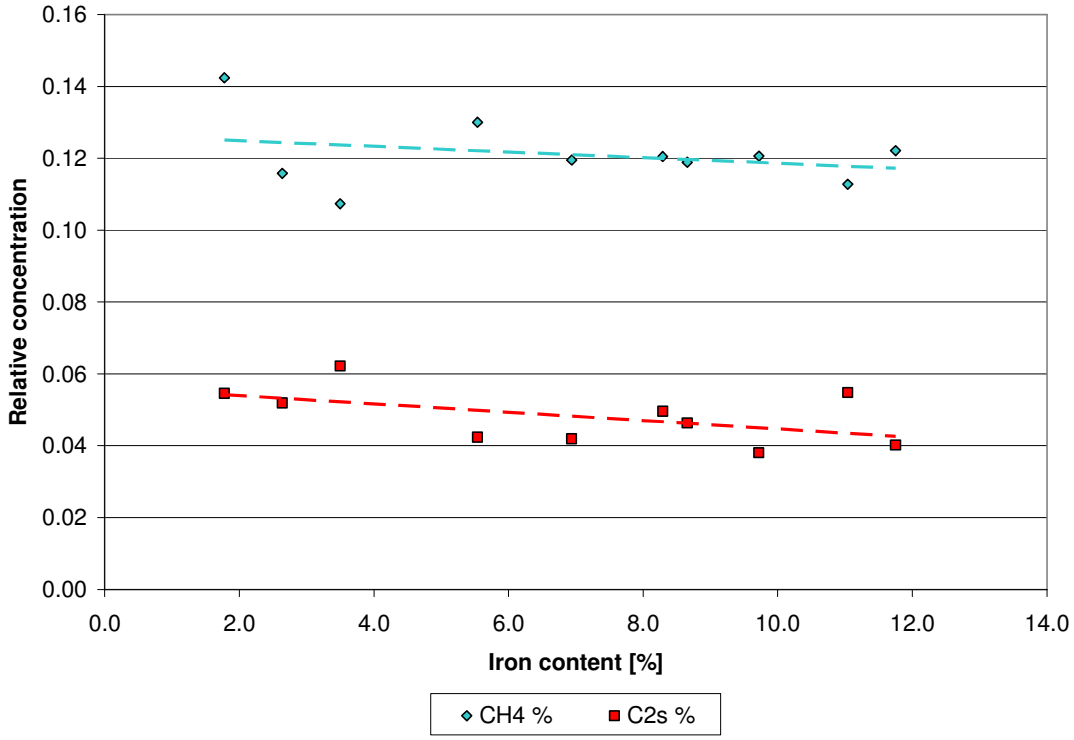

Figure 4.10 – Reduction of methane and C2 hydrocarbon gases in the producer gas with bed materials of increasing iron content.

4.6. CONCLUSIONS

Bed Material composition has significant effects both on gasifier performance and producer gas composition. All the bed materials tested resulted in significant deviations from the greywacke sand 'base case'. The amount of calcium in the bed material significantly affected the hydrogen concentration in the producer gas, indicating that the effect of calcium on the water gas shift reaction is profound. Iron was shown to have a positive influence on reforming of light hydrocarbon gases, to a lesser degree.

Maximum gasifier performance measurements were obtained using a mixture of 25% calcite in olivine, giving an overall bed material composition of 35% magnesium, 14% calcium and 8% iron, with silica the balance. A producer gas yield of 0.877 Nm^3/kg wood fed was obtained with an LHV of 14.2 MJ/Nm^3. The resultant cold gas efficiency was 51.4%. Maximum hydrogen yield of 0.317 kg H_2/kg wood fed (40% hydrogen concentration) was obtained using a 50% calcite in olivine mixture. This bed material had the highest concentration of calcium of all the materials tested at 27.5%, with additional 24% magnesium, which may exhibit similar CO_2-pumping properties.

From the results it is anticipated that depending on producer gas end use, the gasifier bed material could be tailor-made to give appropriate concentrations of hydrogen and carbon monoxide. This can be achieved by simple mixing of readily-available minerals.

5. Gasifier Experiments: Operational Tests and Results

5.1. BACKGROUND

During the course of the bed material testing experiments, several other parameters were measured and results gained. These contribute to the overall comparisons of performance between the University of Canterbury's dual fluidised bed gasifier and other gasifiers of similar type around the world, and help to gauge the ongoing effects of operation of a dual fluidised bed gasifier. The UC gasifier is a constantly changing and complex system, where no two runs are completely alike, so continuous monitoring of other experimental parameters is necessary to establish the condition of the gasifier and evaluation of its fitness-for-purpose.

Whilst the primary aim of trialling different bed material types was to improve the hydrogen composition of the producer gas gasifier performance, overall producer gas quality was also an important consideration. Any downstream utilisation and processing of the producer gas depends on the extent of impurities such as tar and particulates, while accurate assessment of the gas composition and water vapour content is required for evaluating heat recovery potential and overall gasifier efficiency. The ability of the system to cope with various fuels is imperative for its success as an energy plant and opens the economic potential for the system as a hydrogen or liquid fuel production method.

5.2. BIOMASS TARS

5.2.1. Introduction and Characterisation of Biomass Tars

A combined IEA/EU/US DOE definition of biomass tars states that 'tar' is all organic components with a molecular weight larger than benzene [Milne, 1998]. Tars are typically aromatic hydrocarbons of 1 to 5 rings, predominately naphthalene and acenaphthalene [Devi, 2003]. Most tars condense below 300°C, causing significant problems for downstream processes; while gas turbines can tolerate some heavy hydrocarbon components due to having a high gas inlet temperature, gas engines require cooling of the fuel gas to ambient conditions to maintain volumetric efficiency [Bull, 2008]. Catalytic processes such as liquid fuels production and fuel cell electricity generation are significantly adversely affected by more than part-per-million level contamination by polyaromatic hydrocarbons.

At the exit of the gasification column on the UC gasifier biomass tars present themselves as a blue smoke and characteristic odour in the producer gas stream. Particulates with diameter greater than around 45µm are removed from the producer gas stream by cyclone, with large amounts of condensed tars being found on the surface of the particles. In the cyclone particle trap, the tars harden and coat the inside of the trap as a black, glassy substance as shown in Figure 5.1.

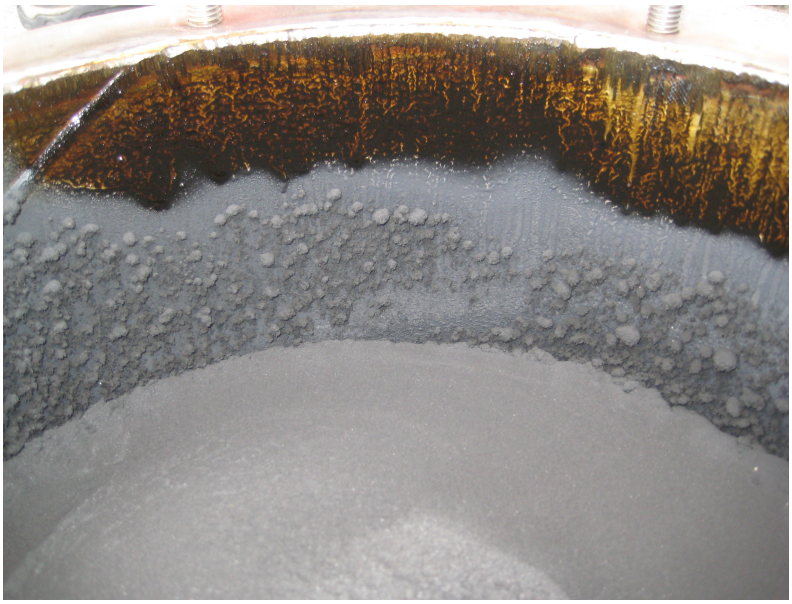

Figure 5.1 – Interior of cyclone particle trap following gasifier run. In addition to the accumulation of particulates, tars have condensed as a brown layer over the surface of the container, particularly apparent around the top of the trap.

In practice there are two categories of tar removal techniques. Primary tar removal is practised with optimisation of gasifier operation which reducing the formation of tars within the gasification reactor itself, by gasifying at elevated temperatures (greater than 800°C), reducing biomass moisture content, or utilising a catalytically active bed material to promote tar cracking (usually nickel oxide, olivine or dolomite). Secondary tar removal is carried out in downstream processing. Two main secondary tar removal processes are reported. They are tar reforming, where the producer gas is heated to 1100°C in a bed of dolomite, or cold gas scrubbing with biodiesel. The latter has been used successfully at the 8MW biomass gasification facility in Güssing, Austria since 2002 [Pfeifer, 2008].

5.2.2. Tar Sampling, Extraction and Measurement

The primary objectives of tar sampling and measurement are to identify and characterise the tar being produced in the gasifier by concentrations of major components, and quantify the tar yield. From this, it may be determined that certain bed materials are catalytically active at promoting tar cracking. Tar from the producer gas stream can be sampled using the combined sampling device as described in Chapter 4. At the front end of the device sits a Bakerbond 3mL amino normal phase SPE column through which is pulled 100mL of producer gas per sample. This SPE column retains the tar and prevents it from entering the gas sample syringe and contaminating the Micro GC analysis equipment.

The quality of the gas is immediately apparent from the condition of the SPE column following sampling. Typically, a dark stain forms on the white amino phase of the column as the gas sample is drawn. On later runs using catalytic bed materials, the reduction in tar components was obvious from the minimal staining of the amino phase that occurred during sampling as shown in Figure 5.2.

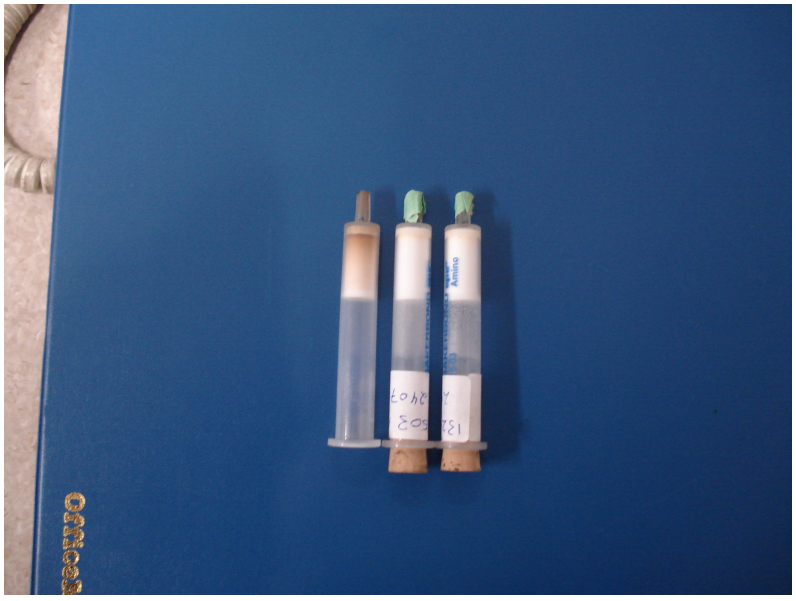

Figure 5.2 – Comparison of SPE columns following producer gas sampling. The leftmost column is typical for producer gas generated with inert bed materials, while the second and third columns resulted from gasification with magnetite and dolomite as bed materials, respectively]

Following gas sampling, the SPE column is removed and sealed, then stored at 4°C until the tars can be extracted from the column for separate analysis. The low storage temperature reduces the evaporation of some of the lighter tar components, improving the accuracy of the analysis. Extraction of the tars involves soaking the column with 6mL dichloromethane

(DCM) in three batches. Firstly, the column is weighed on a four decimal place balance. The first 2mL DCM is injected into the top of the column and the solid phase is allowed to soak, which is apparent from a colour change from white to colourless. As the DCM soaks through the column the tars form a brown solution in the DCM which drips from the column inlet. Slightly positive pressure is applied by pushing air with a syringe from the top of the column, forcing the DCM through until the meniscus of the DCM is level with the upper layer of solid phase. The procedure is repeated twice more with additional 2mL doses of DCM. Finally, the remaining DCM is forced through the SPE column with positive air pressure from the syringe. The tar sample dissolved in 6mL dichloromethane is then centrifuged to remove solid components (usually small char particles are caught during gas sampling) and analysed with a flame-ionisation detection Varian CP 3800 gas chromatograph. Sixteen major tar components can be identified from a sample using this method, as shown in Table 5.1 below.

Table 5.1 - Major components identified from tar sample analysis and typical concentrations (from Hill Labs analysis)

	Sample 1	Sample 2	Sample 3	Sample 4	Average	St. Dev
			µg			
Acenaphthene	9.2	7.2	6.0	9.2	7.9	1.58
Acenaphthylene	83.4	40.0	27.7	84.4	58.9	29.33
Anthracene	14.7	8.1	6.2	13.8	10.7	4.19
Benzo[a]anthracene	4.7	2.7	1.9	4.5	3.5	1.37
Benzo[b]fluoranthene	4.4	2.4	1.6	4.1	3.1	1.35
Benzo[a]pyrene	4.3	2.1	1.5	3.8	2.9	1.34
Bezno[g,h,i]perylene	1.8	0.9	0.6	1.2	1.1	0.51
Benzo[k]fluoranthene	1.9	0.9	0.6	1.6	1.3	0.60
Chrysene	4.2	2.5	1.8	4.0	3.1	1.16
Dibenzo[a,h]anthracene	1.2	0.5	0.4	0.7	0.7	0.36
Fluoranthene	11.4	6.0	4.4	10.1	8.0	3.31
Fluorene	31.1	16.3	12.1	28.7	22.1	9.28
Indeno(1,2,3-c,d)pyrene	2.3	1.1	0.7	1.5	1.4	0.68
Naphthalene	72.2	44.7	29.8	114.0	65.2	36.99
Phenanthrene	42.8	23.8	18.0	41.2	31.5	12.43
Pyrene	12.7	7.5	5.7	12.1	9.5	3.44
TOTAL µg/100mL gas	302	167	119	335	231	104.17

5.2.3. Gravimetric Tar Yield Analysis

A gravimetric method of tar yield measurement was proposed initially, based on the weights of the SPE column before and after tar extraction. Accurate measurement of the weights of the SPE columns following gas sampling was made using a four-decimal-place balance. For each run, a number of samples were made throughout the course of the experiment. Table 5.2 reports the average before and after weights of the SPE columns for several runs, and the bed material in use at the time.

Table 5.2 – Average SPE column weights before and after tar extraction, compared with bed material used in the respective gasifier run

Run Date	Bed Material	Avg. SPE initial wt [g]	Avg. SPE final wt [g]	Weight difference [g]
25 Sep 08	Greywacke	3.2366	3.2014	0.0352
20 Jan 09	Greywacke[1]	2.8135	2.7207	0.0762
3 Feb 09	Olivine (fresh)[1]	2.8262	2.7409	0.0650
16 Feb 09	Olivine (sintered)	2.7889	2.7461	0.0428
2 Mar 09	25% Calcite in Olivine	2.8261	2.7729	0.0532
13 Mar 09	50% Calcite in Olivine	2.8216	2.7729	0.0487

Note:
1. Indicates that two extractions were required

The results above are far in excess of the assumed 'maximum' tar yield observed heretofore from biomass gasification. The weight differences reported are per 100mL of gas as samples, at a temperature between the temperatures at the top of the gasification column (typically approximately 650°C) and at the sample point (approximately 100°C). Scaling up to the typical measurement of grams of tar per normal cubic metre of producer gas, the above results suggest a tar yield of 350–760 g/Nm³. As well as being far above the normally accepted levels of tar production, it disagrees with the Hill Labs analysis which concluded tar concentrations were approximately 3 g/Nm³.

It is suggested that the discrepancy is a result of accumulation of water vapour in the SPE column. Given that the amount of water vapour in the producer gas is variable depending on steam input, bed material quality and gasification reaction extent, and that these parameters are poorly controlled and measured, gravimetric determination of tar yield is unreliable. Addition of a pre-drying step to the SPE extraction régime may reduce the water content, but would not improve the integrity of the result. In light of this situation, gravimetric tar yield analysis was discontinued.

5.2.4. GC-FID Analysis

Following extraction from the SPE columns, the tar samples dissolved in dichloromethane were analysed using gas chromatography. A standard solution of known concentrations of the

sixteen major tar components was prepared and analysed as a basis for comparison of the extracted tar samples. The standard was analysed using the GC with a pre-formulated pyrolysis method, and the plot peak sizes were compared to the known concentrations of the individual components. Subsequently, major components in the extracted tar samples could be identified. Figure 5.3 shows the GC plot with six major components peaks identified.

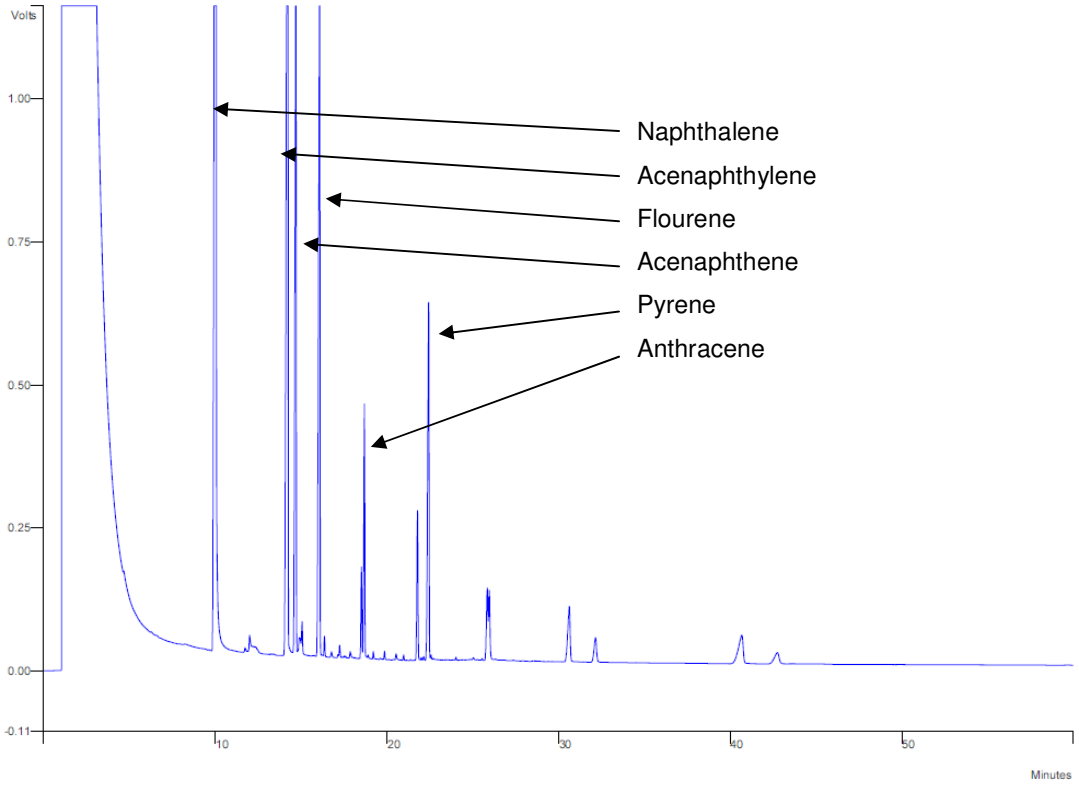

Figure 5.3 – GC-FID analysis of tar standard mixture with major peaks identified.

In order to confirm the identification of the major chemical components, three samples including one flue gas sample were analysed using GC-Mass Spectroscopy (GCMS), which compares the individual compound spectroscopy signatures with an in-built database. Of the samples, one was corrupted from inappropriate storage, while the flue gas sample identified only straight-chain hydrocarbons, not the aromatic hydrocarbons characteristic of biomass tars. Analysis of the third sample as shown in Figure 5.4 was able to positively identify a number of components, including some major components not previously identified or used for the standard composition.

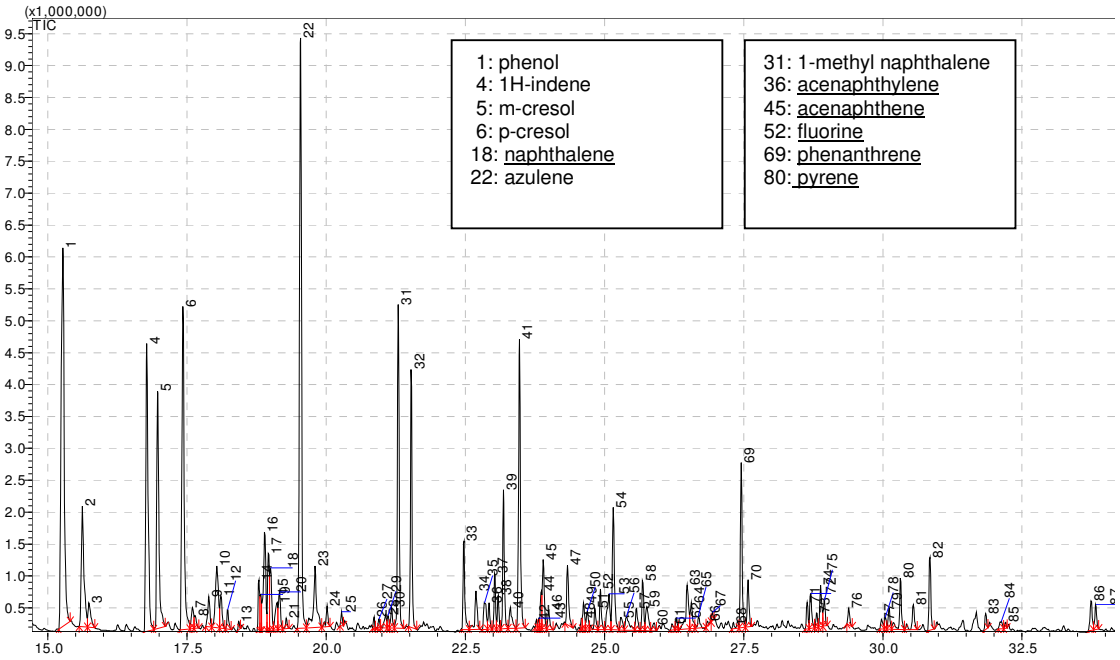

Figure 5.4 – Chromatogram of gasifier tar sample with major components identified where available. Components also included in the tar standard are underlined.

Recent work within the department on the gasifier has focussed on analysing samples doped with known concentrations of specific major components in an effort to use GC analysis as a method of determining tar yield. It is expected that once the analytical method is established, analysis of the samples gathered over the course of the experimental runs will determine positively whether bed material composition has any effect on tar yields and composition.

5.3. PRODUCER GAS VAPOUR CONTENT

5.3.1. Water Vapour Content as a Performance Indicator

Prior research has established that the steam supplied to the gasification column does not react entirely with the biomass fuel to produce gas. Comparison of the equilibrium model with producer gas composition measured in the experiments has indicated that the gasifier operates with an effective steam to biomass ratio of 0.35. The actual steam/biomass ratio of the feeds however was 0.77, suggesting that approximately 55% of the steam injected into the gasifier does not react with the biomass. It can be concluded therefore that the fluidised bed mixing is poor and inferred that steam channelling occurs up the walls of the reactor.

Steam is fed to the gasifier at three points: into the gasification column distributor, into the chute and into the siphon. All of the steam supplied to the BFB either reacts or is exhausted through the producer gas outlet. Previous research by Bull [Bull, 2008] has attempted to establish the degree to which steam in the chute and siphon flows into the gasification side of the system, and has determined that the siphon fluidisation steam is not generally transferred to the gasification side. Chute fluidising steam however is transferred to the BFB against the flow of bed material. Low siphon pressures during recent experiments may also have led to steam infiltration from the siphon to the gasification side, though this steam is unlikely to participate in gasification reactions as it will not flow down into the bed against the flow of outgoing producer gas.

Measurement of vapour content concurrently with producer gas and tar measurements gives an indication as to the degree of mixing in the fluidised bed and the potential of the bed material to enhance reactivity.

5.3.2. Vapour Content Measurement and Calculations

Producer gas moisture content is measured directly by sampling the producer gas through silica gel. As shown in Figure 5.5, a U-tube filled with silica gel and plugged with glass wool as a particulate filter is weighed to four decimal places. The tube is fitted to the producer gas sampling line and one litre of producer gas is manually pulled through the silica gel. The tube is disconnected and reweighed, with the difference in weight between this measurement and the previous being the vapour quantity in the producer gas.

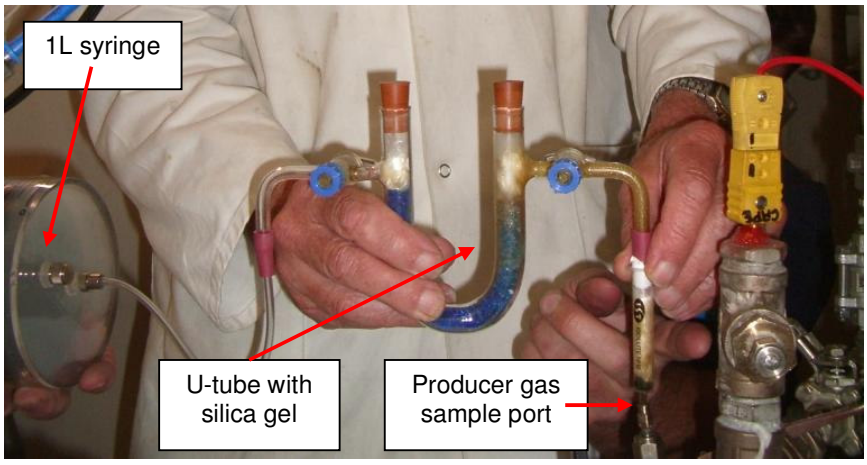

Figure 5.5 – Moisture content sampling system. The SPE column fitted to the producer gas sampling port is not used now as it was found to absorb moisture; instead, a brass fitting with glass wool to trap particulates is used.

As the producer gas is not held at a constant temperature, comparison of different experimental results requires the raw data to be normalised for the same temperature. It is assumed that on sampling, the gas is cooled immediately to ambient conditions. This is guaranteed by ensuring the sample is pulled slowly, allowing the gas to cool and contract to the appropriate volume. The temperature of the surroundings allows the normal (1atm, 0°C) volume of gas to be calculated according to the ideal gas law. Comparison of this result with the volumetric flow of dry producer gas allows calculation of the amount of moisture exiting the gasification column, and determination of the extent of conversion of the fluidising steam.

5.3.3. Results and Discussion

Moisture content measurements were taken for most of the producer gas samples over the course of the experimental programme. Each sample's results deviated substantially, suggesting that steam is not intimately mixed with producer gas at the exit of the gasification column. Figure 5.6 shows the average effective (i.e. reacting) steam/biomass ratio for each of the bed materials tested, calculated based on a moisture balance about the gasification column. Results for the greywacke trials are not available.

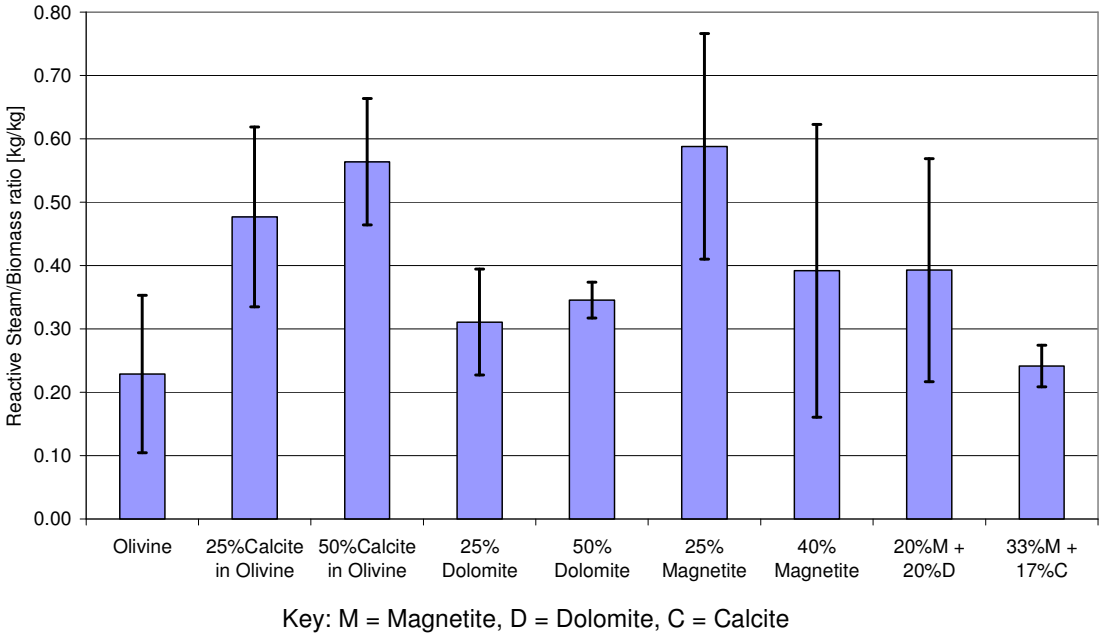

Figure 5.6 – Effective (reactive) steam/biomass ratios for most of the bed materials tested.

Figure 5.6 shows that the variation in reacted steam/biomass ratio between experimental runs for the various bed materials is profound. The reacted steam does not appear to be related to

the degree of influence of a bed material on the water gas shift reaction, as materials which have given high hydrogen content producer gas such as calcite and dolomite do not show consistently high steam reactivity. Alternatively, it was thought that particle fluidisability may have an effect on steam utilisation, as finer particles may allow smaller bubbles of steam to form in the bed, promoting mixing. However, comparison of Archimedes Number and particle diameter with average reacted steam/biomass ratio gives poor correlations, as shown in Figure 5.7. No explanation can be given at this stage for the high variation in reacted steam between runs, except to assume that the unreacted steam and producer gas mix poorly, perhaps due to the formation of large bubbles in the fluidised bed which do not interact with the producer gas.

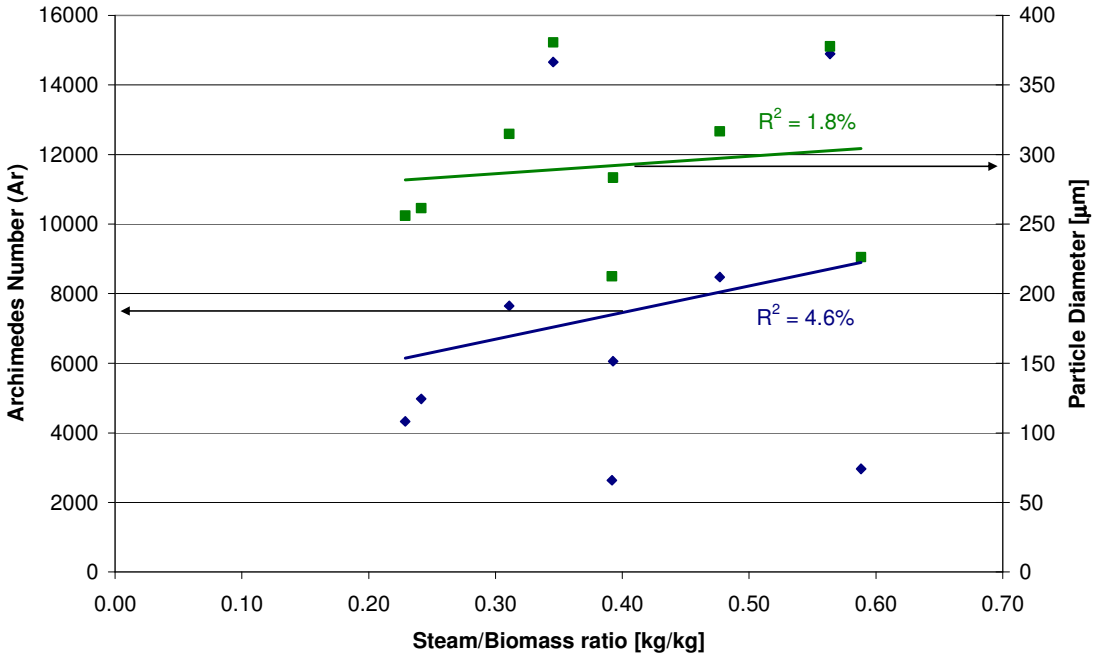

Figure 5.7 – Comparison of reacted steam/biomass ratio with Archimedes number and average particle diameter of each of the bed material combinations tested.

The effect of steam/biomass ratio on producer gas yield and quality from the UC gasifier was extensively investigated by Bull [Bull, 2008] who showed that variation of dry producer gas yield with amount of steam supplied is small. Several authors have discussed the effects of steam/biomass ratio on hydrogen production [Franco, 2003; Lv, 2007; Rapagnà, 1998]. Figure 5.8 gives the relationship between specific dry producer gas yield and hydrogen composition with reacted steam/biomass ratio from this work. Both variables appear to be independent of reactive steam, regardless of bed material. This is inconsistent with the

conclusions of most authors who suggest that hydrogen production is positively influenced by increasing steam/biomass ratio in a certain range.

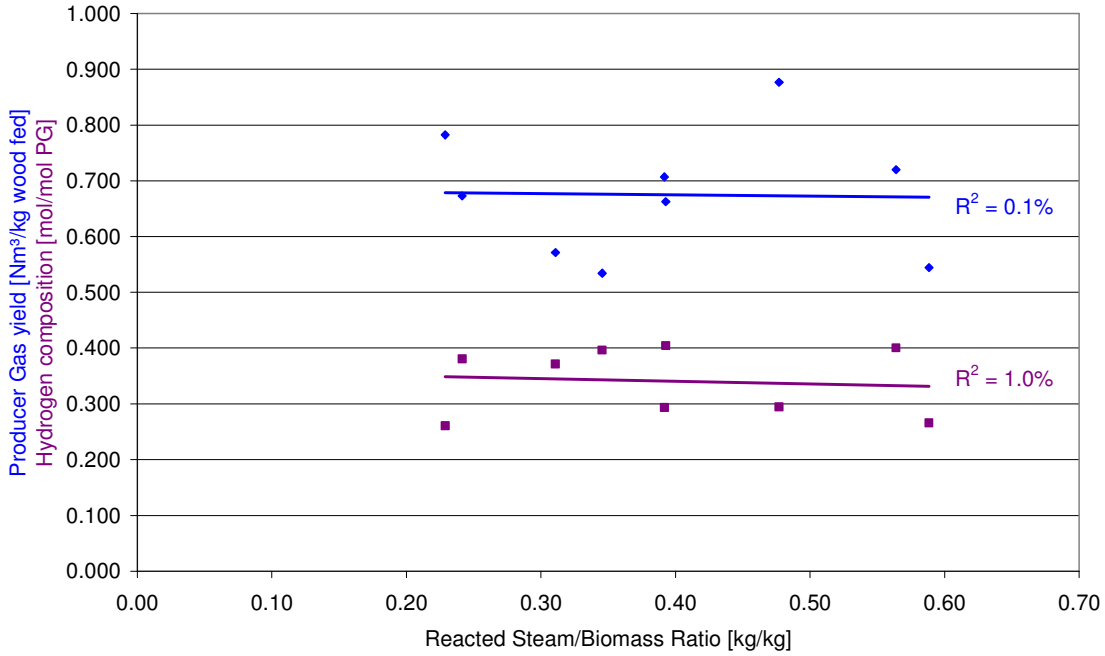

Figure 5.8 – Variation in specific producer gas yield and hydrogen composition with reacted steam/biomass ratio based on results from this work. Note that the two comparisons share a common y-axis scale.

5.3.4. Conclusions

A gravimetric method for measuring moisture content of biomass gasification producer gas has been developed based on silica gel absorption. Results from the measurements suggest there is little correlation between steam utilisation and bed material used, despite the positive influence of some bed materials on the water gas shift reaction which would increase steam reactivity. Contrary to expectation, there appears to be no correlation between the amount of reacted steam and degree of bed fluidisation, based on analysis of different bed material particle diameters and Archimedes numbers. Steam utilisation does not appear to affect either dry producer gas yield or hydrogen composition, contrary to the findings of several authors. More analysis is required to verify these findings, and independent validation of the moisture sampling method is required.

5.4. BIOSOLIDS GASIFICATION

5.4.1. Background

The major economic potential of biomass gasification lies in its ability to upgrade all types of carbonaceous fuels to a useable medium calorific value gas. Until 2009, prior experimental work with the University of Canterbury gasifier has focused solely on utilising wood pellet fuel, due to the consistency of moisture content and fuel calorific value. This allows accurate analysis of the gasifier system without having to account for fuel quality as a variable.

In March 2009 the opportunity arose to investigate dry biosolids, also known as digested sewage sludge, as an alternative fuel source. In accordance with the research programme of Andreas Schabauer, a visiting student from Technical University of Vienna (Technical University Wein or TUW), a series of experiments were performed with the UC gasifier to investigate the applicability of biosolids as a fuel for gasification. In the experiments, the biosolids obtained were in the form of pellets and blended with wood pellets at varying ratios. Typical operations were used to determine the gasification performance characteristics of the new fuel and the effect of the new fuel on the producer gas quality, particularly in regard to the generation of hydrogen.

5.4.2. Biosolids Characterisation and Availability

Biosolids is an end product of the municipal waste water treatment process after sewage sludge dewatering and drying. It is available in substantial quantities in all major population centres and is effectively a continuous, renewable energy resource. Christchurch city in New Zealand's South Island is considered as an example of a large metropolitan centre employing advanced water treatment. Currently, the Christchurch Wastewater Treatment Plant processes around 200,000 m^3 of waste water each day, with a resultant solids flow of around 33,000 kg/day.

The waste water treatment process involves a number of separation stages of increasing orders of magnitude of efficiency. Initially, sewage from a large urban centre such as Christchurch flows through one or more physical separation stages utilising screens to remove coarse solid objects. Aeration and sedimentation processes remove a large portion of the remaining solids. The solids is then fed to anaerobic digesters operating the mesophilic temperature range (around 37°C), which devolatilises much of the carbonaceous material producing a biogas of approximately 60% methane and 40% carbon dioxide. This biogas is

used to fuel gas engine generators, supplying electricity to the treatment plant and the rest of the city. The digested solid solution is then dewatered from 5% solids to around 20% solid content by means of a belt press. Presently, the remaining solids fraction of this process is disposed of in local landfills. Rising landfill dumping costs and increased environmental awareness have led the Christchurch City Council to implement a further thermal drying process to reduce water content of the biosolids and stabilise it, rendering it non-pathogenic and safe for general transport and beneficial reuse, particularly as applied to land remediation.

The end stream of the thermal drying process is a solid with approximately 8% moisture content. The solid is approximately 66 wt% undigested carbonaceous material, with the remainder being ash which consists largely of nitrates (5.4 wt%), phosphates, sulfur (1.1 wt%), heavy metals and other biological nutrients. A full analysis of the biosolids tested is presented in Appendix B.

5.4.3. Biosolids Gasification Experiments

In total five gasifier runs were accomplished, utilising mixtures of wood pellets and biosolids. Proportions of 10%, 20%, 40%, 60%, 80% and 100% biosolids with wood pellets were trialled. Prior to the runs the appropriate proportions of biosolids and wood pellets were mixed completely and stored appropriately to prevent absorption of moisture. During the gasification runs the fuel mixture was fed to the gasifier at an equivalent pellet flow of 15.5 kg/h, and the actual flow calculated later from a calibration curve accounting for the difference in bulk density with the added biosolids. Average gasification temperature was 720°C. The bed material for four runs was inert greywacke river sand, with the fifth run on a reactive 25% calcite/ 75% olivine mixture using a fuel composition of 20% biosolids in wood pellets. Due to operational difficulties the 40% and 60%, and 80% and 100% biosolids/wood pellet mixtures were tested on the same runs.

The biosolids material tested was sourced from FloDry in Auckland, as the biosolids drying process proposed for the Christchurch Wastewater Treatment Plant is not yet operational. The biosolids was dried firstly using a moving belt followed by a rotary drum dryer, in which the solids formed into particles of diverse size range. In order to minimise screw conveyor blockage and maintain consistency with the wood pellets, particles of around 4mm average size were used for the trials. As the biosolids has a different bulk density to wood pellets, fuel

feed auger calibration for each of the biosolids/wood pellet mixtures was conducted in order to determine the amount of fuel being fed to the gasifier.

5.4.4. Gasifier Performance Results and Discussion

Overall, increased biosolids loading in the fuel feed led to poorer gasifier performance. Producer gas production was significantly reduced with high biosolids proportions, leading to poorer gasifier cold gas efficiency. Additionally, more auxiliary fuel was required for sustained gasifier operation, suggesting that either the smaller biosolids particle size led to higher gasification reactivity, or that the biosolids did not have equivalent calorific value to wood as was assumed.

Table 5.3 gives the gasifier performance results from the five runs, with increasing biosolids proportion in the fuel. Figure 5.9 shows the changes in producer gas composition with varying biosolids composition. The results given in Table 5.3 are the averaged values per unit mass of fuel fed. A general trend can be observed in the results that producer gas production was decreased at higher biosolids proportions. In part this can be explained by the much higher ash quantity per unit mass of the biosolids compared with wood pellets (30% compared with 1%). The lower gas production is also supported by the fact that the biosolids are biologically digested prior to gasification, which effectively strips off reactive carbon, reducing the gas yield from the devolatilisation reactions observed prior to wood gasification.

Table 5.3 - Producer gas, hydrogen and energy yields from the experimental runs, with increasing biosolids proportion in the fuel.

% Biosolids fed		0%	10%	20%	40%	60%	80%	100%	20% O/C[1]
Producer Gas Yield	Nm^3/kg	0.729	0.802	0.672	0.628	0.607	0.365	0.345	0.564
Hydrogen Yield	kg/kg	0.170	0.214	0.169	0.184	0.184	0.118	0.118	0.162
Net Calorific Value	MJ/Nm^3	16.2	15.7	16.4	16.2	16.3	16.5	16.9	16.0
Energy Efficiency		45.3%	48.0%	42.9%	36.9%	35.5%	19.4%	19.0%	31.1%

Note:
1 20% O/C refers to the experiment run with the reactive olivine/calcite bed material mixture using 20% biosolids in the feeding fuel.

The increased hydrogen content in the producer gas at higher biosolids proportions shown in Figure 5.9) can be explained by increased rates of the gasification reaction, perhaps due to the

smaller biomass particle size compared with wood pellets. Despite increasing hydrogen composition in the producer gas, hydrogen yield drops off significantly with biosolids composition greater than 60% in the fuel.

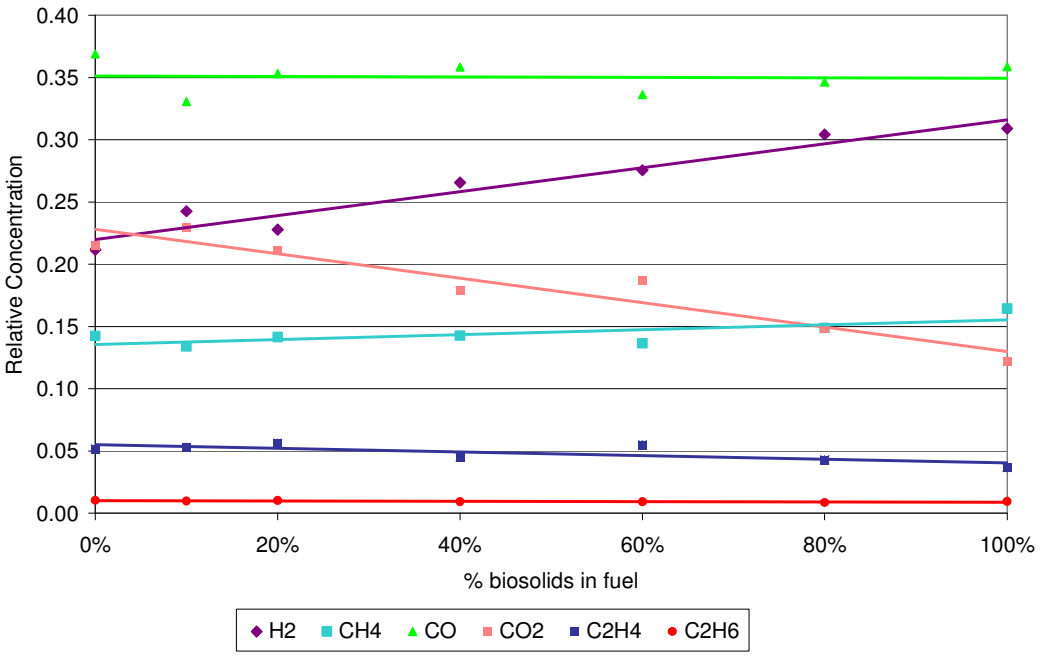

Figure 5.9 - Producer gas composition varying with relative proportion of biosolids in the fuel.

Interestingly, the catalytic bed material trial utilising a mixture of 25% calcite in olivine did not yield the expected improvements, as was demonstrated in previous wood pellet trials. The 25% calcite in olivine mixture was chosen as it was the most energy efficient bed material tested, with highest producer gas yields and good producer gas quality. In these biosolids/wood pellet fuel trials however, the equivalent biosolids loading in greywacke sand yields better results. Producer gas yield was lower when trialled with the olivine/calcite mixture leading to lower cold gas efficiency. Despite this, hydrogen yield was maintained due to higher hydrogen composition in the producer gas, as shown in Table 5.4 below. It is suggested that due to the operational difficulties realised in testing a highly elutriating material such as calcite, much of the initial charge of calcite in the bed material was not still present in the gasifier at the time of gasification starting. Clearly the producer gas results show some calcite remained, enhancing the water-gas shift reaction, as indicated by higher hydrogen and carbon dioxide and lower carbon monoxide concentrations. However, other circumstances such as fuel – bed material interaction or degree of fluid bed mixing may be influencing gasifier performance over and above the positive effects of the catalytic bed

material. This will be discussed in more detail in Chapter 6, along with discussion of the operational observations from the biosolids trials.

Table 5.4 – Producer gas compositions for 20% biosolids fuel loading, in greywacke and 25% calcite in olivine bed materials.

	Greywacke	25% Calcite in Olivine
Hydrogen	23%	31%
Methane	14%	16%
Carbon Monoxide	35%	36%
Carbon Dioxide	21%	12%
Ethene	5.6%	3.7%
Ethane	1.0%	1.0%

5.4.5. Conclusions on the Biosolids Fuel Trials

Dried biosolids (digested sewage sludge) offers a constant, renewable energy source that can be converted through gasification to combustible producer gas which can then be used for electricity and heat. Due to devolatilisation from microbial digestion processes in the sewage sludge pre-treatment, gasifying biosolids has a lower producer gas yield and, consequently, a lower energy efficiency compared with gasifying wood pellets. Producer gas yield fell from 0.729 Nm³/kg with 100% wood pellet fuel to 0.345 Nm³/kg with 100% biosolids fuel, a 47% reduction. However, compared to gasification of pure wood pellets, the producer gas from gasification of biosolids has higher hydrogen content observed with increasing biosolids fuel loadings.

6. Gasifier Operation, Modifications and Development

6.1. INTRODUCTION

Under Objective 2 of the BIGCC programme at the University of Canterbury, a 100 kW dual fluidised bed gasifier was constructed and commissioned over the course of four years, from 2005 – 2008. The dual fluidised bed design was selected from a number of gasifier types, for application to the thermal conversion of waste woody biomass to a combined heat and electrical power load. Figures 6.1 show the gasifier in its current configuration with the appropriate nomenclature overlain. Reference should be made to these figures for clarification of the gasifier components referred to in this chapter.

Over this time a number of mechanical and operational difficulties have been encountered, and many have been overcome. Continued operation and experimenting with the gasifier has been integral to increasing the knowledge base which larger-scale systems will incorporate into their design. Bull [Bull, 2008] undertook as part of a Masters of Engineering qualification a significant review of the design and operation of the as-built gasifier (described in Brown [Brown, 2006]). The results of his analysis are summarised in this chapter. The gasifier underwent a major refit and recommissioning at the end of 2008, to repair mechanical failures and implement recommended design improvements. Over the course of the 2009 experimental campaign, further repairs have been made, and new designs implemented to cope with the new catalytic bed materials which are anticipated to become part of normal gasifier operation in the future.

6.2. 2007-2008 CAMPAIGN: REVIEW

6.2.1. Bed Material Circulation

Initially, many modifications were required to the mechanical design of the plant to achieve stable operation. Poor understanding of solid circulation through the plant and contamination of producer gas with the flue gas stream was improved by installation of transparent viewing sections in the plant and cold-testing. It was shown that the level of sand in the standpipe section of the siphon, and consequently the siphon pressure, was critical to plant performance. Figure 6.2 shows diagrammatically the operation of the gasifier upper section and the correct siphon condition.

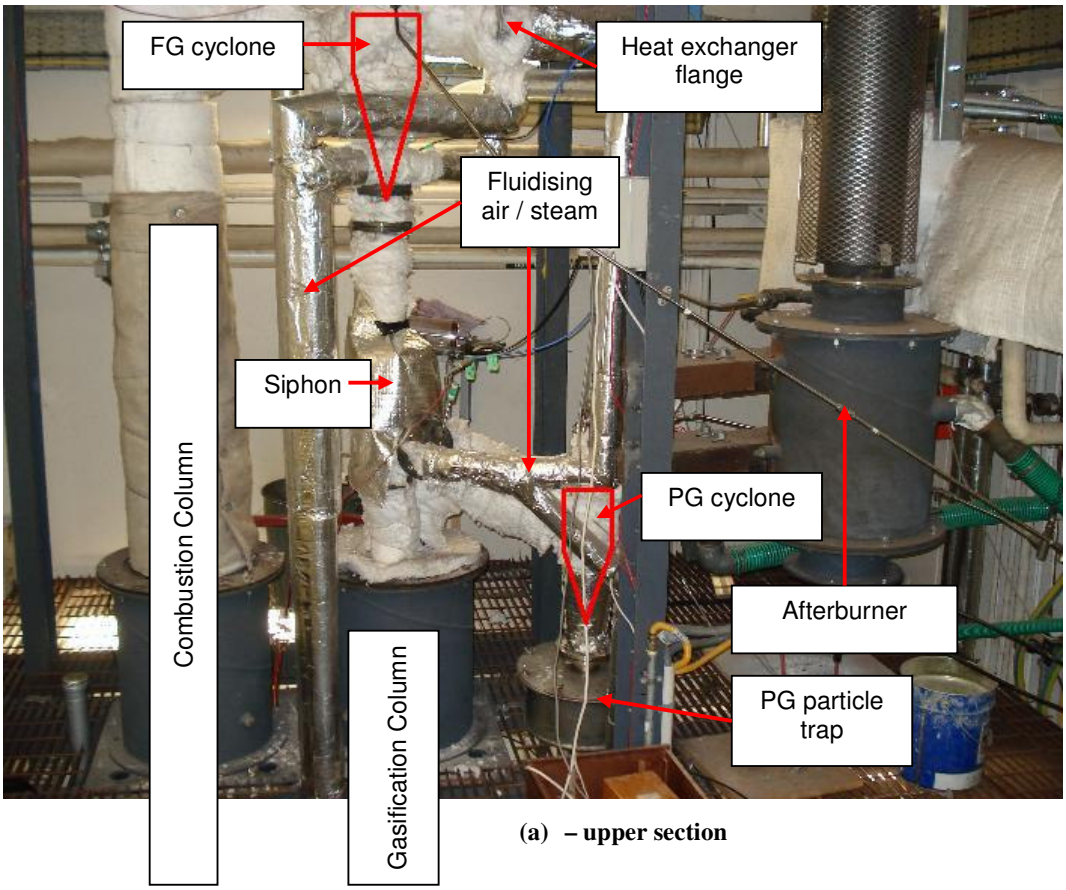

(a) – upper section

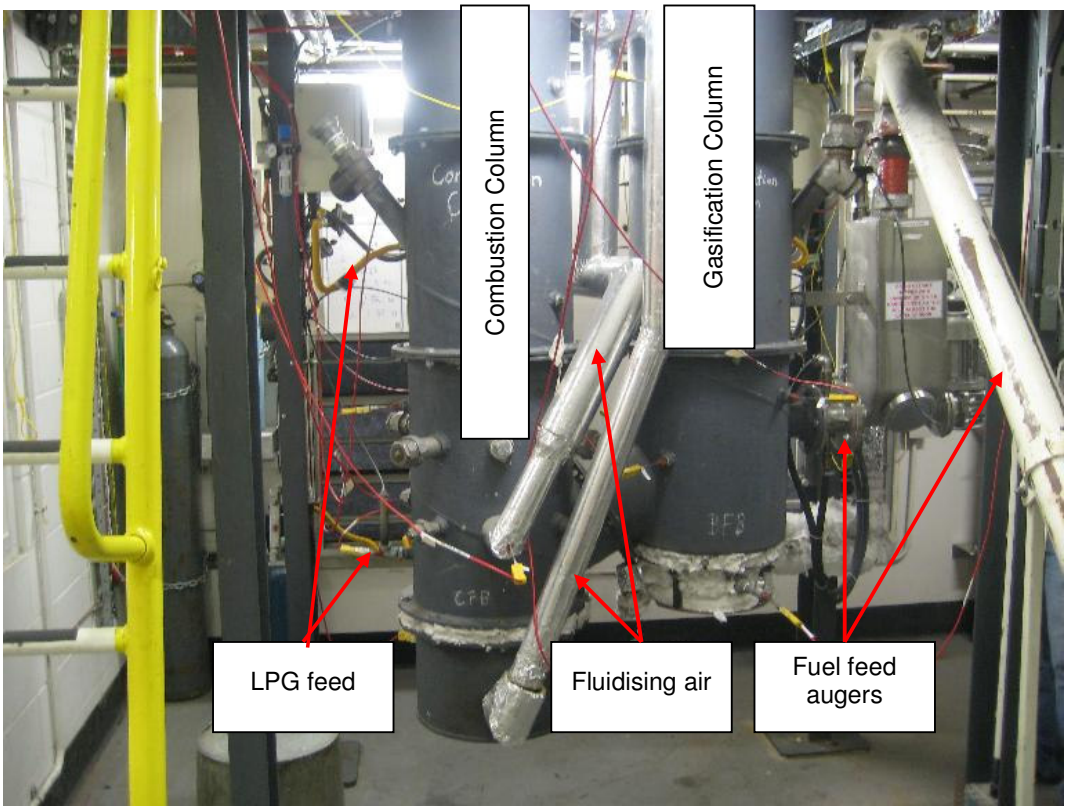

(b) – lower section

Figures 6.1 (a) and (b) – Upper and lower sections of the 100kW UC gasifier in its current configuration, with significant areas indicated 'PG' = producer gas, 'FG' = flue gas.

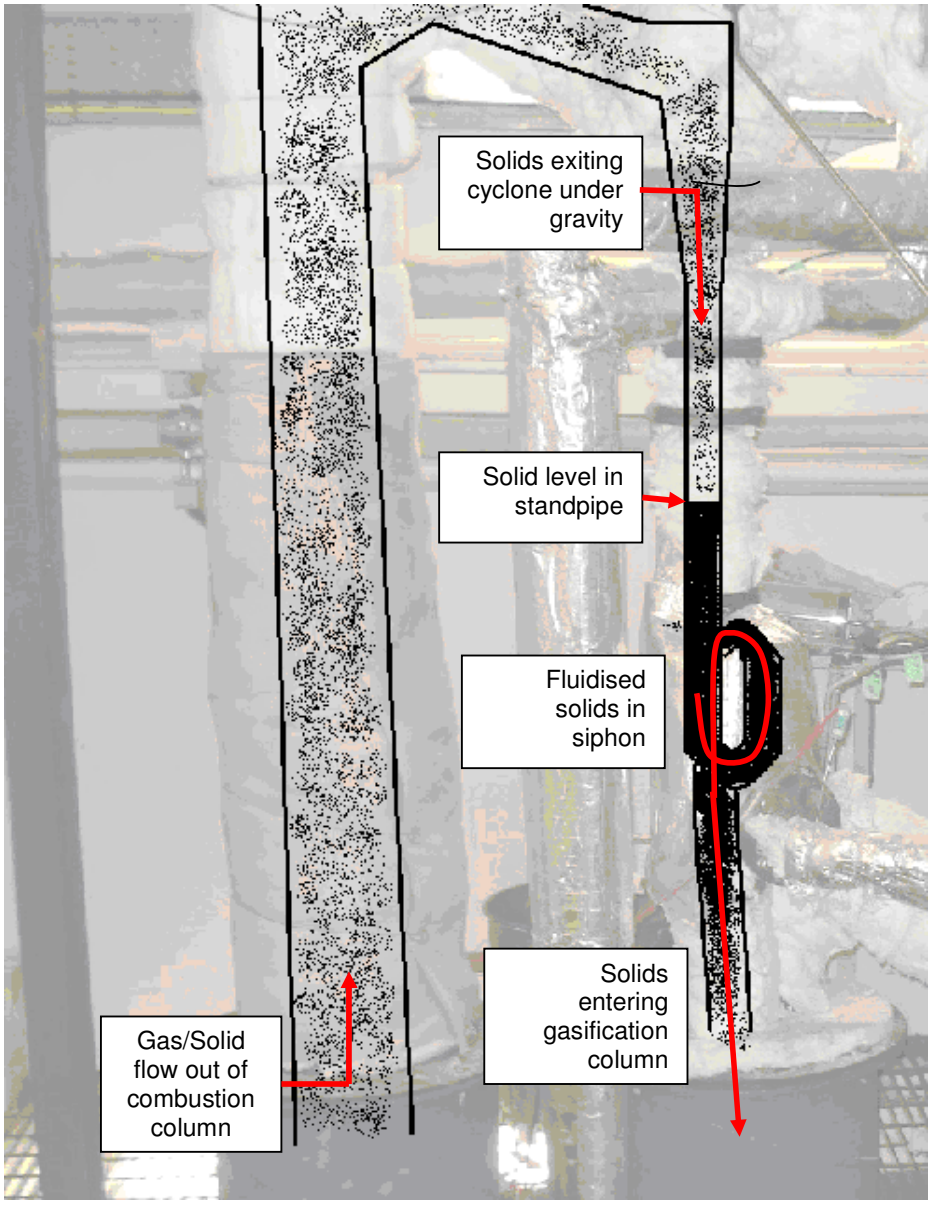

Figure 6.2 – Normal operating conditions of the gasifier upper section, showing transfer of solids (bed material and ash) from the combustion column to the gasification column.

Installation of viewing ports allowed observation of the siphon section under cold testing and later at operating conditions. This became very important to controlling plant operation, as monitoring sand level in the siphon standpipe is the first indication of any abnormalities in bed material circulation.

6.2.2. Investigation of Fluidising Media

Whilst air is required for combustion column fluidisation and steam is required for gasification column fluidisation, it was not known what media was appropriate for use in the chute and siphon sections for effective bed material circulation. Additionally, steam was used during start-up in the siphon which was a great hindrance to fluidisation at low temperatures, due to condensation and caking of the bed material. The chute and siphon fluidising media were rearranged to incorporate using pre-heated air during start-up, while maintaining the use of steam as an option for normal operation. Following this change, heat-up of the system to operating temperature was made significantly easier. Further investigation of different combinations of air and steam fluidisation at the siphon and chute showed that whilst no infiltration of fluidising gas into the gasification column occurred from the siphon, when air was used in the chute section, nitrogen content of the producer gas increased significantly, indicating air infiltration. This allowed further runs to generate producer gas uncontaminated by fluidising air in the chute section during normal operation.

6.2.3. Gasifier Feed System Modification

The original design of the gasifier utilised a screw auger to feed the fuel pellets into the gasification column with wood pellets. A single hopper was mounted atop an inclined auger, which fed the wood pellets onto the top of the bed. This caused two problems. Firstly, the hopper was of too small a size to accommodate sufficient wood pellets (100kg) for a run, so the top of the hopper needed to be removed periodically to refill the hopper. This exposed the operators to potentially harmful producer gas which was back-flowing down the auger. Secondly, it was found that heat transfer to the wood pellets could be vastly improved if instead of the pellets being fed onto the top of the bubbling bed, they were fed into the base of the bed.

To necessitate safe wood pellet replenishment, a lock hopper system was installed that allowed the feed hopper to be isolated while the wood pellets were added to the second hopper (above the feed hopper). When pellets have been added to the upper hopper and the hopper lid replaced, the knife-gate valve between the two hoppers is opened, allowing the pellets to fall through into the feed hopper.

Figure 6.3 - Gasifier wood pellet handling system mounted at base of feed auger (Reproduced from Bull, 2008)

To improve the feeding location of the pellets into the gasification column, the original system was modified to include a horizontal auger mounted near the base of the gasification column, just above the reducing point where the column diameter shrinks to the gas distributor diameter. The original auger was mounted to an intermediate hopper mounted on top of the new horizontal auger which in turn feeds the new auger. Commissioning of the new setup immediately achieved improved producer gas yield.

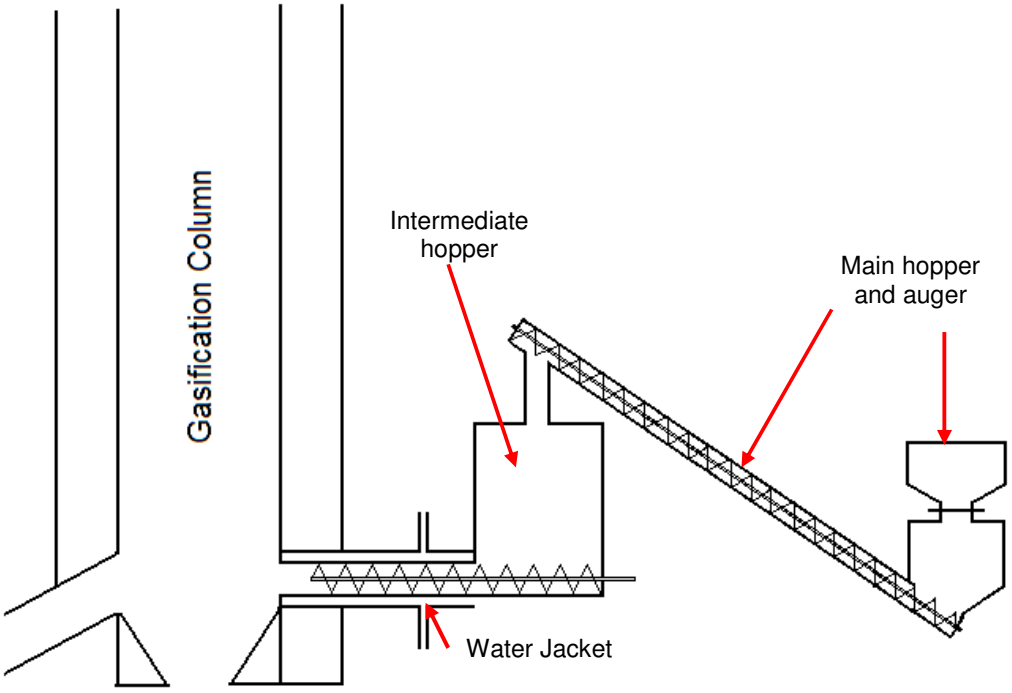

Figure 6.4 – Schematic diagram of new fuel feed system, showing main auger feeding a smaller intermediate hopper. The fuel is then fed into the base of the gasification column.

6.2.4. Producer Gas Flow Measurement

The gasifier presents unique problems for gas flow measurement, due to the very high temperature of the gas and the need not to obstruct gas flow by even a small back pressure. After discounting conventional flow measurement devices such as orifices, venturis, rotameters and pitot tubes, indicator gas injection was chosen as a suitable alternative. Helium is injected at a known flow rate into the producer gas stream near the sampling outlet, and after a sufficient mixing length the producer gas is sampled. The concentration of helium in the producer gas sample is measured by gas chromatography with the rest of the gas components. By knowing accurately the flow rate of helium (set permanently at 2.43 L/min) and the concentration of helium in the producer gas, the producer gas flow rate can be determined by dividing helium flow by helium producer gas concentration.

6.2.5. Producer Gas Sampling System

Originally, a product sampling system was implemented in accordance with the IEA tar sampling protocol for biomass gasification systems [Good et. al., 2005]. A vacuum pump was installed to draw a sufficient sample volume from a slipstream placed inside the main

producer gas outlet line. The pump drew the sample through a solvent train which removed the tar and moisture from the sample. The clean gas sample was then analysed by Micro GC. Several problems were encountered with this method which reduced the integrity of the results substantially. These problems included extensive sample line length, which due to gas losses prevented accurate gas sampling, and the inability to measure reliably the quantity of tar removed by the solvent train reliably, or be able to clean and replace the sample system. This impinged on tar reduction as one of the critical optimisation objectives, as it was difficult to make observations before and after a change in operating parameters to see whether it had any influence on tar production. This led to implementation of the manual combined sampling device as described in §4.1.5. By this method, gas samples were reliably delivered to the Micro GC for sampling, with little tar and moisture contaminating the gas sample. To date, an accurate method for quantifying tar yield from the samples gathered using the SPE columns has not been established, although work within the Department is continuing.

6.3. TRANSITION PERIOD – REPAIR AND RECOMMISSIONING

Following the previous two years experimental work [Bull, 2008], the success of the gasifier operation led to unexpected wear and tear on the plant, particularly on the cyclones. It was discovered that a large hole had been worn in the impact surface of the bed material separation cyclone on the flue gas line. In addition, repeated heating up and cooling down cycles as part of the experimental runs had forced large cracks to open in the refractory lining of the gasifier interior, which led to fracture at the areas where the column bases are removed following runs. It was also observed that by the end of the runs bed material loss had become significant, often surpassing 30% of initial bed material charge. Therefore the decision was made to suspend operations in lieu of a major overhaul of the gasifier top end.

6.3.1. Cyclone Damage

The flue gas line cyclone fulfils a key role in the gasifier operation, as the primary separation unit of entrained bed material from the carrier flue gas. As the combustion column operates in the pneumatic flow régime, bed material is entrained in the flue gas as it travels out the top of the column. The heated bed material is the separated by the cyclone and is pneumatically conveyed into the gasification column. The flue gas is piped to a disengaging space and filter trap to reduce fine particulate emissions before exhausting to atmosphere.

A significant quantity of air is fed to the combustion column to support efficient combustion of char and LPG, and after LPG injection approximately 53.5 Nm³/h of 800°C flue gas with entrained bed material exits from the top of the combustion column. The combined flue gas/bed material stream travels down a 30° incline and impacts at full speed, approximately 60 m/s or 0.09*c*, on the cyclone wall. Over time, the 316 stainless steel wall has worn away, as shown in Figure 6.5. This would have been discovered sooner (perhaps catastrophically for any operators in the vicinity) were it not for the many layers of kaowool insulation bound tightly to the steel walls.

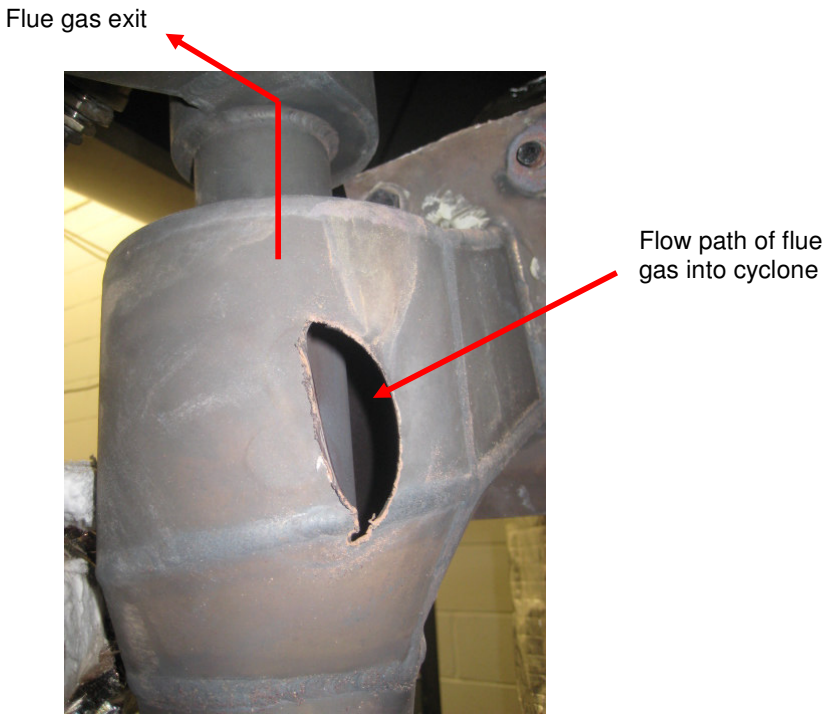

Figure 6.5 – Cyclone damage caused by normal wear of hot flue gas stream and entrained bed material

6.3.2. Siphon Drop Chute Extension

At the conclusion of the 2008 experimental campaign bed material losses from each run were becoming significant, sometimes exceeding 30% of the initial charge. While undoubtedly the cyclone hole contributed to this, the interaction between bed material return to the gasification column and the producer gas exit was identified as being problematic. Bed Material loss is a significant factor in efficient operation of the gasifier. Attrition of the sand over time leads to a smaller average particle size. The smaller particles are more likely to remain entrained in the flue gas and producer gas streams and not be separated efficiently by the respective cyclones, leading to less bed material being available to transport heat from the combustion column to

the gasification column. The original siphon exit design consisted of a 90° bent tube at the top of the gasification column. The horizontal direction was deemed necessary to direct the incoming bed material to the far wall of the column, away from the chute, hence preventing straight-through bed material flow and allowing a bed to accumulate in the base of the gasification column. It was suggested that the proximity of the siphon outlet to the producer gas outlet was contributing to bed material entrainment and loss through the producer gas stream.

To rectify the situation and separate the siphon exit/producer gas outlet, a drop tube was designed that allowed the siphon to discharge 400mm down the column. By discharging at this lower level a greater freeboard height exists which provides a disengaging space for the particle entrainment in the producer gas and allows greater residence time for gas phase reactions. Care was also taken to ensure the tube did not impinge on the height of the bubbling bed and thereby restrict bed material discharge. The tube was again designed to impact the wall opposite the chute inlet to maximise bed loading. Figures 6.6 compare photographs of the 'before' and 'after' arrangements of the siphon discharge. A drawing of the modified siphon discharge system is provided in Figure 6.7. Following replacement of the siphon outlet a build-up of semi-solid bed material was discovered in the horizontal portion of the 90° bend, which may have been restricting bed material flow into the gasification column.

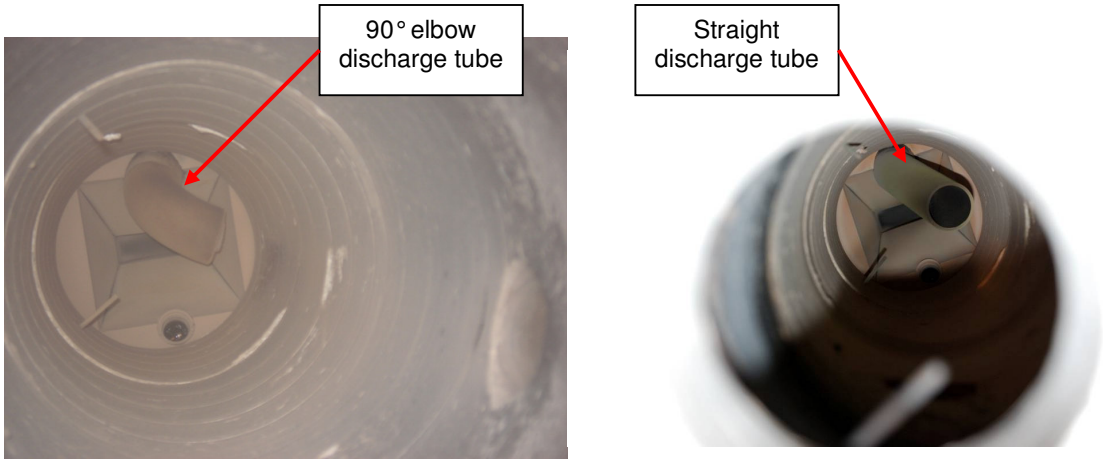

(a) **(b)**

Figures 6.6 (a) and (b) - Photographs of the siphon discharge arrangement (a) before and (b) after modification

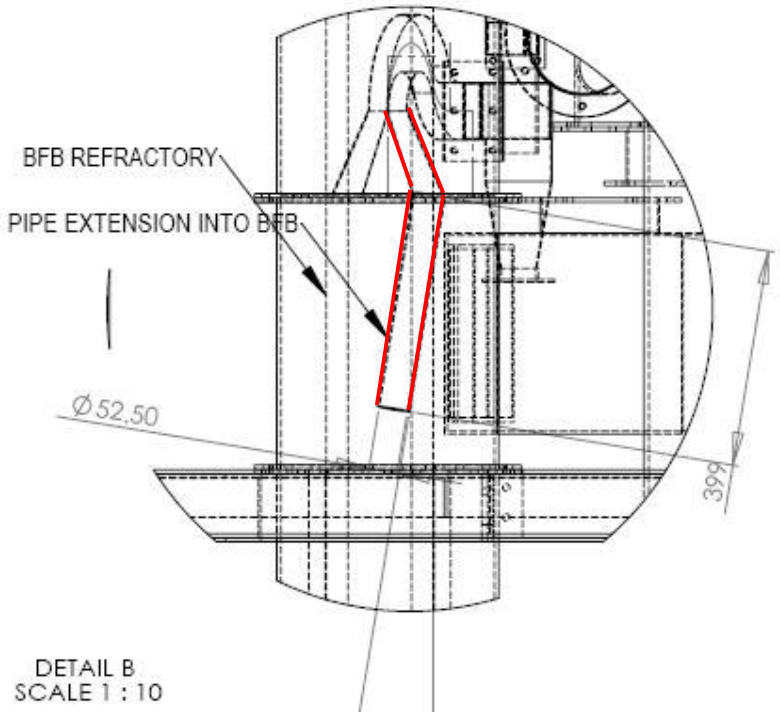

Figure 6.7 – Diagram of modified siphon discharge tube showing discharge angle (care of Lim, M. T., internal publication)

6.3.3. Other Repairs

The gasifier suffers in its capacity as a research plant. The repeated operation of warming up at 2.5°C/min to 770°C (total time approximately 5 hours), short operation time, and cool down over 24-36 hours stresses the plant continuously. The continuous cycling up to operating temperature and back to ambient following a run places great strain on nearly all of the gasifier components. Frequent maintenance is required to minimise material failure. In particular, the steel flange connecting the flue gas exit to the heat exchangers exhibited significant bowing following the year's operations, resulting flue gas leakage and loss of gasifier efficiency. Bed material flow restrictions around the gasifier generally were caused by large cracks in the refractory column internals, especially around the base of the chute, which required repair to improve bed material circulation and gasifier efficiency. Other minor repairs were completed and the gasifier was ready for recommissioning on 20 January 2009.

6.4. BED MATERIAL HANDLING

The work discussed in Chapter 4 shows bed material chemical composition is of critical importance to gasifier performance. Of equal if not greater importance is understanding of the critical physical parameters of the bed material that affect the operation of the plant. Three

factors were identified which play a crucial role in this understanding: fluidisation, agglomeration and comminution (elutriation, particle wear). Experimental observations have led to the design and commissioning of ancillary bed material handling equipment which has improved gasifier operation and performance markedly. Future progress will enable the use of all bed materials for long periods of time, vastly improving the operability and experimental utility of the large scale rig and allow it to become a true proof-of-concept demonstrator.

6.4.1. Bed Material Fluidisation

Fluidisation theory is summarised by Grace [Grace et. al., 1997]. A bed of particles fluidised by a gas stream travelling at increasing velocity U will go through a series of fluidisation régimes, depending on the bed material particle properties. Figure 6.8 shows the transition through the different fluidisation régimes as a function of fluidising velocity. As discussed in §4.3.1, solid particulate materials are classified according to their Geldart groups, which indicates qualitatively the degree of energy required for fluidisation.

The minimum (incipient) fluidisation velocity can be calculated from by considering a correlation between the Reynolds and Archimedes Numbers, given in equation 6.1.

$$\mathrm{Re}_{mf} = \sqrt{\left(27.2^2\right) + 0.0408 Ar} - 27.2 \qquad 6.1$$

$$Ar = \frac{\rho_g \left(\rho_p - \rho_g\right) d_p^3 g}{\mu_g^2} \qquad 6.2$$

$$\mathrm{Re}_{mf} = \frac{d_p u_{mf} \rho_g}{\mu_g} \qquad 6.3$$

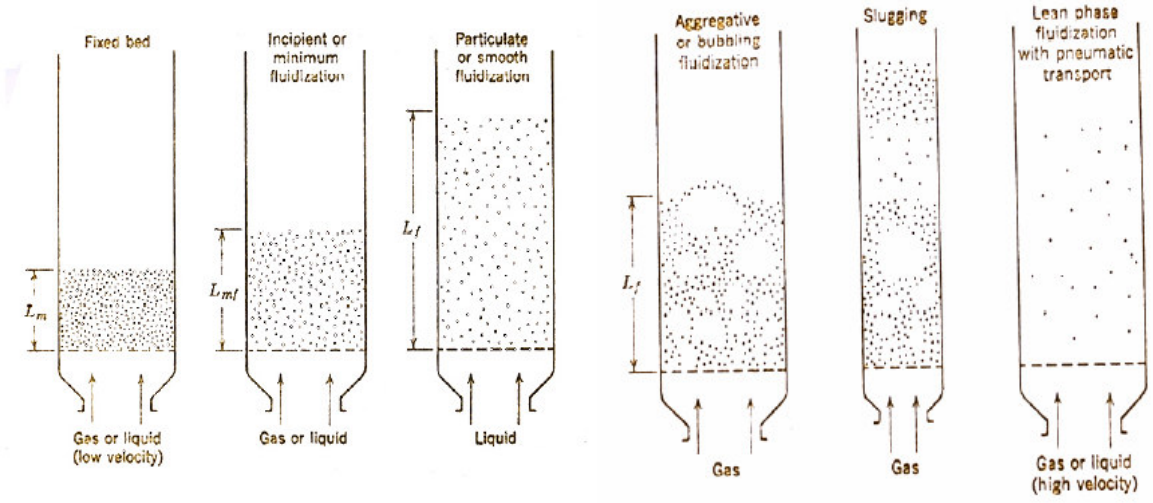

Figure 6.8 – Modes of fluidisation [Chase, n.d.].

Table 6.1 describes the fluidisation properties of bed material components tested in terms of their theoretical fluidisability at the conditions found in the combustion and gasification columns. Average particle diameter is measured by sampling with a 10-stage particle size distribution, usually following sieving to remove most particulates less than 200μm and greater than 1000μm. These limits are imposed based on cyclone separator design and experience with fluidising greywacke sand. The graphical results of the distribution measurement are given in Figure 6.9. Particle density is calculated based on measured bulk density and assuming void fractions of 0.74 for greywacke, olivine and magnetite and 0.5 for calcite and dolomite. These void fractions were estimated by considering particle shape, which was roughly spherical for the first three bed materials and irregular for calcite and dolomite, and typical reported values for the minerals. Minimum fluidisation velocities are calculated using the known density and viscosity values for air at 300°C and 1 bar, and steam at 200°C and 6 bar. As the superficial velocities are much less than 30% of sonic velocity, compression effects have not been factored into the calculations. The calculations and full summary table are given as Appendix E.

Table 6.1 – Fluidisation parameters for the five bed materials trialled.

	Avg particle diameter μm	Particle Density kg/m³	Geldart Group	U(mf) - hot air m/s	Combustion U/U(mf)	U(mf) - steam m/s	Gasification U/U(mf)
Greywacke	249	2068	B	0.021	121.2	0.056	0.6
Olivine	256	2378	B	0.026	97.0	0.068	0.5
Magnetite	157	3243	B	0.008	308.1	0.036	0.9
Calcite	500	2720	D	0.222	11.5	0.228	0.1
Dolomite	512	2840	D	0.249	10.2	0.243	0.1

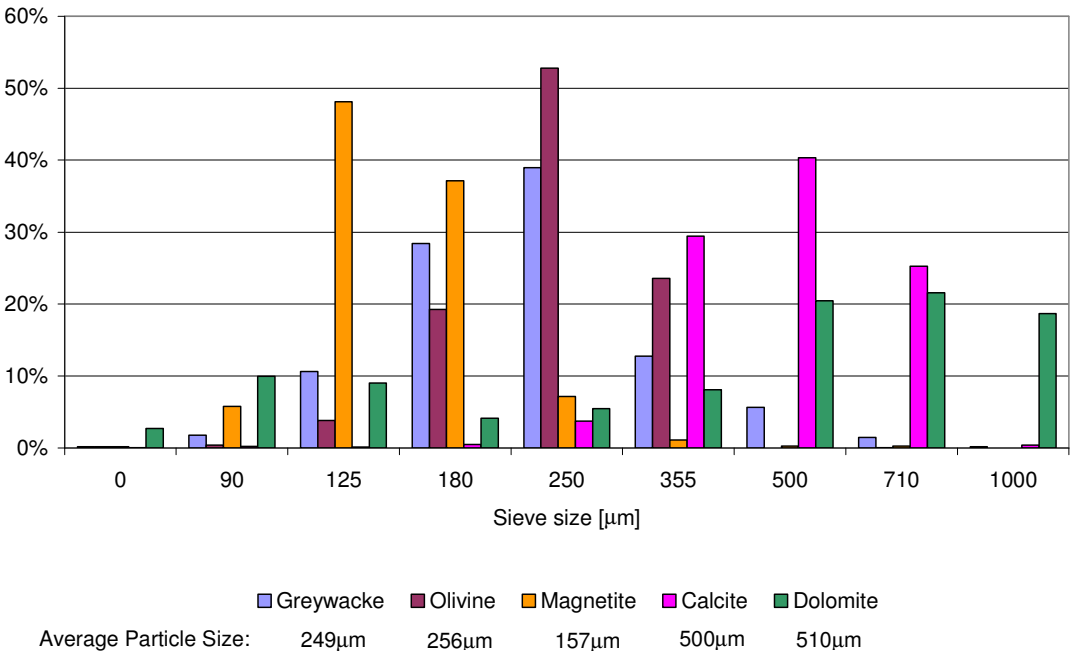

Figure 6.9 – Particle size distributions for the five minerals tested.

The dimensionless superficial velocity ratio U/U_{mf} is used to compare the fluidisability of the different bed materials at the conditions in the combustion and gasification columns. As an example, bubbling fluidisation is typically considered to hold where U/U_{mf} is approximately equal to 6. Despite having much higher particle density, magnetite is theoretically the easiest compound to fluidise, which though unexpected was corroborated during testing. Even so, the calculations suggest that steam flows through the BFB are insufficient to fluidise past incipient fluidisation. In one way this is misleading, as the velocity of steam through the distributor jets is 1.3m/s, or 43 times the superficial velocity through the column. This jet velocity allows the bed to move slightly around the distributor and the bed material to be transferred through the chute; however it also may explain the poor steam conversion and reaction rate in the gasification column, possibly due to channelling through the bed. Calcite and dolomite do not fluidise well, with U/U_{mf} being approximately equal to 11 in the combustion column, suggesting that at least initially a charge of these minerals will sit at the base of the combustion column and not circulate. However, given the softness of these minerals and rapid elutriation that they exhibit under these conditions, reduction in average particle diameter increases the velocity ratio significantly, to the point where pneumatic transport will occur. The variation of velocity ratio with particle size has been investigated for calcite and dolomite under combustion column conditions and plotted in Figure 6.10.

Observations from experimental handling of the different bed material combinations are discussed later in Section 6.5.

6.4.2. Bed Material Agglomeration

During initial commissioning of the gasifier, bed material agglomeration was a significant problem. Agglomeration is generally the result of solid materials with relatively low melting points becoming entrained in local 'hot spots', leading to excessive point heating and melting. Minerals exhibiting this property are predominately compounds of alkali metals such as sodium and potassium. Steam is known to exacerbate the process, perhaps by encouraging formation of mineral hydroxides [Cusumano et. al., 1978]. Conversely, compounds of calcium and magnesium are through to inhibit bed material agglomeration [Lin et. al., 2009]. The molten material then flows to cooler areas of the plant, congeals and traps solid particles in an amorphous matrix. An example of these agglomerates is shown in Figure 6.11. It was encountered following a run using greywacke as the bed material.

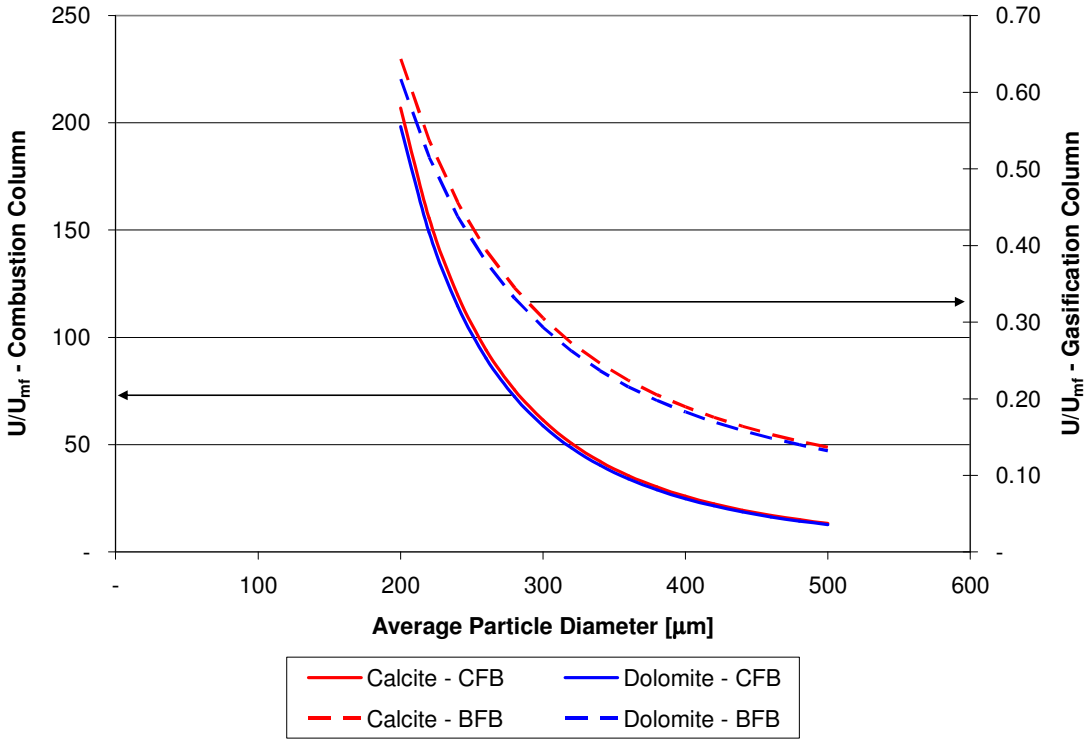

Figure 6.10 – Relationship between dimensionless velocity ratio U/U_{mf} and particle diameter for calcite and dolomite in the combustion (CFB) and gasification (BFB) reactor columns

Figure 6.11 – An instance of agglomeration of bed material that has caused premature plant shutdown. This was taken from the base of the gasification column, surrounding the distributor.

As a result of the above issues operational routines were developed that prevented agglomeration from occurring. Principally, this involves maintaining higher flow rates of air on start-up to ensure sufficient fuel/air mixing during the heat up phase, and to prevent entrainment of bed material which fluidises poorly at low temperatures. Additionally, the shut down procedure was modified to 'drop' the plant immediately, cutting all fuel, air and steam flows and allowing the plant to cool as a solid mass. This ensures that no defluidisation occurs while air and fuel are still flowing, preventing hot spots forming in the bed. Following implementation of these operational procedures, no further agglomeration was experienced for any of the bed materials tested.

6.4.3. Bed Material Comminution

Bed material losses affect gasifier operation as reduction of bed material mass means less heat transfer from the combustion column to the gasification column, limiting gasification reactions. At constant fuel feed rate, it also increases the proportion of char particles in the bed material, effectively increasing average particle size and limiting fluidisation. Prior to modifications to the gasifier allowing addition and removal of bed material during the run, the system effectively operated on a fixed time frame, governed by the rate of bed material comminution.

The elutriation of bed material became most apparent with use of calcite and dolomite minerals. As these minerals are much softer than greywacke or olivine, their rate of wear in the fluid bed environment was severe enough to limit runs to 6 hours or less, compared to the 8-10 hours of normal operation previously available. In extreme cases, the loss of bed material was so great that the producer gas particle trap filled completely, blocking the cyclone and allowing particle-laden gas to the afterburner, where the fines blocked the burner, shutting the plant down.

The rates of bed material comminution were investigated for greywacke, olivine, calcite and dolomite based on the weights of bed material before and after each run. Biomass ash accumulation was not accounted for on the assumption that the ash particle size would be small enough to be entrained in the flue gas and producer gas on formation, and therefore would not accumulate in the bed material. Table 6.2 below shows the average rates of elutriation of the four materials analysed.

Table 6.2 – Average rates of bed material comminution observed during gasifier operations

Bed Material	Elutriation rate [kg/h]
Greywacke	0.25
Olivine	0.26
Calcite	0.57
Dolomite	0.48

6.4.4. Bed Material Feed System

In response to the elutriation of bed material causing short run times and premature plant shut down, a modification to the gasifier was designed and commissioned that allowed addition of bed material while the gasifier is in operation. It was found that the fuel feed augers would not be able to adequately transfer small particles of bed material into the gasifier with the fuel feed, thus a separate system was designed for this purpose.

The bed material feeder makes use of the existing sight-glass tube mounted on the side of the combustion column, which is used to monitor fluidisation in that reactor. An elbow was mounted to the tube allowing a knife-gate valve and a capped vertical storage tube to be attached. Figure 6.12 shows the configuration of the bed material feed system.

Operation of the feeder prefers two people, one on the ground floor and one on the second level of the laboratory. The lower operator checks the knife-gate valve closed, permitting the upper operator to remove the cap and add approximately 1.5 to 2.5 kg of bed material, depending on the bulk density. Once the material is added the cap is replaced and the lower operator gradually opens the knife-gate valve, allowing the bed material to enter the combustion column slowly, preventing large thermal shock to the environment. Figure 6.13 shows the temperature profile of the gasifier during the commissioning of the feed system on 24 July 2009. Since that date, the feeder has greatly improved gasifier operations, allowing soft bed materials to be added later in the run and maximising the materials' effects on producer gas composition.

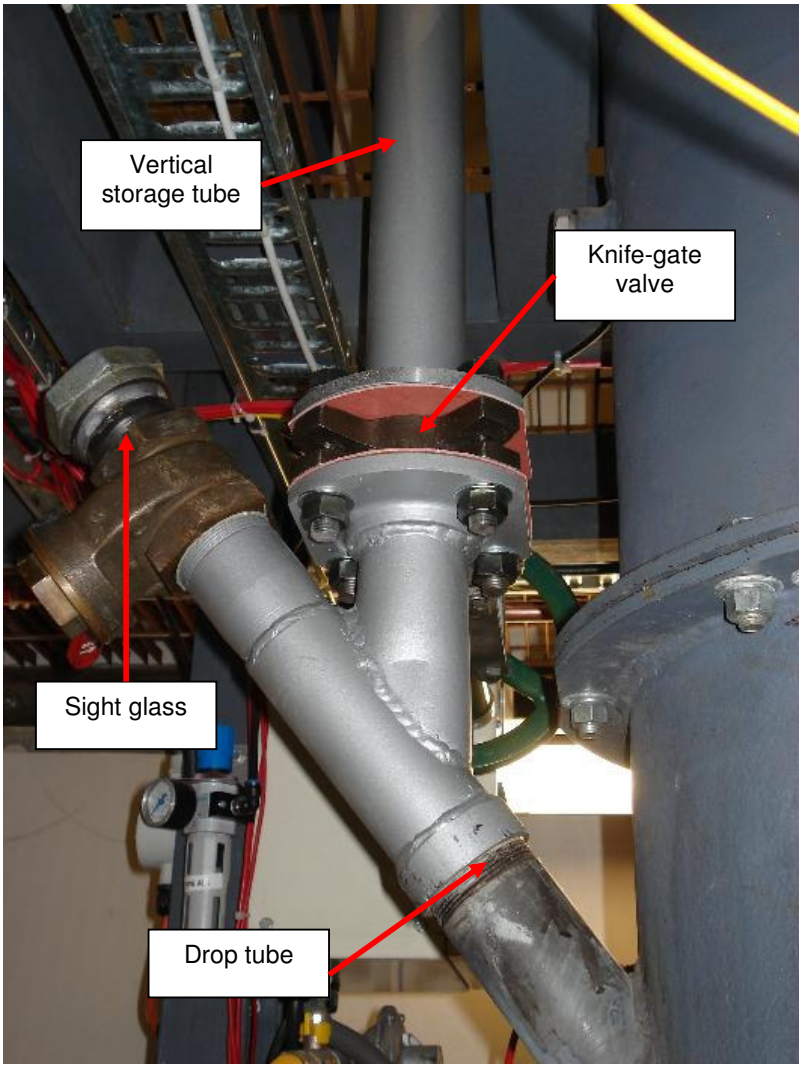

Figure 6.12 – Bed material feeder system with vertical storage tube, knife-gate valve, drop tube and sight glass indicated.

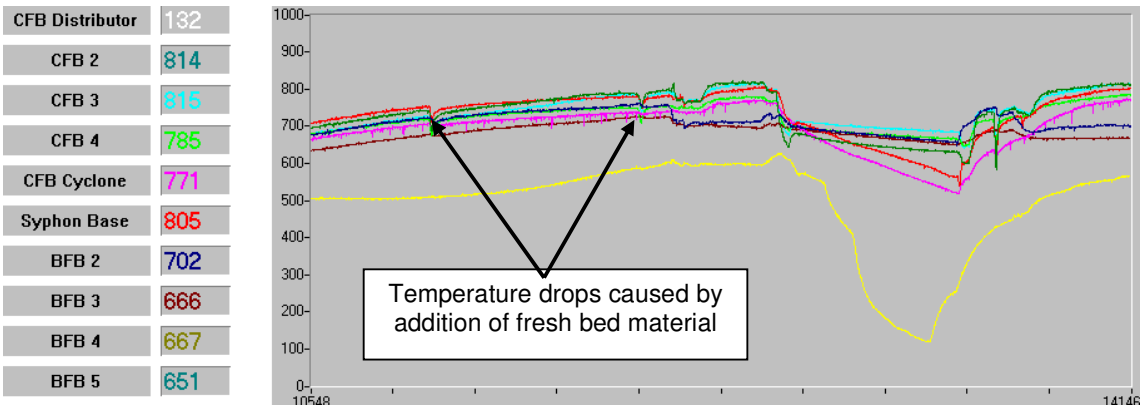

Figure 6.13 – Temperature profile of gasifier operation during run on 24 July 2009. Indicated are the small temperature drops caused by addition of cold fresh bed material.

6.4.5. Producer Gas Particle Trap Modification

Following a number of gasifier runs using soft bed materials, particle separation problems were encountered. Particles entrained in the flue gas and producer gas streams are separated by cyclones prior to downstream exhausting or combustion of the gases. The flue gas cyclone allows bed material to be transferred to the gasification column, with any smaller entrained particles removed in a specially designed particle trap downstream. However, the producer gas cyclone must remove as much particulates as possible as any transfer of solids to the afterburner will cause burner failure. During runs with calcite and dolomite, the amount of fines produced by the elutriation of the bed material exceeded the capacity of the producer gas cyclone's particle bin. This caused the particles to travel downstream into the afterburner, blocking the burners and ending the runs.

In order to enable the gasifier to operate for as long as required in these conditions, a mechanism was developed which allowed the producer gas particle trap to be cleared during operation. This capability was deemed very important as producer gas quality is significantly improved with the use of calcite and dolomite, both of which have high rates of elutriation in the fluid bed environment.

Figure 6.14 shows the modified producer gas cyclone particle trap. The initial design consisted of a cyclone with a particle trap drum mounted directly underneath the cyclone solids outlet. Removing the drum during operation of the gasifier would expose operators to hot, flammable producer gas. The new system allows material to accumulate below the cyclone atop a closed valve. The valve could then be opened during the run to drop the

accumulated particles into the drum. The line could be sealed by closing a second valve and the drum removed, allowing the particles to be removed during operation. The system has not yet been commissioned, but due to its simple design is not expected to cause difficulty.

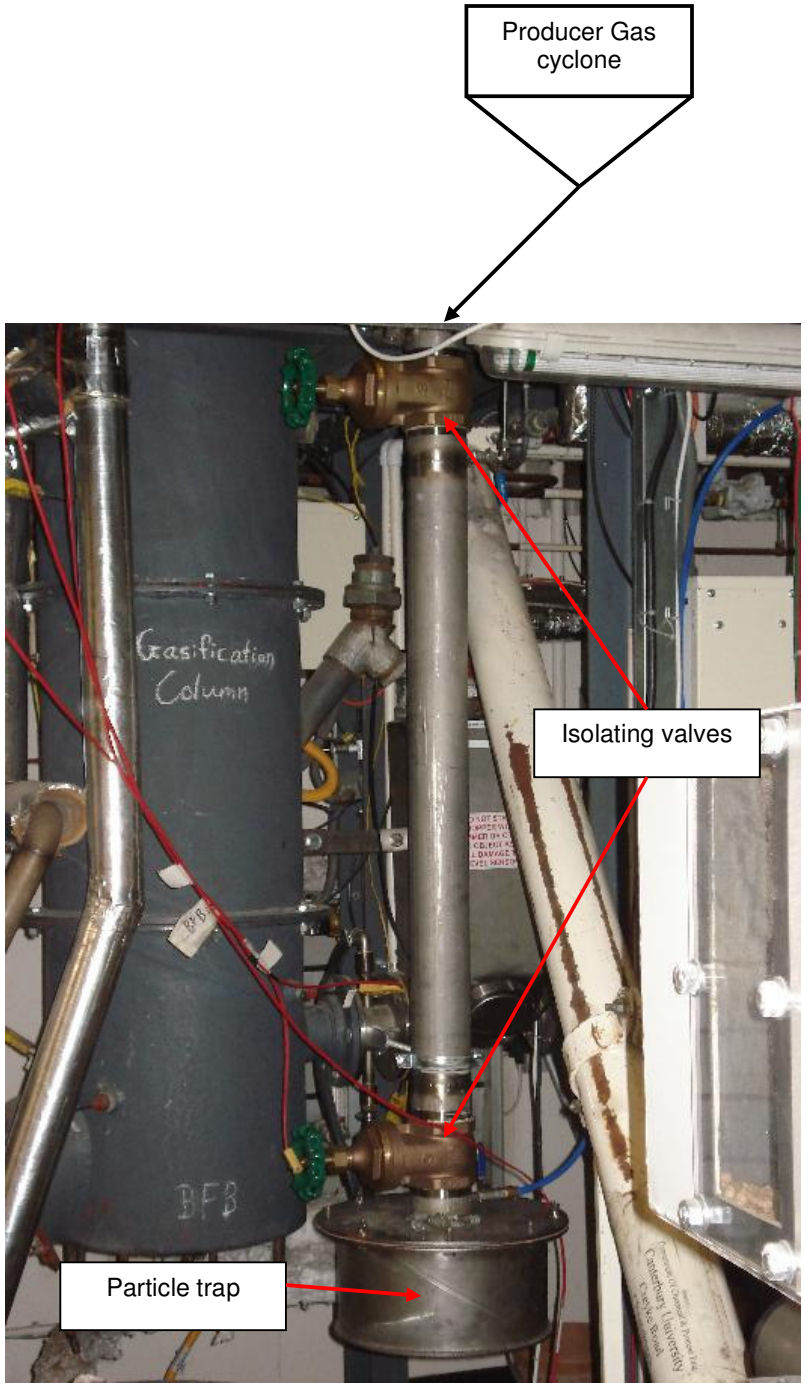

Figure 6.14 – Photograph of the modified producer gas cyclone particle trap with key devices indicated.

6.5. OPERATIONAL OBSERVATIONS

Following commissioning of the repaired gasifier on 20 January 2009, 19 gasification runs were conducted, of which 16 were successful and delivered useful results. The remaining three encountered significant problems prior to measurements being made. Observation of the peculiarities of gasifier operation during this time has revealed numerous issues which may affect future experiments using the 100 kW UC gasifier, and influence the design and operation of any similar larger scale plants commissioned in the future. A selection of significant operational observations is discussed in this section.

6.5.1. Effects of bed material loss

As discussed briefly in §6.4.3 the gradual reduction in quantity of bed material and subsequent emission of fines has a significant effect on bed material circulation, overloading cyclones and fouling burners. These effects limit the operability of the gasifier over time to the point where it must be shut down.

During two runs using a mixture of 50% calcite and 50% olivine as bed material, the elutriation of calcite reduced the quantity of bed material to a dangerously low level. It was theorised that the constant fuel flow and loss of bed material mass caused the average particle diameter of solids in the fluid beds to increase, reducing fluidisability of the bed. This became apparent first in the chute section, where a flow restriction formed. Without the usual quantity of bed material in the combustion column, temperatures rose rapidly, at one point exceeding 1000°C. Conversely, the high quantity of bed material resting in the gasification column increased reactions of the biomass fuel, causing significantly more producer gas to evolve in a short period of time, which was made noticeable by a large flame from the afterburner and a 'roaring' sound. The increased pressure caused by more bed material in the gasification column eventually forced the bed material through the chute into the combustion column, rapidly reducing the combustion column temperatures to approximately 700°C. The onset of the cyclical temperature phenomenon and fear of mechanical failure of the plant led to plant shutdown. Figure 6.15 shows the temperature profile of the gasifier during one of these events.

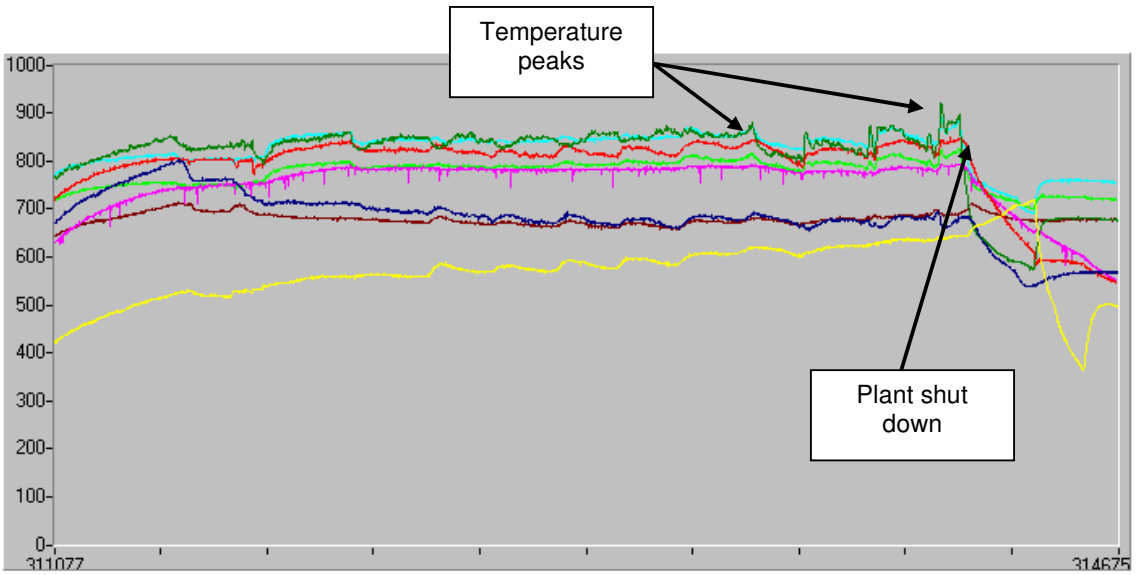

Figure 6.15 – Temperature profile of gasifier during cycling operation caused by low bed material mass with high fuel loading.

In conclusion, biomass fuel loading in the bed material was shown to have a profound effect on solids fluidisation and plant stability. The ability to add bed material during the run to counter losses from attrition has enabled the gasifier to run for long periods with highly comminuting bed materials without showing this instability.

6.5.2. Effects of Fuel Quality

As discussed in section 5.4, experiments were also conducted on biosolids gasification (digested sewage sludge). It was observed that the biosolids showed poorer reactivity than wood pellets, with the 100% biosolids fuel producing roughly half the yield of producer gas than normally observed with wood pellets. In combination with the increased auxiliary fuel requirement, this resulted in a gasifier cold gas efficiency of 19%. Although the best information available suggested the biosolids fuel has roughly the same net calorific value as the wood pellets (18-20 MJ/kg) [Bouman, 2009], this was not consistent with the results of the gasification experiments. However, the fuel structure may be at least partially the cause for the resultant decrease in gasifier performance.

Wood pellets are made from sawdust by using high compressive forces to bind the sawdust into a pellet. Examination of the wood pellet char particles following the gasifier runs shows that despite large residence times in a highly abrasive environment, the pellets continue to hold their form. Conversely, the biosolids was dried and formed in a rotary dryer / drum granulator, resulting in particles of lower density and amorphous structure. During the biosolids fuel experiments, run times were notably shorter due to producer gas particle trap

overloading. On examining the particles collected in the trap, a large amount of unreacted fuel was present in the mixture, mostly from the biosolids. It is suggested that the amorphous nature of the biosolids pellets resulted in premature breakdown in the fluid bed, with the smaller fuel particles becoming entrained in the gas and drawn out of the gasifier far sooner than char from the wood pellet fuel. This fuel loss appears to be at least one cause of the reduced gasifier efficiency and lower producer gas yield.

It is recommended that operators of future trials of alternative fuels in the gasifier need to examine the suitability of the fuel which needs to resist the highly abrasive environment within the dual fluidised bed system. In addition to the drying stage of fuel pre-treatment, compression of amorphous fuels such as biosolids and sawdust into pellets would greatly enhance the residence time of the fuel in the reactors, improving gasifier performance.

6.5.3. Performance of New Fuel Feed System

In October 2008, the new fuel feed system was commissioned which allowed fuel to be fed into the base of the bubbling fluidised bed in the gasification column, which increased heat transfer to the fuel compared to the previous top-fed system, and improved gasifier performance [Bull, 2008].

During the 2009 experimental programme, the fuel feeder largely performed very well. However on two occasions, gasifier runs had to be stopped prematurely due to fuel feed blockage. In the first instance, a plug developed at the mouth of the in-bed feed port. On examination the plug appeared to be an agglomeration of fused bed material and partially gasified sawdust. Attempts during the run to clear the plug by force resulted in significant damage to the shaftless screw auger, as shown in Figure 6.16.

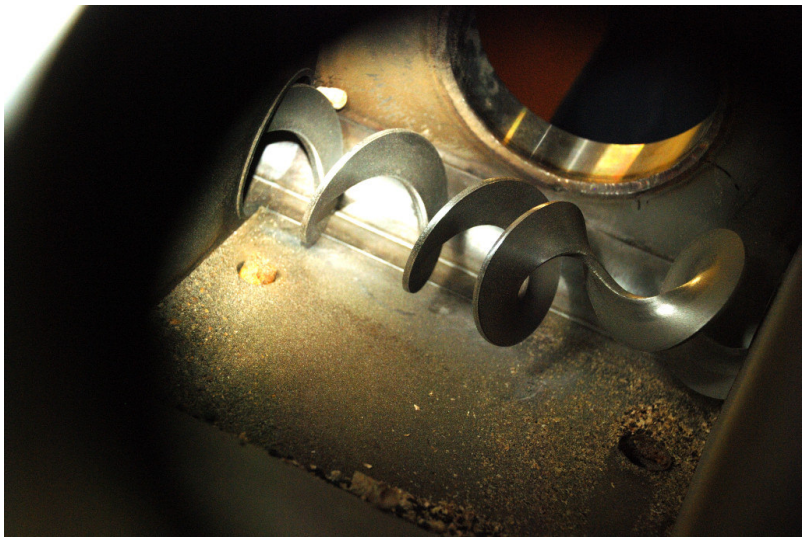

Figure 6.16 – Warping of the in-bed screw auger following attempts to force through a solidified plug at the feeder outlet.

Following this damage, the auger was removed and a shaft was added to strengthen the auger flighting. A second encounter with plugging was experienced on a subsequent run, and although no damage was caused to the auger in trying to clear the plug, the plug could not be removed by increase in power from the motor. Following this second event a torque rod was added to the shaft of the auger so manual torque could be applied to clear any plugs in future. Additionally, pre-run operating procedure was updated to ensure no plugging was present before the next experiment.

6.5.4. Damage to the Gasifier during 2009 Experiments

Following the series of experiments performed in 2008, numerous repairs were undertaken and the gasifier was recommissioned prior to further operation, as discussed in Section 6.2. At the conclusion of the 2009 experimental programme, many of the same mechanical faults experienced in the previous year were present, in addition to other damage caused by normal operation. Analysis of this damage has revealed some design faults which require further investigation.

Constant thermal expansion and contraction has caused significant wear and tear to the column internal walls and other refractory sections, as shown in Figures 6.17. The formation of cracks leads to abrasion of the refractory by the hot sand flow, causing sand loss and further damage. In the chute, fracturing of the refractory has caused large sections to fall away, which could restrict bed material flow during operation and has led to defluidisation of the bed material in the chute.

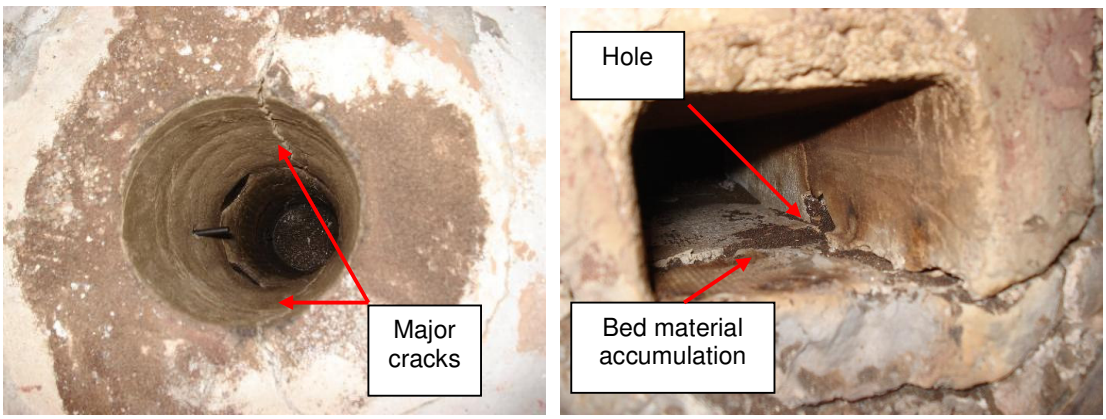

(a) (b)

Figures 6.17 (a) and (b) – Damage caused to (a) the combustion column and (b) the chute section by repeated heating and cooling of the plant. Note the accumulation of bed material in the chute and the presence of holes and cracks.

The opening of cracks caused by expansion and contraction of dissimilar materials has caused damage to the chute fluidising sparger. A hairline crack in the supply tube caused steam to bore a large hole in the surrounding refractory material, which has limited steam supply to the chute and consequently reduced fluidisation, causing infiltration of flue gas into the gasification column. Figures 6.18 show the location of the crack in the supply tube and the hole in the refractory, which are currently undergoing repairs.

(a) (b)

Figures 6.18 (a) and (b) – Damage to the chute refractory (a) caused by a hairline crack in the chute sparger supply tube (b) (circled).

In addition to the thermal damage to the refractory, extraordinary wearing was present on the steel sections of the plant. Shortly after recommissioning a small fissure developed around the weld connecting the steel combustion column riser to the refractory reactor section, as shown

in Figure 6.19. This allowed hot bed material to escape the column and caused the third run of the programme to end prematurely.

Figure 6.19 – Crack in weld at union of combustion column riser and refractory sections.

Similarly, the repaired flue gas cyclone was again damaged due to wear from the flue gas stream after a series of gasification runs. As shown in Figures 6.20, the damage to the cyclone was almost identical to that from the previous incident as described in §6.3.1. Discussions regarding an improved design for the cyclone are continuing within the Department.

(a) **(b)**

Figures 6.20 (a) and (b) – Damage to the flue gas cyclone caused by ongoing wear from the solids-laden flue gas stream. The original hole is shown in (a) while the second hole following the 2009 programme is shown in (b).

6.6. CONCLUSIONS AND RECOMMENDATIONS

Following the 2008 experimental programme, numerous design changes and repairs were made to the gasifier which have improved gasifier performance. Repairs to the flue gas cyclone and heat exchanger flanges were necessary for the gasifier to run in the new year, and at the time the opportunity was taken to redesign and replace the bed material drop pipe from the siphon to the gasification column in an effort to limit bed material losses. A new system for feeding fuel into the gasification column was installed and verified to operate well during the 2009 experiments, showing improvements in gasifier performance.

Following commissioning and in accordance with the aims of the research, further changes were made to the bed material handling system. Highly comminutive bed materials such as calcite and limestone need to be constantly replenished to maintain their positive effect of gasifier performance and producer gas composition. A bed material feed system and modifications to the producer gas particle trap have allowed addition of bed material and removal of fines during gasifier runs, improving system stability and extending run time.

Analysis of the physical properties of the bed materials tested showed small particle sizes are required for gasifier operation, with larger particles (diameters above 500μm) highly resistant to fluidisation. Using the theories of fluidisation presented in Grace [Grace et. al., 1997] it was shown that the superficial velocity of steam into the gasification column at normal flow rates is insufficient to maintain bubbling fluidisation. It was suggested that this could be a cause of the predicted poor utilisation of steam by the gasification reactions. Further investigation of the fluidisation of the bubbling bed is recommended to ascertain the extent to which gasifier performance is being impeded.

Operation of the gasifier throughout 2009 has raised a number of issues which require attention to ensure successful running in the future. Bed material loss and consequently high fuel pellet loading in the bed has shown to cause system instability and eventual failure. This has been corrected by the addition of the bed material feed system and modification to the producer gas particle trap. Experiments using soft, amorphous grains of biosolids suggest that fuel quality has a significant effect on gasifier performance, as compressed wood pellets showed higher resistance to elutriation and hence higher residence time in the gasifier. Normal operation of the gasifier creates a lot of stress on the refractory and steel structure of the system, and regular maintenance of the flue gas cyclone and chute section especially is required for optimal, safe operation.

7. Economic Analysis

7.1. INTRODUCTION

7.1.1. Value-Added Biomass Gasification

Biomass gasification has been developed principally as a conversion technology for renewable energy generation. Experimental investigation in this project including the catalytic bed material investigation in this research has shown that not only is the biomass gasification producer gas suitable for combined heat and power (CHP) generation, but with improvements to the process the high-hydrogen content producer gas is also suitable for production of pure hydrogen and synthetic liquid fuels. Previous study undertaken by this research team [Penniall & Williamson, 2009] has included economic evaluations of biomass gasification systems applied to sawmills and Medium Density Fibreboard (MDF) and Laminated Veneer Lumber (LVL) process plants. This study has considered that the producer gas is used for either cogeneration of heat and electricity, or for production liquid fuels by the Fisher-Tropsch process. The study has concluded that whilst the process has a positive payback, high capital costs and relatively inexpensive electricity in New Zealand conspire to render the Biomass Integrated Gasification Combined Cycle (BIGCC) processes utilising either gas turbines or gas engines uneconomic in the timber industry for which the technology has been traditionally intended. Other authors have considered hydrogen production from biomass gasification and evaluated its economic potential in various international contexts [Gnanapragasam et. al., 2009; Ji et. al., 2009; Sequeira et. al., 2007; Koppatz et. al., 2009; Sues et. al., 2009].

Hydrogen and synthetic liquid fuels are higher value products compared to electricity, especially in the New Zealand context where large capacity hydroelectric and geothermal plants generate relatively cheap electricity much of the time. Conversely, 48% of hydrogen globally is produced from diminishing resources of natural gas [US DOE, 2009], while crude oil is also becoming increasingly less available at current drilling capacity. The values of these commodities remain largely speculative and very sensitive to numerous economic and geopolitical factors. Despite this, in both cases it is nearly certain that in the long term, and barring any significant technological paradigm shifts, their value will increase, as combating climate change and responding to diminishing fossil fuel resources become governmental priorities. The long-term economic potential of biomass gasification therefore lies in its

ability to produce these commodities, whilst limiting the high capital cost that to date has rendered combined heat and power applications uneconomic.

7.1.2. Summary of existing modelling

The biomass gasification technology developed by this research team has been initially targeted to be used in wood processing plants with annual production of approximately 80,000 to 120,000m³ of respective products of sawn timber, MDF and LVL. [Rutherford, 2006; Penniall & Williamson, 2009]. These processes have associated waste woody biomass streams which are used as energy plant fuel. The energy requirements of the processing plants are approximately 1.5 to 5 MW electrical power and 8 to12 MW thermal power. The modelling methodology has incorporated the gasification chemical equilibrium model developed by Rutherford [Rutherford, 2006] which can be used for predictions for the producer gas composition and yield. This model has been run with HYSYS software together with an economic model as well as energy demand model in order to perform feasibility studies. The key equipment sizing parameters are applied to capital plant cost relationships developed by Ulrich and Vasudevan [Ulrich & Vasudevan, 2004] and Bouman [Bouman et. al., 2005].

The results of the modelling have shown that as energy plant, biomass gasification is uneconomic for sawmill and LVL process plants of 100,000m³ annual production scale. Applied to MDF plants, the economic modelling is more favourable, with low break even electricity costs and a 12.5 year discounted payback period. The main reasons for the poor economics are the high capital costs of biomass drying plant, the value of the risk associated with implementing 'new' technology, and the relatively low cost of electricity in New Zealand. This results showed that the breakeven cost of electricity for the plant ranges from 4.0 ¢/kWh in the MDF scenario to 11.6 ¢/kWh in the sawmill [Penniall & Williamson, 2009], compared with the average wholesale electricity price of approximately 5 ¢/kWh for 2009 [M-Co, 2009]. The results have shown significant sensitivity to capital cost and it is likely that further development of the technology will improve its economic potential.

7.1.3. Hydrogen utilisation

In the proposed Hydrogen Economy, the utility of the resource is maximised through the use of fuel cells. As discussed in §1.4.2, numerous fuel cell technologies are currently available or in development, which are categorised as being mobile, small-scale units ('stacks') of up to

200 kW_e capacity, or stationary, large-scale stacks exceeding 1 MW_e output. Based on current technology two types of fuel cell are considered in this analysis, Molten Carbonate Fuel Cells (MCFC) and Proton Exchange Membrane Fuel Cells (PEMFC). MCFCs operate at 650°C and utilise both hydrogen and carbon dioxide as fuel, making them particularly suitable for integration with biomass gasification plant for stationary power generation. Though still under development, commercialisation of this technology is expected in the near future and researchers suggest electrical efficiencies of 55-60% may be obtained [Bischoff, 2006]. PEMFCs have received considerable attention recently as automotive power plants, as hydrogen produced from renewable sources offers the only means of completely displacing carbon dioxide emissions from fossil fuels. PEMFC-powered cars such as the Honda FCX Clarity (as shown in Figure 7.1, with performance figures given in Table 7.1 below) are on the edge of commercialisation and currently operate in southern California, where hydrogen refuelling infrastructure already exists. The Honda is notable as it was the first Fuel Cell Vehicle to boast competitive performance figures when compared to similarly-sized fossil-fuelled vehicles.

Figure 7.1 – Honda FCX Clarity Fuel Cell Electric Vehicle [American Honda Motor Co. Inc., 2009]

Table 7.1 – Comparative performance figures for the Honda FCX Clarity fuel cell vehicle and the equivalent petrol-powered model, a 2008 Honda Accord Euro

	Honda FCX Clarity 2008	Honda Accord Euro 2008
Power plant	PEMFC, 100kW	2.4L petrol engine, 140 kW
Torque	256 Nm	234 Nm
Max Speed	160 km/h	227 km/h
Fuel Capacity	3.92 kg H_2 (5000psi)	65L
Range	430 km	730 km

7.1.4. Scenarios for Analysis

The economic analysis presented here considers two scenarios for hydrogen production from biomass gasification. Firstly, a dedicated hydrogen production facility is considered, for providing the Canterbury region with hydrogen in the event of significant demand for fuel cell powered vehicles. Alternative industries with significant demand for high purity hydrogen include the petroleum industry where hydrogen is used in hydrocracking processes, or in the production of ammonia. Neither of these alternative industries presently exists in the region. The proposed facility would utilise all of the available biomass wastes from timber processing in the region, which have been evaluated by Li [Li, 2008]. In addition to a pure hydrogen product stream, a medium calorific value producer gas by-product would be used as a fuel for an energy plant, with a heat/electricity split based on demand. The proposal is unique compared to the previous models as it considers a far larger biomass feed stream and details the purification equipment necessary for the production of fuel-cell grade hydrogen.

The second scenario considers utilisation of the same biomass feed stock presented in Scenario 1 in a centralised power plant producing electricity using MCFC stacks and a steam bottoming cycle from the waste heat produced in the plant. The gas conditioning requirements are less stringent for generation of electricity with an MCFC compared with producing pure hydrogen; consequently less capital plant expenditure is expected.

7.2. SCENARIO 1 – PURE HYDROGEN PRODUCTION

7.2.1. Description of the Process

A schematic diagram of the process is given in Figure 7.2. Raw biomass feedstock is transported to a centralised biomass gasification–hydrogen production facility in the Canterbury region. Total available biomass is estimated at 120,000 oven-dried tonnes (odt) per year [Li, 2008], which has an initial moisture content of 120% (dry basis). The waste is classified on site with any larger pieces ground to suitable size, then dried to a moisture content of less than 12%.

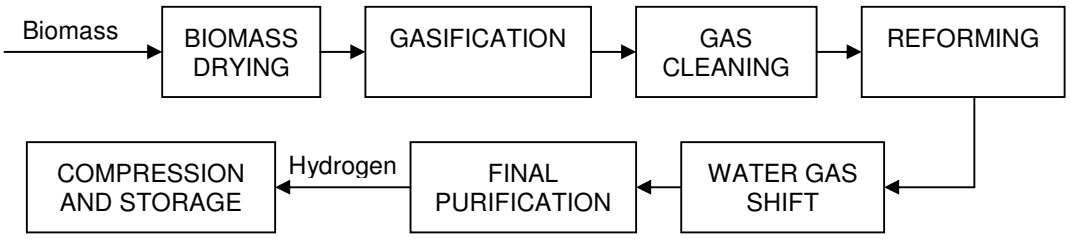

Figure 7.2 – Block flow diagram of the hydrogen production from biomass gasification process.

The dried biomass is fed to a dual fluidised bed gasifier of similar design to the UC gasifier. This type of gasifier is chosen based on the high hydrogen content producer gas and experience of design and operation from the current studies. Above these, the technology has been proven at an 8MW CHP plant in Güssing, Austria [Koppatz, 2008]. The feed rate equates to 15 t/h, or 84 MW based on a lower heating value of 20.13 MJ/kg (see Appendix A). At a steam/biomass ratio of 0.8 approximately 12 t/h steam is required, or 9.3 MW. The gasifier produces approximately 41,400 Nm³/h of 800°C flue gas which is bag filtered then passes through a heat recovery chain, heating gasifier air and steam and finally fuelling a heat recovery steam generator (HRSG). Using the optimum values of producer gas yield from the research presented in Chapter 4 as an estimate, approximately 10,600 Nm³/h dry producer gas (47.4 MW lower heating value) is formed with a composition presented in Table 7.2.

Table 7.2 – Producer gas composition and flow assumed for modelling study, based on figures from CO_2-absorption enhanced gasification at CHP-Güssing in Austria [Koppatz, 2009].

Component	mol%
Hydrogen	51
Methane	13
Carbon monoxide	17
Carbon dioxide	13
Ethene	5
Ethane	1
Flow rate [Nm³/h]	12660
Moisture [kg/h]	1932
LHV [MJ/Nm³]	16.1
Temperature [°C]	650

The producer gas then goes through clean up and upgrading operations. The gas is cooled to 180°C and bag filtered, then goes through a biodiesel scrubbing system to remove tar and moisture. Based on the gas cleaning technology developed by Mwandila [Mwandila, 2008], biodiesel is used for scrubbing the tars from the producer gas and then a stream of hot air

flows through the used biodiesel in a stripper for tar recovery. Finally the tar-loaded hot air is fed to the combustion column for incineration. The value of recycling the biodiesel is currently high due to the price and scarcity of the resource: other models estimate that a biodiesel scrubbing system without recycle would consume approximately 5mL-biodiesel/ m³-gas, with a value of approximately $1.2M annually. After the gas cleaning process, the producer gas, now at approximately 40°C, is compressed in a multi-stage turbocompressor to 32 bar and heated to 850°C for reforming which converts 99% of the light hydrocarbon gases and residual tar to carbon monoxide and hydrogen. The reformed gas consists of hydrogen, carbon monoxide and carbon dioxide with some residual water. This gas is shifted in high temperature and low temperature reactors to increase hydrogen content and reduce CO concentration to a minimum. Finally, CO_2 and other gaseous impurities are absorbed using Pressure Swing Adsorption (PSA). The final product is 99.9999% pure hydrogen with a recovery selectivity of 85% [Criscuoli et. al., 2001]. This is compressed to 700 bar for storage. Figure 7.3 shows the detailed flow diagram for the process, while Tables 7.3 and 7.4 summarise the key parameters of the major streams.

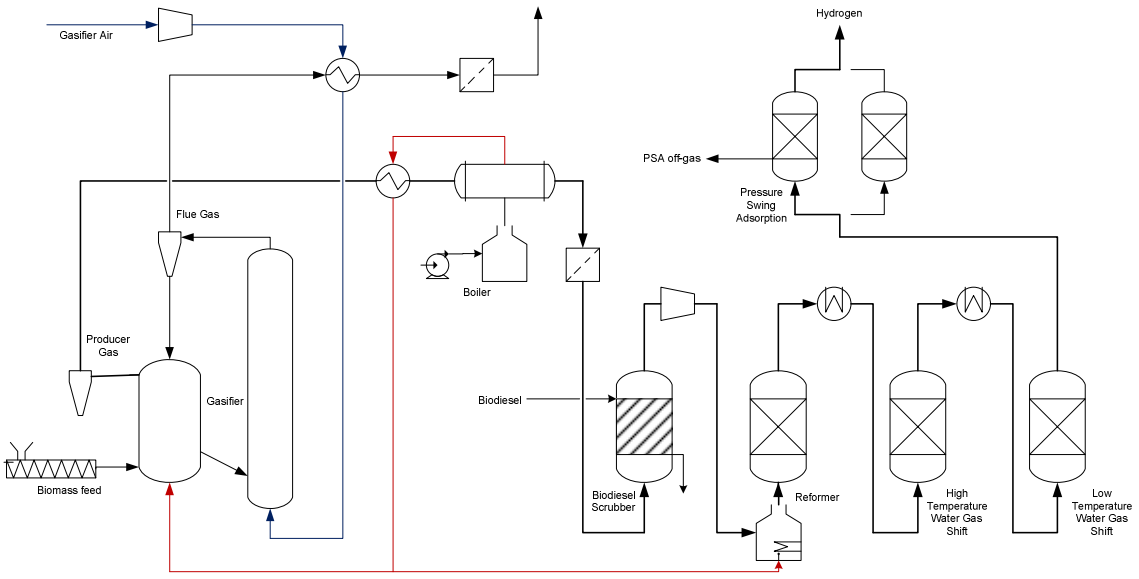

Figure 7.3 – Flow schematic of Scenario 1 process.

Table 7.3 – Description of Scenario 1 major streams

Stream	Description	Stream	Description
1	Raw wood waste to dryer	8	Producer Gas to Reformer
2	Gasifier wood feed	9	Reformed Gas to WGSR
3	Gasifier steam	10	Shifted Gas to PSA
4	Gasifier air	11	Hydrogen Product
5	Producer Gas ex Gasifier	12	PSA off-gas
6	Cooled Producer Gas	13	Flue Gas ex Gasifier
7	Producer Gas to Scrubber	14	Flue Gas exit

Table 7.4 – Summary of Scenario 1 mass flows and conditions of the major streams described above

Stream		1	2	3	4	5	6	7
Pressure	bar	1	1	6	2	1.2	1.2	1.2
Temperature	°C	20	40	433	420	650	440	180
Flow	kmol/h	0	0	666.1	2701	672.1	672.1	672.1
	kg/h	33000	15000	12000	-	-	-	-
	Nm³/h	-	-	-	-	-	-	-
Composition	H2	-	-	-	-	0.510	0.510	0.510
	CH4	-	-	-		0.130	0.130	0.130
	CO	-	-	-	-	0.170	0.170	0.170
	CO2	-	-	-	-	0.130	0.130	0.130
	C2H4	-	-	-	-	0.050	0.050	0.050
	C2H6	-	-	-	-	0.010	0.010	0.010
	N2	-	-	-	0.790	-	-	-
	O2	-	-	-	0.210	-	-	-
	wood	-	1.000	-	-	-	-	-
Moisture	kg/kg	1.2	0.12	1	-		-	-
	kmol/kmol	-	-	-	-	0.19	0.19	0.19
	kmol/h					127.7	127.7	127.7

Stream		8	9	10	11	12	13	14
Pressure	bar	32	30	29	29	29	1.2	1.2
Temperature	°C	850	850	250	20	250	800	180
Flow	kmol/h	564.8	1078	1534	725.8	808	2088	2088
	kg/h	-	-	-	1463	-	-	-
	Nm³/h	-	-	-	-	-	-	-
Composition	H2	0.510	0.669	0.734	1.000	0.292	-	-
	CH4	0.130	0.008	0.006	-	0.017	-	-
	CO	0.170	0.245	0.002	-	0.005	-	-
	CO2	0.130	0.078	0.258	-	0.686	0.097	0.097
	C2H4	0.050	-	-	-	-	-	-
	C2H6	0.010	-	-	-	-	-	-
	N2	-	-	-	-	-	0.835	0.835
	O2	-	-	-	-	-	0.068	0.068
	wood	-	-	-	-	-	-	-
Moisture	kg/kg	-	-	-	-	-	-	-
	kmol/kmol	-	0.151	0.241	-	0.458	0.115	0.1149
	kmol/h	0.0	162.8	369.6	0.0	369.6	239.9	239.9

7.2.2. Capital Cost Analysis

The cost of major plant items as shown in Table 7.5 and Figure 7.4. The scale of the plant has been determined by using various HYSYS-based thermodynamic models to establish key parameters upon which the cost correlations are based, as described in Table 7.5. These cost correlations have been adapted from previous analyses by the research team, in order to maximise comparability between the models. The extents of the reforming and water gas shift reactions have been modelled according to typical yields based on numerous literature sources [Lobachyov & Richter, 2007; Criscuoli et. al., 2001].

Table 7.5 – Cost correlations used for capital cost estimation.

Equipment type	Cost Parameters	Cost Correlation	Reference
Rotary drum dryer	Moisture removed x [t/h]	MPIC (NZ$) = $3.5\times10^5 x + 3.5\times10^5$	Penniall, 2008
Column (empty)	Diameter D [m] Height H [m]	MPIC (NZ$) = $(3952D + 965)H^{(0.9749 - 0.0518D)}$	Rutherford, 2006
Cyclone	Flow q [m³/s]	MPIC (NZ$) = $2330q^{0.912}$	Rutherford, 2006
Blower	Flow q [m³/s]	MPIC (NZ$) = $771q + 2.4\times10^3$	Rutherford, 2006
Burner		MPIC (NZ$) = 12,000	Rutherford, 2006
Steam generator	Heating duty [kW]	Figure 5.25, Ulrich & Vasudevan, 2004	
Heat exchanger[1]	Area A [m²]	MPIC (NZ$) = $15600A^{0.566}$	Bouman, 2005
Bag filter	Flow q [m³/s]	MPIC (NZ$) = $23355q^{0.6622}$	Penniall, 2008
Scrubber column	Flow q [m³/s]	MPIC (NZ$) = $22199q^{0.5973}$	Penniall, 2008
Packed column[2,3]	Internal Volume [m³]	Figure 5.33 (Vertical tower gas contactor), Ulrich & Vasudevan, 2004	
Reformer furnace	Heating Duty [kW]	Figure 5.27, Ulrich & Vasudevan, 2004	
Compressor[4]	Fluid Power w_f [kW]	MPIC (NZ$) = $1210w_f$	Bouman, 2005
Contingency and Fee		15% × Plant Capital	Sinnott, 2005
Working Capital		1% × Plant Capital	Sinnott, 2005

Note:

1 Heat exchanger area is calculated from values for UA which are calculated by HYSYS. Value for U = 56.8W/m².K comes from Douglas [Douglas, 1988].

2 Reformer column and Pressure Swing Adsorption columns are based on residence times of 0.1s for reforming and 15s for PSA

3 Water gas shift reactor sizes are calculated by simple plant scale-up calculation, with a scale factor = 0.66, from Criscuoli [Criscuoli et. al., 2001].

4 Compressor fluid power is calculated by HYSYS, using an isentropic efficiency of 75%.

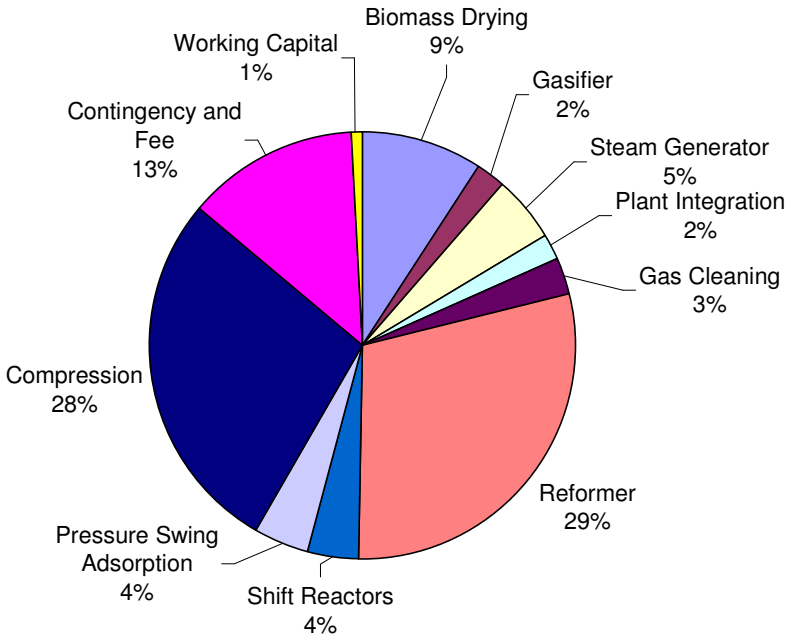

Figure 7.4 – Capital cost breakdown of proposed hydrogen production plant

7.2.3. Operational Cost and Cost of Hydrogen

Operational cost approximations are based on figures available in Coulson and Richardson's Chemical Engineering Textbook series Volume 6 [Sinnott, 2005], and have been used by previous authors [Rutherford, 2006; Penniall, 2008]. Operational costs are summarised in Table 7.6, with consumables unit prices included for reference. Woody biomass has been given an intrinsic cost of $2.00/GJ which equates to approximately $40/oven dried tonne (odt). Transport of wood waste has initially not been included in the operational cost analysis as no reliable information on the cost of transport throughout the region was available, however, transport cost has been taken as a variable for later sensitivity analysis. The cost of biodiesel used in the gas scrubbing process has not been included as the biodiesel is heavily recycled, thus total usage would be negligible compared with other material costs. 95% of the electricity consumed is used by the compressors, due to their high power requirement. In this setting however it is likely that another motive force would be used, most likely the off-gas from the pressure swing adsorption process which has a heat flow of 29.2MW. Labour has been calculated based on two full time operators with associated supervision. As costs for water-gas shift and steam reforming catalysts and pressure-swing adsorbents are unavailable, this has been factored into the Operating Supplies.

Table 7.6 – Operational cost summary for the proposed hydrogen production plant

Item		Unit Cost			Total
Raw Materials	Wood	$ 2.00	/GJ	$	4,831,000
	Transport	$ -	/t	$	-
Utilities	Electricity	$ 0.10	/kWh	$	4,125,000
	Biodiesel				negligible
Labour	Operators	$ 20.00	/h	$	320,000
	Supervisors	15%	*Op Lab	$	48,000
	Admin & O/H	60%	*Lab + Maintenance	$	1,090,000
Other	Maintenance	2%	*Cap Cost	$	1,449,000
	Local Taxes	1%	*Cap Cost	$	725,000
	Insurance	1.5%	*Cap Cost	$	1,087,000
	Operating Supplies	15%	*Maintenance Cost	$	217,000
TOTAL				**$**	**13,892,000**

Based on the capital and operational costs calculated, a net present value analysis shows that for this plant with a 20 year lifetime and at a discount factor of 8%, the break-even cost of hydrogen production is $1.73/kg ($1.73/gallon of gasoline equivalent, 'gge'). This compared very favourably with the US Department of Energy's goal of US$2.00-$3.00/gge, based on the energy efficiency of a fuel cell vehicle on a cost-per-mile basis [US DOE, 2005]. A plant of this type selling hydrogen at US$2.00/kg (NZ$3.64/kg) would be cash-flow positive after the first year, and have paid back the capital investment in 3 years. The model does not account for tax on revenue or tax back from depreciation. If a tax on revenue of 30% is imposed, with 10% straight line depreciation from which tax is claimed back, the cost price of hydrogen over the 20 year lifetime of the plant is $2.29/kg.

7.2.4. Discussion

In general, the economic analysis of hydrogen production from biomass gasification appears to be very favourable. The plant as designed would produce approximately 11,700 tonnes of hydrogen annually. The ability of the plant to sell the hydrogen however is contingent upon either widespread adoption of fuel cell vehicles, or the establishment of a major industrial consumer in the region, for instance an oil refinery in the event of a large discovery in Pegasus Bay or Southland.

The demand for personal transport in New Zealand is high, and based on 2006 census figures for the Canterbury region, an estimated 270,000 people have access to at least one motor

vehicle (95% of the population aged over 15) [Statistics New Zealand, 2006]. Using the Honda FCX Clarity as an example of a typically-performing fuel cell vehicle, a 4kg 'tank' of hydrogen fuel will power the car for 430km. Assuming an average yearly distance travelled of 15,000km per person, the hydrogen production from the plant would supply the fuel needs of approximately 31% of the travelling public in the region and would displace approximately 289,000 tonnes of carbon dioxide emissions annually[3] [MfE, 2008]. Moreover, at $2.00/gge the demand for hydrogen-powered vehicles is likely to be high, as the cost to the consumer per 'tank' of fuel would be only $8.00, compared with the $50-$100 experienced by the average motorist today. From these figures, the social and environmental impact of this alternative to fossil fuelled vehicles would be profound. However, significant investment into a hydrogen infrastructure would be necessary for any of these benefits to be realised.

The model as presented does not account for the displacement of the wood waste feedstock from the current process consumption, nor the cost of transporting the wood waste from around the region to a central facility. Wood wastes are currently in high demand, both at the points of processing where wood waste is generally used as thermal fuel, and around the region where operators of boilers consider wood waste an attractive alternative to 'dirty' coal or costly diesel or LPG. Additionally, harvesting residues are difficult to collect and currently uneconomical to transport over long distances. The cost of hydrogen is particularly sensitive to the cost of woody biomass and biomass transport, and as Figure 7.5 shows, a transport cost of $61/odt (total biomass cost of $101/odt) is the upper limit before the US DOE target cost of hydrogen is no longer being realised. Current estimates of transport costs around the region amount to approximately $10/odt, which gives a combined cost of biomass feedstock as $50/odt. This results in a break even hydrogen price of $1.86/kg [Pooch, 2009]. Current costs of woody biomass wastes in the Canterbury region vary significantly based on type of residue. Sawdust is typically sold with low moisture contents for between $96 - $156/tonne, while wood chips for fuel are values at $45 - $120/tonne based on moisture content [Brorens & Taylor, 2009]. Wet landing residues have been valued by SCION at $35/tonne delivered [Hall, 2007]. The plant utilising biomass feed stocks as described in Scenario 1 has drying capability, therefore would endeavour to pay for the cheaper, higher moisture content residues where available.

[3] Calculation of carbon dioxide emissions values are based on the CO_2-equivalent emissions factor for 2008 of 234g CO_2-e/km for a petrol powered car [MfE, 2008]

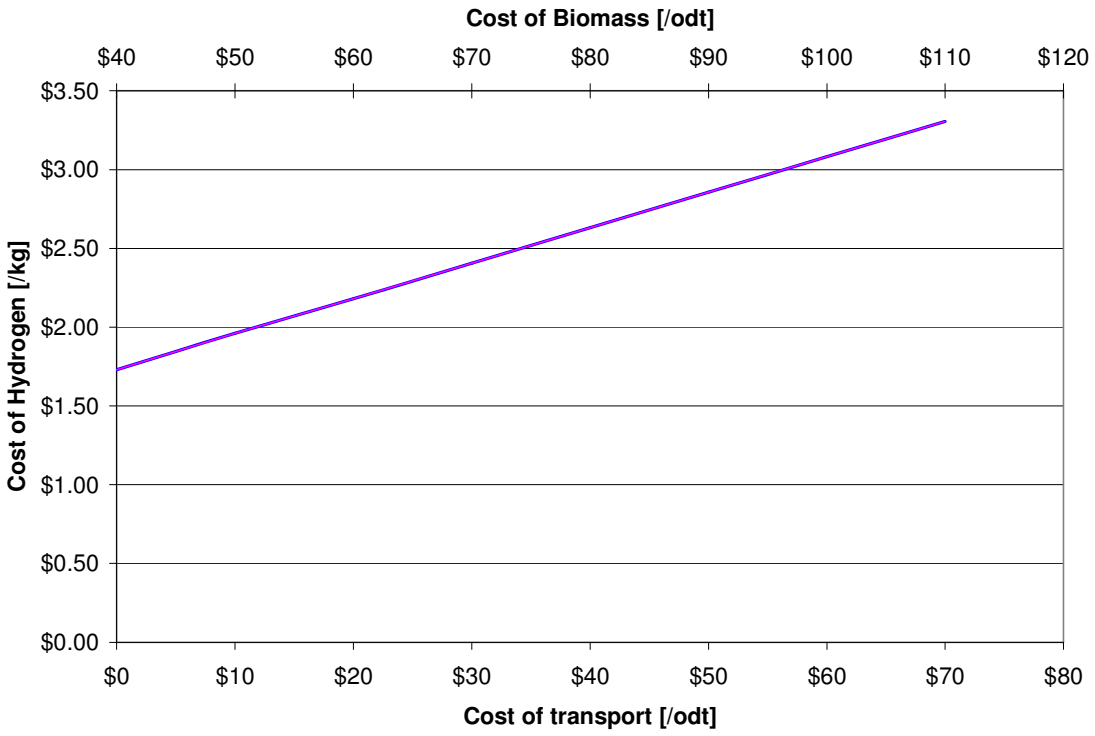

Figure 7.5 – Variation in the cost of hydrogen with increasing cost of transport per tonne of wood waste

From the above analysis, the plants internal thermal requirements are met with process integration and combustion of the PSA off-gas, which contains a significant amount of unrecoverable hydrogen. The excess thermal energy from the plant is 14.1 MW which can be used for electricity generation or exported for process heating elsewhere. The value of this stream has not been calculated.

Given the high relative cost of the reforming stage, the specific benefit of this operation has been questioned. Removing the reforming stage would save $24.6M on the capital cost, but produce significantly less hydrogen, as 3 moles of hydrogen are produced for every one mole of methane (2.5mol/mol ethane and 2 mol/mol ethene). The overall reduction in hydrogen production from omitting the reforming stage is 813 kg/h, valued at $13M/y for a $2.00/kg price of hydrogen. This loss makes the plant less economic, with a breakeven price of hydrogen of $2.52/kg. The added heating value to the PSA off-gas from the unreformed hydrocarbon gases amounts to a 3MW increase. If all of the excess thermal energy in this scenario were used by the plant to generate electricity in the best-case scenario of 55% efficiency for a combined-cycle system, 74.8 GWh would be generated annually with a value of approximately $7.5M. Offsetting the electricity use by the plant as assumed in the first case, the cost of hydrogen to make this plant break even over its 20 year lifetime would be

approximately $1.73/kg, the same as the original case. The production of hydrogen in this case would supply hydrogen to roughly 14% of the Canterbury motoring population. It is evident that thorough knowledge of the demand for hydrogen in the region is important to gauge the degree of initial investment.

7.3. SCENARIO 2 – ELECTRICITY FROM MCFC

7.3.1. MCFC – Technical summary

MCFCs are an attractive alternative electricity generator that is approaching commercialisation. A number of factors determine their appeal, chief among which are the relatively low cost compared with other fuel cells utilising expensive platinum (PEMFC) or yttrium-stabilised zirconia (SOFC) electrolytes, and high operating temperature of 650°C which provides good opportunities for heat recovery and enables efficient integration to the gasification plant. Several commercial-scale test cells are in operation internationally, with the most successful displaying continuous operation with an internally-reformed natural gas fuel stock for 17,000 hours [Hengeveld & Revankar, 2007]. A production capacity of 2 MW_e is typical with current technology. The analysis presented here assumes a fuel utilisation of 80% of the available hydrogen, and a internal reforming extent of 100% for the C2 hydrocarbons and 75% for methane.

The MCFC electrochemical conversion differs from other fuel cells in that it requires both hydrogen and carbon dioxide as fuels. Hydrogen is converted to water as normal at the anode via electrochemical oxidation, while at the cathode carbon dioxide is used to replenish the molten carbonate electrolyte. In this way it is particularly suitable for operation with a dual fluidised bed gasifier operating with internal CO_2 removal, described as adsorption enhanced reforming (AER). The electrochemical reactions describing the MCFC operation are given in R-7.1 and R-7.2. As can be seen from R-7.2, a composition ratio of CO_2:O_2 of 2 is required in the flue gas stream.

Anode:	$H_2 + CO_3^{2-} \rightarrow H_2O + CO_2 + 2e^-$	R-7.1
Cathode:	$0.5O_2 + CO_2 + 2e^- \rightarrow CO_3^{2-}$	R-7.2

Compared with the producer gas requirements imposed for pure hydrogen production and even gas turbines, MCFCs are more robust, being able to handle higher particulate concentrations as shown in Table 7.7. MCFCs are still susceptible to damage from tars and

sulfur compounds, but nitrous oxides have been shown to have no negative effect on MCFC operation [Kawase, 2002]. Because the fuel cells operate at high temperature and employ internal reforming, light hydrocarbons in the producer gas are converted to hydrogen and are not treated as impurities.

Table 7.7 – Particulate and impurity limits required for MCFC operation [Lobachyov & Richter, 1998].

	BIGCC	BIG-MCFC
Tar content	No tars	No tars
Alkali metals level	0.1-0.2 ppm	1-10 ppm
Particulate loading	0-10 pm	<100 ppm

7.3.2. Description of the Process

Scenario 2 proposes the use of MCFC stacks for generating electricity directly from biomass gasification producer gas (Biomass Integrated Gasification-Molten Carbonate Fuel Cell, BIG-MCFC), and recovering the waste heat in a Rankine bottoming cycle. Figure 7.6 gives the flow schematic diagram of the process. Biomass conditioning and gasification operations are nearly identical to those proposed in Scenario 1 (Figure 7.2), but with a higher steam/biomass ratio of 0.92 for gasification as required for downstream reforming of the light hydrocarbon gases in the producer gas. A higher operating pressure in the gasifier is also required, at approximately 4 – 5 bar. Based on the experience gained in operating the UC gasifier and from literature reports, it is expected that neither slightly higher steam/biomass ratio nor increased pressure will have a significant effect on dry producer gas composition and yield.

Following gasification high temperature gas cleaning is used for both the producer gas and flue gas streams. Flue gas cleaning is required as it is used as an MCFC feed stock, fed to the cathode side of the cell. Particulate removal to acceptable levels is achieved by using high temperature ceramic candle filters on both streams. Following filtration, the producer gas is heated to 1000°C, and then fed to a fluidised bed tar cracker typically using dolomite or olivine as a bed material. Heat recovery on both streams heats water for the steam bottoming cycle, after which the producer gas and flue gas streams are fed to the MCFC stack, consisting of 36 cells. 50.5 MW_e is generated by the fuel cells. The exhaust gas of the fuel cell stack is combusted in 4% excess air to eliminate reactive species, then is delivered to a heat recovery steam generator to generate steam for the Rankine cycle. The turbine throttles 13.5 t/h steam from 70 bar to 7 bar in two stages producing 1.7 MW_e. The expanded steam is then preheated by the remaining heat in the fuel cell exhaust and fed to the gasifier. The fuel cell exhaust

stream is expanded from 2 bar to 1 bar, which is used to compress the flue gas entering the fuel cell. Overall power output from the plant is 47.5 MW_e, giving an electrical energy efficiency of 57%. Utilisation of the 11.3 MW_{th} of waste heat would give an overall plant efficiency of 70%. Consequently, placement of the plant adjacent to a plant with high thermal load (such as one of the timber processors producing the wood waste) would be advisable.

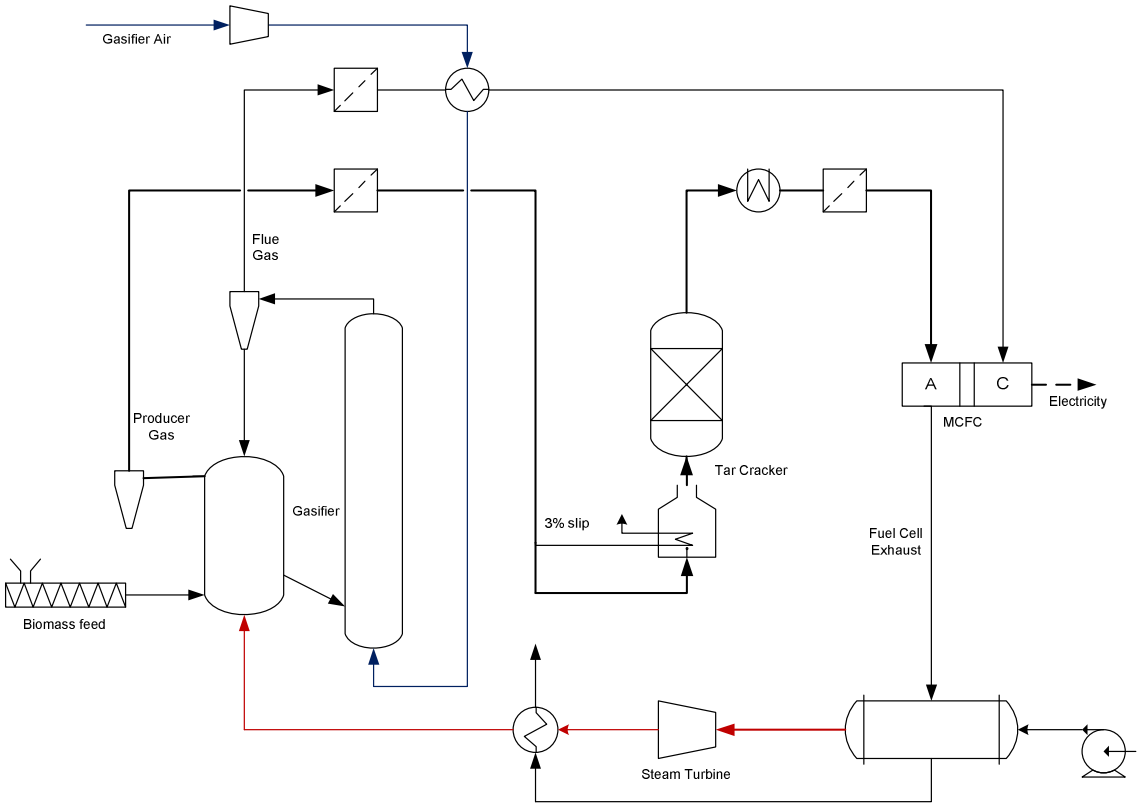

Figure 7.6 – Flow schematic of Scenario 2 process.

Table 7.8 - Summary of Scenario 2 mass flows and conditions of the major streams described above

Stream		1	2	3	4	5	6
Pressure	bar	3.0	3.0	6.0	3.0	3.0	3.0
Temperature	℃	20	40	433	500	650	1,000
Flow	kmol/h	-	-	749.4	2,701	672.1	672.1
	kg/h	33,000	15,000	13,500	-	-	-
	Nm^3/h	-	-	-	-	-	-
Composition	H2	-	-	-	-	0.510	0.510
	CH4	-	-	-		0.130	0.130
	CO	-	-	-	-	0.170	0.170
	CO2	-	-	-	-	0.130	0.130
	C2H4	-	-	-	-	0.050	0.050
	C2H6	-	-	-	-	0.010	0.010
	N2	-	-	-	0.790	-	-
	O2	-	-	-	0.210	-	-
	wood	-	1.000	-	-	-	-
Moisture	kg/kg	1.20	0.12	1.00	-		-
	kmol/kmol	-	-	-	-	0.19	0.19

Stream		7	8	9	10	11	12
Pressure	bar	2.0	3.0	2.0	2.0	70	1.0
Temperature	℃	650	850	650	650	505	433.8
Flow	kmol/h	672.1	2,088	2,088	3,610	749	3,610
	kg/h	-	-	-	-	13,500	-
	Nm^3/h	-	-	-	-	-	-
Composition	H2	0.510	-	-	-	-	-
	CH4	0.130	-	-	-	-	-
	CO	0.170	-	-	-	-	-
	CO2	0.130	0.097	0.097	0.250	-	0.250
	C2H4	0.050	-	-	-	-	-
	C2H6	0.010	-	-	-	-	-
	N2	-	0.835	0.835	0.683	-	0.683
	O2	-	0.068	0.068	0.067	-	0.067
	wood	-	-	-	-	-	-
Moisture	kg/kg	-	-	-	-	1.00	-
	kmol/kmol	0.19	0.11	0.11	0.23	0.151	0.241

7.3.3. Capital Cost Analysis

In addition to the cost correlations used in Table 7.5, Table 7.9 shows the cost correlations required for the different operations used in Scenario 2. The biomass drying system and gasifier capital costs are the same as for Scenario 1, but gas cleaning is accomplished using a high temperature tar cracker and candle filters. The tar cracker has been modelled as a circulating fluidised bed with associated cyclone, similar to the gasifier combustion column. The column dimensions have been determined based on the required fluidisation velocity for pneumatic transport in a bed of 500μm diameter dolomite particles. The candle filter cost has been modelled as having equivalent cost as dry electrostatic precipitators (ESP). In reality

however, the cost of a candle filter is likely to be competitive compared with a dry ESP, so this offers a conservative cost estimate. MCFC cost is difficult to estimate, with other authors anticipating the cost of a 1-2MW scale MCFC to be between $240,000/cell [Hengeveld & Revankar, 2007] and $356,000/cell [Lobachyov & Richter, 1998]. An average of these prices is used initially. The capital cost breakdown for Scenario 2 is demonstrated in Figure 7.7, while full cost information is provided as Appendix F.

Table 7.9 – Additional cost correlation information used for Scenario 2.

Equipment type	Cost Parameters	Cost Correlation	Reference
Candle Filter	Flow [m³/s]	Figure 5.56, Ulrich & Vasudevan, 2004	
Steam Turbine	Shaft Power [kW]	Figure 5.21 Ulrich & Vasudevan, 2004	

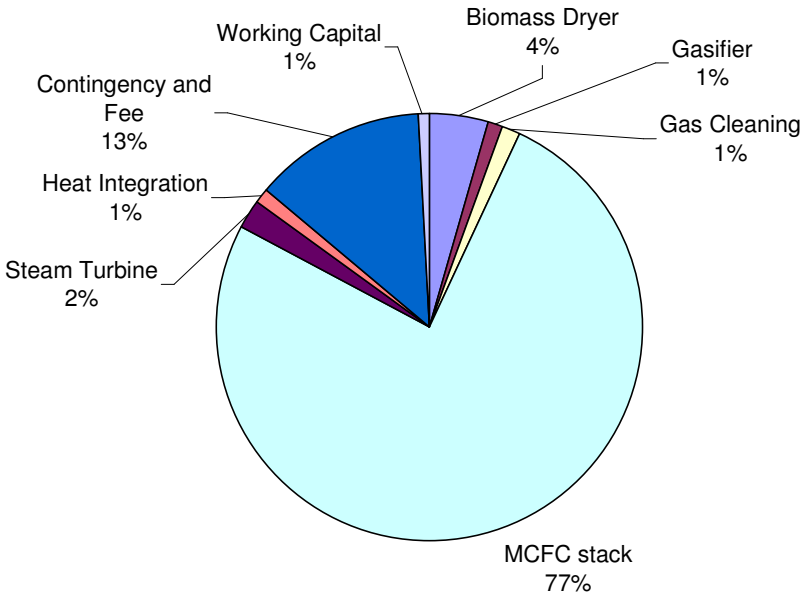

Total Capital Cost = NZ$154,055,000

Figure 7.7 – Capital cost breakdown of proposed BIG-MCFC power plant

7.3.4. Operational Cost Summary and Net Present Value

Table 7.10 gives the operational cost estimates for the Scenario 2 proposal, which are determined from the same sources as Scenario 1. Again, the intrinsic cost of woody biomass feedstock of $2.00/GJ ($40/odt) has been used. In this instance a wood transport cost of $10/odt has been used, giving a total woody biomass cost of $50/odt. All of the organic

electricity requirement is met by the plant's generation so is not considered. Biodiesel consumption is set at zero, assuming no auxiliary fuel is required for gasification (a condition of steady state operation).

Revenue is summarised in Table 7.11. The revenue is based on a breakeven electricity price over the 20 year lifetime of the plant, with an associated income tax of 30%. Depreciation is assumed to be 10% per year straight line depreciation with an associated tax refund of 30% per year. Based on the net present value calculations, the cost of electricity produced by the plant is 10.57 ¢/kWh.

Table 7.10 – Operational cost summary for the proposed BIG-MCFC power plant.

Item		Unit Cost		Total
Raw Materials	Wood	$ 2.00	/GJ	$ 4,831,000
	Transport	$ 10.00	/t	$ 2,640,000
Utilities	Electricity	$ -	/kWh	$ -
Labour	Operators	$ 20.00	/h	$ 320,000
	Supervisors	15%	*Op Lab	$ 48,000
	Admin & O/H	60%	*Lab + Maintenance	$ 2,069,000
Other	Maintenance	2%	*Cap Cost	$ 3,081,000
	Local Taxes	1%	*Cap Cost	$ 1,541,000
	Insurance	1.5%	*Cap Cost	$ 2,311,000
	Operating Supplies	15%	*Maintenance Cost	$ 462,000
TOTAL OPERATING COSTS				**$ 17,303,000**

Table 7.11 – Revenue summary of the proposed BIG-MCFC power plant

Item		Rate		Total
Revenue	Electricity	$ 0.1057	/kWh	$ 40,153,000
Less Tax		-30%		-$ 12,046,000
				$ -
Depreciation		10%		$ -
Tax refund		30%		$ 3,984,000
				$ -
TOTAL REVENUE	**<10y**			**$ 32,091,000**
	>10y			**$ 28,107,000**

7.3.5. Discussion

The Biomass Integrated Gasification-MCFC power plant proposed is a promising system utilising increased hydrogen producer gas from a biomass gasifier. An analysis of the electricity output compared with energy input yields a system efficiency of 57% which is unprecedented in current technology, but very close to the efficiency of natural gas-combined cycle power generation (around 55%). The analysis assumed an electrical generation efficiency of the MCFCs of 55%. Fuel cell technology is currently under development and close to commercialisation. It is likely that in the near future, plants such as described in this Scenario will offer efficient, near-carbon neutral generation to countries with high costs of electricity, or large base load thermal generation. In New Zealand where the majority of electricity is produced from hydroelectric plants cheaply, the costs of a BIG-MCFC power plant are uneconomic at the present time. However, proponents of thermal base load generation, arguing that the intermittency of hydroelectricity experienced to date is unacceptable in a modern, developed nation, may take comfort in the possibility of clean, efficient, continuous power generation that this system would provide for developed nations where the intermittency of hydroelectricity supply experienced to date is unacceptable.

As demonstrated in Figure 7.8, the cost of the fuel cell stack accounts for 70% of the total capital cost, suggesting that the value of electricity produced by this plant is highly sensitive to variations in MCFC cost. As stated earlier, the technology is close to commercialisation with several demonstration sites operating around the world. It is inevitable that as demand for the technology increases and the technology is improved further, the cost will reduce considerably. Figure 7.8 shows the sensitivity of breakeven electricity cost to MCFC cost. The results of the sensitivity analysis show that at the low end of MCFC cost (US$149,000/cell), breakeven electricity price drops to 7.3 ¢/kWh. Currently, wholesale electricity prices average around 5 ¢/kWh in New Zealand, varying between 0.1 ¢/kWh to more than 35 ¢/kWh when climatic conditions conspire to reduce lake levels to less than 80% of the historical average [M-Co, 2009]. In this market climate, the BIG-MCFC will offer an attractive alternative to current thermal generation options in the near future.

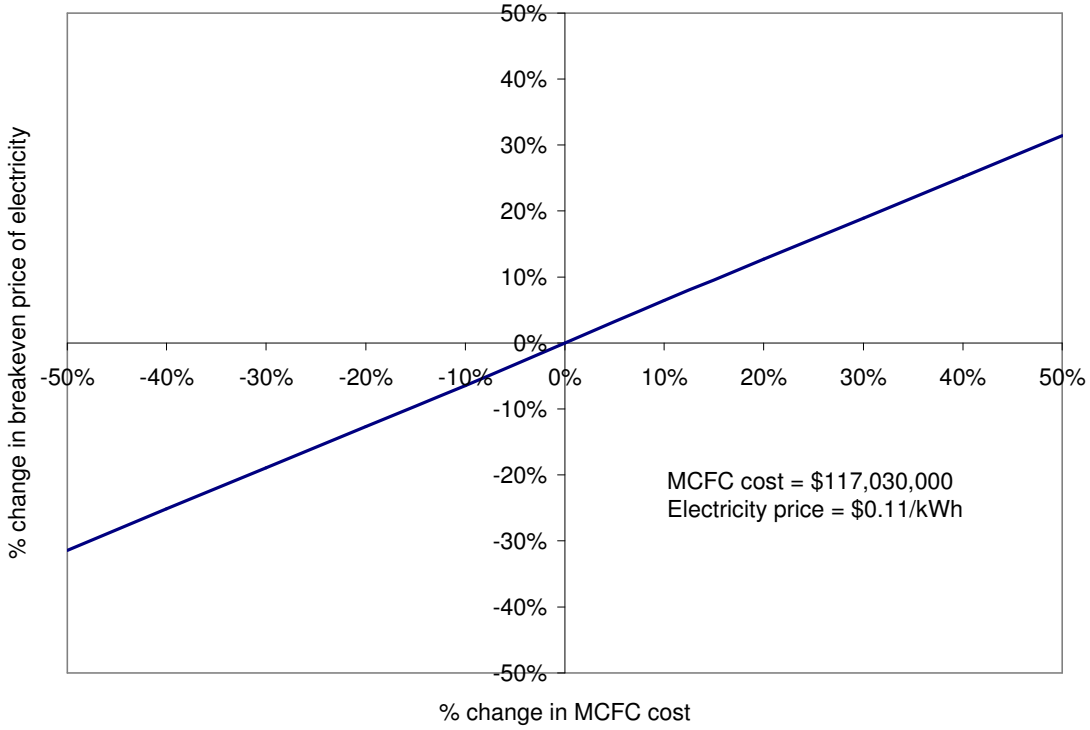

Figure 7.8 – Sensitivity of breakeven electricity price to fuel cell cost.

7.4. CONCLUSIONS

Hydrogen production from biomass gasification will have strong economic potential in the near future with hydrogen expected to become a major part of a global renewable energy economy. Two possible sectors of hydrogen utilisation are transport, where pure hydrogen is a potential fuel for Fuel Cell Vehicles, and electricity generation, incorporating stationary Fuel Cell stacks.

Economic analyses considering the potential for biomass gasification to produce hydrogen for the end uses in the two sectors mentioned above are conducted in this project. The analyses adopt utilisation of the available woody biomass resources of the Canterbury region, approximately 120,000 odt/y ($84MW_{th}$), at a centralised gasification plant. Scenario 1 proposed a hydrogen production plant capable of producing 11,700 tonnes of hydrogen annually, at a cost of production of $1.63/kg plus tax. Scenario 2 evaluated the potential for a BIG-MCFC power plant utilising the same feed stock, which is able to produce $47.5MW_e$ at an electrical efficiency of 57%. The cost of electricity production by this method is 10.09 ¢/kWh.

The price of hydrogen determined by Scenario 1 is very competitive internationally, but relies on sufficient demand for hydrogen in the Canterbury region for the process to be considered economic. It is expected that with the development of Fuel Cell Vehicles, demand for hydrogen will shift away from the current industrial consumers to individuals for transport fuel, as an alternative to fossil-fuelled vehicles. Electricity produced from hydrogen fuel cells as considered in Scenario 2 is less economically competitive, but equivalent to current less efficient thermal generators. As demand for less intermittent base load generation increases, the BIG-MCFC process presents an environmentally sound alternative to fossil fuel electricity generation.

8. Conclusions and Recommendations

Biomass gasification has been investigated as a process for production of hydrogen-rich producer gas and ultimately, pure hydrogen. With predictions of impending global shortages of fossil fuels, and wide acceptance of the theory of anthropogenic climate change, renewable energy technologies are coming under intense scrutiny. Several engineering analyses of the current state of the art have shown that neither decarbonisation of fossil energy, nor nuclear energy nor renewable energy alone can fulfil expected demand. With most renewable energy sources being intermittent in nature, continuous energy production via biomass gasification offers an appealing alternative to fossil-fuel consumption. There is potential for utilisation of hydrogen produced from biomass gasification either for electricity generation or as a transport fuel.

This work has focussed on the development and improvement of the dual fluidised bed gasifier technology that has been under development at the University of Canterbury since 2005. Previous studies worldwide have investigated the potential for using different minerals as bed materials of the fluidised bed system to catalyse or otherwise influence the gasification reaction set to improve producer gas quality. Internationally it has been shown that reduction in tar content in the biomass gasification producer gas can be achieved from utilising various bed materials, especially nickel and dolomite containing compounds. Improving producer gas composition has mainly been achieved by adsorption enhanced reforming (AER) which involves gasifying biomass in a calcium-laden bed material to facilitate CO_2 removal from the producer gas stream, increasing hydrogen production.

At the laboratory scale, it has been found that the choice of bed material can influence the homogeneous gas phase gasification reactions across a range of temperatures up to 700°C. The reverse water gas shift reaction was shown to dominate in an idealised producer gas mixture at temperatures between 350°C and 550°C; the latter is considered the lower limit for gasifier operations. Calcite ($CaCO_3$) and iron compounds were shown to catalyse the water gas shift reaction. Therefore it was expected that calcite and iron bed materials would positively influence the forward water gas shift at higher temperatures, thereby enhancing hydrogen production. Use of the lab scale apparatus was fraught with technical difficulties, but persevering with the equipment is recommended, particularly for the investigation of biomass decomposition products and analysis of the heterogeneous gasification reactions.

Simple mixtures of greywacke, olivine, calcite, dolomite and magnetite were tested as bed materials in the UC 100kW-scale DFB gasifier. Extensive experimentation and detailed analysis of the producer gas showed that bed material selection had a profound effect on the performance of the gasifier and the composition of the producer gas. Maximum producer gas yield of 0.877Nm³/kg wood was obtained with a mixture of 25% calcite / 75% olivine bed material, an improvement of 20% over greywacke bed material. The same bed material demonstrated a 5.3% increase in energy yield (MJ of producer gas per kg of wood fed) and a 6% increase in cold gas efficiency. Most importantly from the perspective of hydrogen production, a mixture of 50% calcite / 50% olivine yielded hydrogen at 0.317kg/kg wood fed, an improvement of 85% over the greywacke base case.

During the bed material tests numerous other measurements were taken and understanding of the operation of the dual fluidised bed system has increased. The first chromatograms of tars collected from the gasifier were produced, showing a dominance of certain PAH species. Further development of this analysis and comparison of tar yields from the various bed material trials may fortify speculation that tar yields decreased significantly using calcite and dolomite as bed materials. The measurement of the vapour content of the producer gas showed that the effective steam/biomass ratio varies from 108% above to 90% below the average value of 0.39, suggesting that homogeneous gas mixing is not taking place in the bubbling fluidised bed gasification column.

Investigation of the potential for the use of biosolids (digested sewage sludge) as a fuel in the gasifier has shown that the physical structure of the fuel has high importance, affecting producer gas yield and gasifier operability. Interestingly, high proportions of biosolids in the fuel mixture seem to positively affect producer gas composition, increasing hydrogen content and decreasing carbon dioxide. However, the producer gas yield and cold gas efficiency decreased significantly with increasing proportion of biosolids in the fuel. As the biosolids fuel has zero or negative value there is strong economic potential from gasifying biosolids. It is recommended that further biosolids gasification trials are conducted with a pelletised biosolids fuel to increase fuel residence time in the gasifier.

From an operational perspective, the gasifier has undergone numerous repairs prior to the bed material trials and following these experiments, more repairs and improvements have been required. The majority of these mechanical failures were caused by thermal stressing, but

design changes to the flue gas cyclone to improve resistance to wear, and the chute to ensure fluidisation of the bed material is maintained, are recommended. It is also suggested that the construction of the chute should be modified to remove the refractory and replace it with an insulated rectangular steel tube. Steel construction on other sections of the gasifier has proven to be more robust. To improve handling of soft bed materials such as calcite and dolomite which experience high attrition and elutriation, a bed material feed system and particle trap modification have been designed and commissioned. The bed material feeder has shown extraordinary value already during trials, allowing positive results for the effect of dolomite to be obtained. It is expected that this, in combination with the particle trap modification, will allow experiments to run for a longer period of time, creating opportunities to substantially increase data collection during experiments and to ensure the operation reaches steady state. It is also expected that auxiliary fuel usage will decline at longer run times, improving the cold gas efficiency of the plant.

The economic potential of biomass gasification systems for hydrogen production has been investigated. In the near future, the development of hydrogen fuel cells is expected to have a significant effect on energy usage, offering a zero-emissions alternative to fossil-fuelled vehicles and increased efficiency electricity generation. Utilising the available stocks of woody biomass in the Canterbury region, the economic analysis shows that hydrogen can be produced at a breakeven cost of NZ$1.73/kg, which is very competitive compared with the existing commodity price of around US$4.00/kg. A biomass integrated gasification fuel cell plant has the potential to produce electricity for 10.57 ¢/kWh, which is competitive for base load generation. Both options require development and commercialisation of automotive and stationary fuel cell technology, but even with the current state of commercialisation it is recommended that hydrogen from biomass gasification remains a viable and exciting technology to mitigate fossil-fuel consumption and potentially, climate change.

9. References

Argonne National Laboratory (2005). Basic research needs for solar energy utilization. Report on the US DOE basic energy sciences workshop on solar energy utilization. Publ. Argonne Nat. Lab., 2005

Asadullah, M., T. Miyazawa, et. al.. (2004). "Gasification of different biomasses in a dual-bed gasifier system combined with novel catalysts with high energy efficiency." Applied Catalysis A: General **267**(1-2): 95-102.

Azhar Uddin, M., H. Tsuda, et. al... (2008). "Catalytic decomposition of biomass tars with iron oxide catalysts." Fuel **87**(4-5): 451-459

Begley, S. (2009). *We can't get there from here.* Newsweek magazine, March 23, 2009.

Bischoff, M. (2006). "Molten carbonate fuel cells: A high temperature fuel cell on the edge to commercialization." Journal of Power Sources **160**(2): 842-845.

Bleeker, M. F., S. R. A. Kersten, et. al. (2007). "Pure hydrogen from pyrolysis oil using the steam-iron process." Catalysis Today **127**(1-4): 278-290

Bouman, R.W., Jesen, S.B., Wake, M.L., Earl, W.B. (2005). *Process Capital Cost Estimation for New Zealand 2004*. Society of Chemical Engineers New Zealand, Christchurch

Bouman, R (2009) Personal Communication during meeting with Christchurch City Council Wastewater Treatment Plant managers and engineering consultants.

Brorens, P.H., Taylor, M.E. (2009). "Manufacturing and market for wood polymer composites in New Zealand." Confidential report prepared for the University of Canterbury, AgResearch Client Report CLR 09/52, November 2009.

Brown, J., (2006). *Biomass Gasification: Fast Internal Circulating Fluidised Bed Gasifier Characterisation and Comparison – A thesis submitted in partial fulfillment of the requirements for the degree of Master of Engineering in Chemical and Process Engineering*. University of Canterbury

Brown, R. C. (2003). *Biorenewable Resources: Engineering New Products from Agriculture*: Iowa State Press.

Bull, D. (2008). *Performance Improvements to a Fast Internally Circulating Fluidized Bed (FICFB) Biomass Gasifier for Combined Heat and Power Plants – A thesis submitted in partial fulfillment of the requirements for the degree of Master of Engineering in Chemical and Process Engineering*. University of Canterbury

California Energy Commission (CaEC) (2003). *Fuel Cells.* Retrieved 31 October 2009. http://www.energy.ca.gov/distgen/equipment/fuel_cells/fuel_cells.html

California Energy Commission (CaEC) (2009). *Ocean Energy.* Retrieved 31 October 2009. http://www.energy.ca.gov/oceanenergy/index.html

Chase, G., G (n.d.). *Fluidization*: University of Akron. Retrieved 5 June 2007. http://www.ecgf.uakron.edu/~chem/fclty/chase/Solids/SolidsNotes5%20Fluidization.pdf

Cusumano, J. A., Dalla Betta, R. A., Levy, R. B. (1978). *Catalysis in Coal Conversion.* Academic press NY 1978

Devi, L., M. Craje, et. al.. (2005). "Olivine as tar removal catalyst for biomass gasifiers: Catalyst characterization." Applied Catalysis A: General **294**(1): 68-79.

Di Felice, L., C. Courson, et. al. "Catalytic biomass gasification: Simultaneous hydrocarbons steam reforming and CO2 capture in a fluidised bed reactor." Chemical Engineering Journal **In Press, Corrected Proof**.

Electricity Innovation Institute (2004). *Offshore Wave Energy Conversion Devices* E2I EPRI WP-004-US-Rev1. Retrieved 31 October 2009. *oceanenergy.epri.com/.../wave/.../004_WEC_Device_Assess_Report_Rev1_MP_6-16-04.pdf*

Energy Efficiency and Conservation Authority (EECA) (2007). *New Zealand Energy Efficiency and Conservation Strategy.* New Zealand Government.

Franco, C., F. Pinto, et. al. (2003). "The study of reactions influencing the biomass steam gasification process[small star, filled]." Fuel **82**(7): 835-842.

Fridleifsson, Ingvar B.; Bertani, Ruggero; Huenges, Ernst; Lund, John W.; Ragnarsson, Arni; Rybach, Ladislaus (2008). O. Hohmeyer and T. Trittin. ed. (pdf). *The possible role and contribution of geothermal energy to the mitigation of climate change*. Luebeck, Germany. pp. 59-80. Retrieved 31 October 2009. http://iga.igg.cnr.it/documenti/IGA/Fridleifsson_et_al_IPCC_Geothermal_paper_2008.pdf.

Fuel Cell Today (2009). *Fuel Cell History, Part 1.* Wand, G. (pdf). Retrieved 31 October 2009. http://www.fuelcelltoday.com/media/pdf/archive/Article_1104_Fuel%20Cell%20History%20Part%201.pdf

Geldart, D. and A. L. Radtke (1986). "The effect of particle properties on the behaviour of equilibrium cracking catalysts in standpipe flow." Powder Technology **47**(2): 157-165

Gnanapragasam, N. V., B. V. Reddy, et. al. "Feasibility of an energy conversion system in Canada involving large-scale integrated hydrogen production using solid fuels." International Journal of Hydrogen Energy **In Press, Corrected Proof**

Good, J., Ventress, L., et. al. (2005). "Sampling and analysis of tar and particles in biomass producer gas - Technical Report". Prepared under CEN BT/TF 143 "Organic contaminants ("tar") in biomass producer gases".

Grace, J.R., Avidan, A.A., Knowlton, T.M. (Eds.), *Circulating Fluidized Beds*, Blackie Academic and Professional, 1997

Grassi, G., & Bridgewater, A. V. (1991). *Biomass Pyrolysis Liquids Upgrading and Utilisation*: Elsevier Science Publishers Ltd

Hall, P. (2007). Bioenergy options for New Zealand: Logging residues - Situation analysis: Resource, supply costs and barriers. SCION, 2007.

Haryanto, A., S. Fernando, et. al.. (2007). "Ultrahigh temperature water gas shift catalysts to increase hydrogen yield from biomass gasification." Catalysis Today **129**(3-4): 269-274.

Hildenbrand, N., J. Readman, et. al. (2006). "Sorbent enhanced steam reforming (SESR) of methane using dolomite as internal carbon dioxide absorbent: Limitations due to $Ca(OH)_2$ formation." Applied Catalysis A: General **303**(1): 131-137

Hofbauer, H., Rauch, R. (2001) Hydrogen-Rich Gas from Biomass Steam Gasification. Report to the European Commission Non-Nuclear Energy Programme, 2001.

Hoffert, M. I., K. Caldeira, et. al.. (2002). "Advanced technology paths to global climate stability: Energy for a greenhouse planet." Science **298**(5595): 981-987.

International Energy Agency (IEA) (2006). *Renewables in Global Energy Supply: An IEA Factsheet*. Retrieved 31 October 2009. http://www.iea.org/papers/2006/renewable_factsheet.pdf

Ji, P., W. Feng, et. al. (2009). "Production of ultrapure hydrogen from biomass gasification with air." Chemical Engineering Science **64**(3): 582-592.

Kawase, M., Mugikura, Y., Watanabe, T., Hiraga, Y., Ujihara, T. (2002). "Effects of NH_3 and NO_x on the performance of MCFCs." Journal of Power Sources **104** (2002) 265-271

Kolbitsch, P., C. Pfeifer, et. al. (2008). "Catalytic steam reforming of model biogas." Fuel **87**(6): 701-706

Koppatz, S., C. Pfeifer, et. al. (2009). "H2 rich product gas by steam gasification of biomass with in situ CO2 absorption in a dual fluidized bed system of 8 MW fuel input." Fuel Processing Technology **90**(7-8): 914-921

Li, J. (2008). *Energy Demand and Biomass Supply in NZ Wood Processing Plants.* Presentation to the Biomass Gasification technology and Biomass Energy workshop, University of Canterbury, 13 February 2008.

Lin, C.-L., J.-H. Kuo, et. al. (2009). "Inhibition and promotion: The effect of earth alkali metals and operating temperature on particle agglomeration/defluidization during incineration in fluidized bed." Powder Technology **189**(1): 57-63.

Lv, P., Z. Yuan, et. al. (2007). "Hydrogen-rich gas production from biomass air and oxygen/steam gasification in a downdraft gasifier." Renewable Energy **32**(13): 2173-2185.

Marshall, A.T., Sunde, S., Tsypkin, M. and Tunold, R. (2007). Performance of a PEM water electrolysis cell using IrxRuyTazO2 electrocatalysts for the oxygen evolution electrode. International Journal of Hydrogen Energy, 32, 13, 2320-2324

The Marketplace Company (M-Co) (2009). *Hydrology.* Retrieved periodically. http://www.electricityinfo.co.nz/comitFta/ftaPage.main

Mahishi, M. R. and D. Y. Goswami (2007a). "An experimental study of hydrogen production by gasification of biomass in the presence of a CO2 sorbent." International Journal of Hydrogen Energy **32**(14): 2803-2808.

Mahishi, M. R. and D. Y. Goswami (2007b). "Thermodynamic optimization of biomass gasifier for hydrogen production." International Journal of Hydrogen Energy **32**(16): 3831-3840.

Milne TA, Abatzoglou N, Evans RJ. (1998) *Biomass gasifier ''tars'': their nature, formation and conversion*. National Renewable Energy Laboratory (NREL), reports NREL/TP-570-25357, Colorado, 1998

Miyazawa, T., M. Asadullah, et. al. (2004). Novel Catalysts for Gasification of Biomass with High Energy Efficiency. Studies in Surface Science and Catalysis, Elsevier. **Volume 153:** 85-90.

Murakami, T., G. Xu, et. al. (2007). "Some process fundamentals of biomass gasification in dual fluidized bed." Fuel **86**(1-2): 244-255.

Mwandila, G., Pang, S., Gilmour, I., Williamson, C. (2008). "Tar removal in a hot gas bubble and spray system for gas cleaning after biomass gasification". Proccedings from the Chemeca Conference 2008, Newcastle, Australia

National Institute for Standards and Technology (NIST) Webbook (2008a). *Hydrogen.* Retrieved 6 October 2009. http://webbook.nist.gov/cgi/cbook.cgi?ID=C1333740&Units=SI

National Institute for Standards and Technology (NIST) Webbook (2008b). *Thermophysical Properties of Fluid Systems.* Retrieved 9 November 2009. http://webbook.nist.gov/chemistry/fluid/

National Ocean and Atmospheric Administration (NOAA) (2009) *Total Solar Irradiance.* Retrieved 31 October 2009. ftp://ftp.ngdc.noaa.gov/STP/SOLAR_DATA/SOLAR_IRRADIANCE/IRRAD97.PDF

New Zealand Centre for Advanced Engineering (CAENZ) (2008) *Energy Information Handbook, 3rd ed.* CAENZ, 2008.

New Zealand Ministry for the Environment (MfE) (2008). *Emissions Factors and Methods 2006.*Retrieved 19 November 2009. http://www.mfe.govt.nz/publications/climate/guidance-greenhouse-gas-reporting-apr08/html/page3.html

New Zealand Ministry of Economic Development (MED) (2007). *New Zealand Energy Strategy to 2050.* New Zealand Government, 2007.

Nishikawa, J., T. Miyazawa, et. al. (2008). "Promoting effect of Pt addition to Ni/CeO2/Al2O3 catalyst for steam gasification of biomass." Catalysis Communications **9**(2): 195-201.

Nishikawa, J., K. Nakamura, et. al. (2008). "Catalytic performance of Ni/CeO2/Al2O3 modified with noble metals in steam gasification of biomass." Catalysis Today **131**(1-4): 146-155.

Nordgreen, T., T. Liliedahl, et. al. "Metallic iron as a tar breakdown catalyst related to atmospheric, fluidised bed gasification of biomass." Fuel **85**(5-6): 689-694

Pang, S. (2008) *Overview of Up-To-Date Progresses and Challenges in Biomass Gasification.* Presentation to the Biomass Gasification technology and Biomass Energy workshop, University of Canterbury, 13 February 2008.

Penniall, C.L. (2008) *Feasibility Study into the Potential for Gasification Plant in the New Zealand Wood Processing Industry – A thesis submitted in partial fulfillment of the requirements for the degree of Master of Engineering in Chemical and Process Engineering*. University of Canterbury

Penniall, C. L. and C. J. Williamson (2009). "Feasibility study into the potential for gasification plant in the New Zealand wood processing industry." Energy Policy **37**(9): 3377-3386.

Pfeifer, C., Rauch, R., Hofbauer, H., no date. Hydrogen-rich gas production with a Ni – catalyst in a dual fluidised bed gasifier

Pfeifer, C. (2008). *Biomass Steam Gasification - A Success Story.* Presentation to the Biomass Gasification technology and Biomass Energy workshop, University of Canterbury, 13 February 2008.

Pfeifer, C. and H. Hofbauer (2008). "Development of catalytic tar decomposition downstream from a dual fluidized bed biomass steam gasifier." Powder Technology **180**(1-2): 9-16.

Pidwirny, M. (2006). "Introduction to the Oceans". *Fundamentals of Physical Geography, 2nd Edition*. Retrieved 31 October 2009. http://www.physicalgeography.net/fundamentals/8o.html

Pooch, J.V. (2009). Personal Communication regarding estimates transport costs of wood chips.

Prins, M. J., K. J. Ptasinski, et. al. (2007). "From coal to biomass gasification: Comparison of thermodynamic efficiency." Energy **32**(7): 1248-1259.

Raju, A. S. K., C. S. Park, et. al. (2009). "Synthesis gas production using steam hydrogasification and steam reforming." Fuel Processing Technology **90**(2): 330-336.

Rapagnà, S., N. Jand, et. al. (1998). "Catalytic gasification of biomass to produce hydrogen rich gas." International Journal of Hydrogen Energy **23**(7): 551-557.

Rapagnà, S., N. Jand, et. al. (2000). "Steam-gasification of biomass in a fluidised-bed of olivine particles." Biomass and Bioenergy **19**(3): 187-197

Rutherford, J. (2006). *Heat and PowerApplications of Avdvanced Biomass Gasifiers in the New Zealand Wood Processing Industry: A thesis submitted in partial fulfillment of the requirements for the degree of Master of Engineering in Chemical and Process Engineering*. University of Canterbury

Sanz, A. and J. Corella (2006). "Modeling circulating fluidized bed biomass gasifiers. Results from a pseudo-rigorous 1-dimensional model for stationary state." Fuel Processing Technology **87**(3): 247-258.

Sasol (2005). *Sasol counters factual inaccuracies by the Democratic Alliance.* Retrieved 1 November 2009. http://www.sasol.com/sasol_internet/frontend/navigation.jsp;jsessionid=45F4PJ1KQWQ5JG5N4EZSFEQ?articleTypeID=2&articleId=12400005&navid=4&rootid=4

Sato, K. and K. Fujimoto (2007). "Development of new nickel based catalyst for tar reforming with superior resistance to sulfur poisoning and coking in biomass gasification." Catalysis Communications **8**(11): 1697-1701.

Saw, W. L. (2009). Personal Communication regarding temperature measuring equipment in small scale, high temperature experimental reactors.

Schuster, G., G. Löffler, et. al. (2001). "Biomass steam gasification - an extensive parametric modeling study." Bioresource Technology **77**(1): 71-79.

Sequeira, C. A. C., P. S. D. Brito, et. al. (2007). "Fermentation, gasification and pyrolysis of carbonaceous residues towards usage in fuel cells." Energy Conversion and Management **48**(7): 2203-2220.

Statistics New Zealand (2006). *QuickStats about Canterbury Region*. Retrieved 19 November 2009. http://www.statistics.govt.nz/Census/2006CensusHomePage/QuickStats/AboutAPlace/SnapShot.aspx?id=1000013&type=region&ParentID=

Sues, A., M. Jurascík, et. al. "Exergetic evaluation of 5 biowastes-to-biofuels routes via gasification." Energy **In Press, Corrected Proof**.

Swierczynski, D., S. Libs, et. al. (2007). "Steam reforming of tar from a biomass gasification process over Ni/olivine catalyst using toluene as a model compound." Applied Catalysis B: Environmental **74**(3-4): 211-222

Tasaka, K., T. Furusawa, et. al. "Biomass gasification in fluidized bed reactor with Co catalyst." Chemical Engineering Science **62**(18-20): 5558-5563.

Ulrich G.D., Vasudevan, P.T. (2004). *Chemical Engineering Process Design and Economics (Second Ed)*. Process Publishing, New Hampshire (2004)

United States of America Department of Energy (US DOE) Fuel Cells Technology Program (2009). *Types of Fuel Cells.*Retrieved 31 October 2009. http://www1.eere.energy.gov/hydrogenandfuelcells/fuelcells/fc_types.html

United States of America National Research Council (US NRC), National Academy of Engineering, (2004). *The Hydrogen Economy: Opportunities, costs, barriers and R&D needs*. National Academies Press, Washington D.C., 2004

Wiltowski, T., K. Mondal, et. al. (2008). "Reaction swing approach for hydrogen production from carbonaceous fuels." International Journal of Hydrogen Energy **33**(1): 293-302.

World Wind Energy Association (February 2009). "World Wind Energy Report 2008". *Report*. Retrieved on 16 March 2009 http://www.wwindea.org/home/images/stories/worldwindenergyreport2008_s.pdf.

Appendix A – CRL Wood Pellet Analysis

INTERIM REPORT OF ANALYSIS

Date Received: 26-Aug-05

Client: Canterbury University

Description: Wood Chip pellets and Husk samples supplied by client.

CRL Energy Ltd Reference:			76/050	76/051	76/052
Customer Reference:			Sample#1 Chips	Sample#2 Pellets	Sample#3 Husks
Analysis - As Received Basis					
Moisture	ISO 5068	%	52.6	8.0	9.9
Ash	ASTM D1102	%	0.2	0.4	2.6
Volatile	ISO 562	%	39.8	77.4	73.8
Fixed Carbon	By Difference	%	7.4	14.2	13.7
Gross Calorific Value	ISO 1928	MJ/kg	9.53	18.63	17.08
Carbon	micro analytical	%	24.3	47.2	43.7
Hydrogen	micro analytical	%	2.87	5.35	5.07
Nitrogen	micro analytical	%	<0.1	<0.2	0.56
Sulphur	ASTM D4239	%	0.01	0.01	0.06
Oxygen	By Difference	%	20.0	38.7	38.1
CHN determined by Chemsearch Otago University					
Analysis - Dry Basis					
Ash	ASTM D 1102	%	0.4	0.4	2.9
Volatile	ISO 562	%	84.0	84.1	81.9
Fixed Carbon	By Difference	%	15.6	15.4	15.2
Gross Calorific Value	ISO 1928	MJ/kg	20.10	20.25	18.95
Carbon	micro analytical	%	51.2	51.3	48.5
Hydrogen	micro analytical	%	6.10	5.81	5.63
Nitrogen	micro analytical	%	<0.2	<0.2	0.62
Sulphur	ASTM D4239	%	0.02	0.01	0.07
Oxygen	By Difference	%	42.3	42.4	42.9

Signature:

Date of Issue: **13-Oct-05**

Grant Murray

Laboratory Supervisor

THIS REPORT MUST NOT BE QUOTED EXCEPT IN FULL

Distribution:

Dept of Chemical and Process Engineering, PB 4800, CHCH ATTN: Ian Gilmour

CRL Energy Ltd, Laboratory

Appendix B – Hill Laboratories Biosolids Analysis

Hill Laboratories
BETTER TESTING BETTER RESULTS

R J Hill Laboratories Limited
1 Clyde Street
Private Bag 3205
Hamilton 3240, New Zealand

Tel +64 7 858 2000
Fax +64 7 858 2001
Email mail@hill-labs.co.nz
Web www.hill-labs.co.nz

ANALYSIS REPORT

Client:	Beca Infrastructure Ltd	**Lab No:**	648932	SPv2
Contact:	Hanafin, Annie	**Date Registered:**	08-Jul-2008	
	C/- Beca Infrastructure Ltd	**Date Reported:**	19-Sep-2008	
	119 Armargh Street	**Quote No:**	33282	
	PO Box 13960	**Order No:**		
	CHRISTCHURCH 8141	**Client Reference:**	Biosolids	
		Submitted By:	Hanafin, Annie	

Amended Report

This report replaces an earlier report issued on the 07 Aug 2008 at 5:03 pm
Chloride and heavy metal results have been added to the report at the client's request.

Sample Type: Soil

Sample Name:		Beca 30-Jun-2008	Beca 03-Jul-2008	Beca 07-Jul-2008		
Lab Number:		648932.1	648932.2	648932.3		
Individual Tests						
Dry Matter	g/100g as rcvd	17	18	20	-	-
Soluble Salts	g/100g dry wt	-	0.92	0.96	-	-
Electrical Conductivity (EC)*	mS/cm	-	2.6	2.7	-	-
Ash*	g/100g dry wt	29	28	32	-	-
Total Recoverable Aluminium	mg/kg dry wt	5600	5100	5700	-	-
Total Recoverable Cobalt	mg/kg dry wt	4.4	3.9	4.6	-	-
Total Recoverable Iron	mg/kg dry wt	12000	11000	12000	-	-
Total Recoverable Manganese	mg/kg dry wt	350	300	320	-	-
Total Sulphur*	g/100g dry wt	1.3	1.1	1.2	-	-
Total Recoverable Tin	mg/kg dry wt	59	52	50	-	-
Chloride*	mg/kg dry weight	430	350	320	-	-
Fluoride*	mg/kg dry weight	59	73	53	-	-
pH	pH Units	7.0	7.1	6.9	-	-
Ammonium-N*	mg/kg dry weight	8700	8000	7000	-	-
Nitrite-N*	mg/kg dry weight	< 2.9	< 2.7	< 2.4	-	-
Nitrate-N*	mg/kg dry weight	7.7	6.8	< 3.4	-	-
Nitrate-N + Nitrite-N*	mg/kg dry weight	9.7	7.8	3.7	-	-
Total Organic Carbon	g/100g dry wt	36	33	34	-	-
Total Nitrogen	g/100g dry wt	5.5	5.4	5.1	-	-
Carbon:Nitrogen Ratio		6.4	6.2	6.7	-	-
Oil and Grease	mg/kg dry wt	5800	4900	4800	-	-
Heavy metal screen level As,Cd,Cr,Cu,Ni,Pb,Zn						
Total Recoverable Arsenic	mg/kg dry wt	9.4	11	11	-	-
Total Recoverable Cadmium	mg/kg dry wt	3.2	3.3	3.4	-	-
Total Recoverable Chromium	mg/kg dry wt	390	340	340	-	-
Total Recoverable Copper	mg/kg dry wt	330	280	290	-	-
Total Recoverable Lead	mg/kg dry wt	74	64	75	-	-
Total Recoverable Nickel	mg/kg dry wt	45	37	40	-	-
Total Recoverable Zinc	mg/kg dry wt	1300	1200	1100	-	-
BTEX in Soil by Headspace GC-MS						
Benzene	mg/kg dry wt	< 0.55	< 0.51	< 0.46	-	-
Toluene	mg/kg dry wt	< 0.55	< 0.51	< 0.46	-	-
Ethylbenzene	mg/kg dry wt	< 0.55	< 0.51	< 0.46	-	-
m&p-Xylene	mg/kg dry wt	< 1.1	< 1.1	< 0.92	-	-
o-Xylene	mg/kg dry wt	< 0.55	< 0.51	< 0.46	-	-

Sample Type: Soil						
Sample Name:		Beca 30-Jun-2008	Beca 03-Jul-2008	Beca 07-Jul-2008		
Lab Number:		648932.1	648932.2	648932.3		
Polycyclic Aromatic Hydrocarbons Trace in Soil						
Acenaphthene	mg/kg dry wt	0.050	0.049	0.055	-	-
Acenaphthylene	mg/kg dry wt	0.037	0.036	0.048	-	-
Anthracene	mg/kg dry wt	0.060	0.065	0.067	-	-
Benzo[a]anthracene	mg/kg dry wt	0.10	0.10	0.10	-	-
Benzo[a]pyrene (BAP)	mg/kg dry wt	0.085	0.086	0.097	-	-
Benzo[b]fluoranthene + Benzo[j] fluoranthene	mg/kg dry wt	0.20	0.20	0.23	-	-
Benzo[g,h,i]perylene	mg/kg dry wt	0.086	0.099	0.10	-	-
Benzo[k]fluoranthene	mg/kg dry wt	0.074	0.064	0.061	-	-
Chrysene	mg/kg dry wt	0.11	0.10	0.11	-	-
Dibenzo[a,h]anthracene	mg/kg dry wt	0.033	0.033	0.023	-	-
Fluoranthene	mg/kg dry wt	0.21	0.17	0.19	-	-
Fluorene	mg/kg dry wt	0.11	0.092	0.12	-	-
Indeno(1,2,3-c,d)pyrene	mg/kg dry wt	0.054	0.068	0.077	-	-
Naphthalene	mg/kg dry wt	0.50	0.55	0.61	-	-
Phenanthrene	mg/kg dry wt	0.29	0.36	0.30	-	-
Pyrene	mg/kg dry wt	0.58	0.61	0.58	-	-
Poychlorinated Biphenyls Trace in Soil						
PCB-101	mg/kg dry wt	< 0.00099	< 0.0010	< 0.0010	-	-
PCB-105	mg/kg dry wt	< 0.00099	< 0.0010	< 0.0010	-	-
PCB-110	mg/kg dry wt	< 0.00099	< 0.0010	< 0.0010	-	-
PCB-114	mg/kg dry wt	< 0.00099	< 0.0010	< 0.0010	-	-
PCB-118	mg/kg dry wt	< 0.00099	< 0.0010	< 0.0010	-	-
PCB-121	mg/kg dry wt	< 0.00099	< 0.0010	< 0.0010	-	-
PCB-123	mg/kg dry wt	< 0.00099	< 0.0010	< 0.0010	-	-
PCB-126	mg/kg dry wt	< 0.00099	< 0.0010	< 0.0010	-	-
PCB-128	mg/kg dry wt	< 0.00099	< 0.0010	< 0.0010	-	-
PCB-138	mg/kg dry wt	< 0.00099	< 0.0010	< 0.0010	-	-
PCB-141	mg/kg dry wt	< 0.00099	< 0.0010	< 0.0010	-	-
PCB-149	mg/kg dry wt	< 0.00099	< 0.0010	< 0.0010	-	-
PCB-151	mg/kg dry wt	< 0.00099	< 0.0010	< 0.0010	-	-
PCB-153	mg/kg dry wt	< 0.00099	< 0.0010	< 0.0010	-	-
PCB-156	mg/kg dry wt	< 0.00099	< 0.0010	< 0.0010	-	-
PCB-157	mg/kg dry wt	< 0.00099	< 0.0010	< 0.0010	-	-
PCB-159	mg/kg dry wt	< 0.00099	< 0.0010	< 0.0010	-	-
PCB-167	mg/kg dry wt	< 0.00099	< 0.0010	< 0.0010	-	-
PCB-169	mg/kg dry wt	< 0.00099	< 0.0010	< 0.0010	-	-
PCB-170	mg/kg dry wt	< 0.00099	< 0.0010	< 0.0010	-	-
PCB-180	mg/kg dry wt	< 0.00099	< 0.0010	< 0.0010	-	-
PCB-189	mg/kg dry wt	< 0.00099	< 0.0010	< 0.0010	-	-
PCB-194	mg/kg dry wt	< 0.00099	< 0.0010	< 0.0010	-	-
PCB-206	mg/kg dry wt	< 0.00099	< 0.0010	< 0.0010	-	-
PCB-209	mg/kg dry wt	< 0.00099	< 0.0010	< 0.0010	-	-
PCB-28 + PCB-31	mg/kg dry wt	< 0.00099	< 0.0010	< 0.0010	-	-
PCB-44	mg/kg dry wt	< 0.00099	< 0.0010	< 0.0010	-	-
PCB-49	mg/kg dry wt	< 0.00099	< 0.0010	< 0.0010	-	-
PCB-52	mg/kg dry wt	< 0.00099	< 0.0010	< 0.0010	-	-
PCB-60	mg/kg dry wt	< 0.00099	< 0.0010	< 0.0010	-	-
PCB-77	mg/kg dry wt	< 0.00099	< 0.0010	< 0.0010	-	-
PCB-81	mg/kg dry wt	< 0.00099	< 0.0010	< 0.0010	-	-
PCB-86	mg/kg dry wt	< 0.00099	< 0.0010	< 0.0010	-	-
Total PCB (Sum of 33 congeners)	mg/kg dry wt	< 0.02	< 0.02	< 0.02	-	-

Analyst's Comments

"We were unable to test for Soluble Salts on sample 648932.1 using our standard method because the sample absorbed all

Analyst's Comments

the water added, leaving no free liquid to measure EC on."

SUMMARY OF METHODS

The following table(s) gives a brief description of the methods used to conduct the analyses for this job. The detection limits given below are those attainable in a relatively clean matrix. Detection limits may be higher for individual samples should insufficient sample be available, or if the matrix requires that dilutions be performed during analysis.

Sample Type: Soil

Test	Method Description	Default Detection Limit	Samples
Environmental Solids Sample Preparation*	Air dried at 35°C and sieved, <2mm fraction.	-	1-3
Heavy metal screen level As,Cd,Cr,Cu,Ni,Pb,Zn	Dried sample, <2mm fraction. Nitric/Hydrochloric acid digestion, ICP-MS, screen level.	-	1-3
Total Organic Carbon and Total Nitrogen	Catalytic Combustion (900°C, O^2), separation, Thermal Conductivity Detector [Elementar Analyser]	-	1-3
BTEX in Soil by Headspace GC-MS	Solvent extraction, Headspace GC-MS analysis US EPA 8260B	-	1-3
Polycyclic Aromatic Hydrocarbons Trace in Soil	Sonication extraction, SPE cleanup, GC-MS SIM analysis US EPA 8270C	-	1-3
Poychlorinated Biphenyls Trace in Soil	Sonication extraction, SPE cleanup, GPC cleanup (if required), GC-MS analysis	-	1-3
Dry Matter (Env)	Dried at 103°C (removes 3-5% more water than air dry), gravimetry.	0.10 g/100g as rcvd	1-3
esFIAextn*	2M potassium chloride extraction for FIA determination. Analyst, 109, 549, (1984).	-	1-3
esICextn*	Potassium phosphate extraction for Ion Chromatography. In House.	-	1-3
Total Recoverable digestion	Nitric / hydrochloric acid digestion. US EPA 200.2.	-	1-3
Soluble Salts	1:5 soil:water extraction followed by potentiometric determination of conductivity. SS=EC*0.35 Calculated from EC measurement.	0.050 g/100g dry wt	2-3
Conductivity from soluble salts*	1:5 soil:water extraction, potentiometric conductivity determination (Soluble salts/0.35) .	0.20 mS/cm	2-3
Ash*	Ignition in muffle furnace 550°C, 6hr, gravimetric. APHA 2540 G 21st ed. 2005.	0.040 g/100g dry wt	1-3
Total Recoverable Aluminium	Dried sample, sieved as specified (if required). Nitric/Hydrochloric acid digestion, ICP-MS, screen level. US EPA 200.2.	10 mg/kg dry wt	1-3
Total Recoverable Cobalt	Dried sample, sieved as specified (if required). Nitric/Hydrochloric acid digestion, ICP-MS, screen level. US EPA 200.2.	0.40 mg/kg dry wt	1-3
Total Recoverable Iron	Dried sample, sieved as specified (if required). Nitric/Hydrochloric acid digestion, ICP-MS, screen level. US EPA 200.2.	40 mg/kg dry wt	1-3
Total Recoverable Manganese	Dried sample, sieved as specified (if required). Nitric/Hydrochloric acid digestion, ICP-MS, screen level. US EPA 200.2.	1.0 mg/kg dry wt	1-3
Total Sulphur (Sub)*	LECO SC32 Sulphur Determinator, high temperature furnace, infra-red detector. Subcontracted to SGS, Waihi. ASTM 4239.	0.0050 g/100g dry wt	1-3
Total Recoverable Tin	Dried sample, sieved as specified (if required). Nitric/Hydrochloric acid digestion, ICP-MS, screen level. US EPA 200.2.	1.0 mg/kg dry wt	1-3
Chloride*	Ion Chromatography determination of es potassium phosphate extraction. APHA 4110 B 21st ed. 2005.	3.0 mg/kg dry weight	1-3
Total Fluoride in solids*	Alkaline fusion of sample. Ion selective electrode determination. Methods of Soil Analysis 2nd Edition, Pt2, 26-4.3.3.	10 mg/kg dry weight	1-3
pH	1:2 (v/v) soil : water slurry followed by potentiometric determination of pH.	0.1 pH Units	1-3
Ammonium-N*	2M potassium chloride extraction. Phenol/hypochlorite colorimetry. Discrete Analyser. APHA 4500-NH_3 G 21st ed. 2005.	5.0 mg/kg dry weight	1-3
Nitrite-N*	FIA determination of es 2M potassium chloride extraction. APHA 4500-NO_3^- I (Proposed) 21st ed. 2005.	1.0 mg/kg dry weight	1-3
Nitrate-N*	Calculation: (Nitrate-N + Nitrite-N) - Nitrite-N.	1.5 mg/kg dry weight	1-3
Nitrate-N + Nitrite-N*	Automated cadmium reduction, FIA determination of es 2M potassium chloride extraction. APHA 4500-NO_3^- I (Proposed) 21st ed. 2005.	1.0 mg/kg dry weight	1-3

Sample Type: Soil			
Test	**Method Description**	**Default Detection Limit**	**Samples**
Oil and Grease	Chemical drying, Soxhlet extraction, gravimetric determination of extracted Oil & Grease.	100 mg/kg dry wt	1-3

These samples were collected by yourselves (or your agent) and analysed as received at the laboratory.

Samples are held at the laboratory after reporting for a length of time depending on the preservation used and the stability of the analytes being tested. Once the storage period is completed the samples are discarded unless otherwise advised by the client.

Carole Rodgers-Carroll BA, NZCS
Client Services Manager - Environmental Division

Appendix C – XRD/XRF Analysis of Bed Materials

The following is a summary of the XRF – Rock Majors Program analyses of the bed materials tested. The analyses were performed by the University of Canterbury Geology Department between December 2008 and October 2009.

Sample #	Material	SiO2	TiO2	Al2O3	Fe2O3T	MnO	MgO
32979A	Greywacke - Washdyke	73.76	0.45	11.87	3.28	0.05	1.18
32980A	Greywacke - Rangitata	0.70	0.01	14.24	3.82	0.06	1.48
32981A	Greywacke - Wakanui	69.43	0.53	14.44	3.88	0.06	1.46
32982A	Greywacke - Rakaia	0.70	0.01	14.42	3.59	0.05	1.39
32983A	Greywacke - Ashburton Cliffs	71.32	0.47	13.42	3.44	0.05	1.27
32984A	Greywacke - Kaitorete Barrier	0.74	0.41	12.57	2.98	0.05	1.12
34715A	Olivine (1)	41.12	0.02	0.24	11.04	0.16	46.64
34938A	Magnetite - Barrytown	39.63	14.59	13.04	24.13	2.40	1.07
34939A	Dolomite	0.25	0.01	<0.2	6.00	<0.01	0.25
34941A	Olivine (2)	46.57	0.03	0.69	9.87	0.15	42.08
34943A	Calcite	<0.2	<0.01	<0.2	0.04	0.02	0.33

Sample #	Material	CaO	Na2O	K2O	P2O5	LOI	Total
32979A	Greywacke - Washdyke	2.75	3.16	1.75	0.14	1.73	100.13
32980A	Greywacke - Rangitata	2.59	3.71	2.09	0.15	1.60	100.03
32981A	Greywacke - Wakanui	2.21	3.81	2.32	0.16	1.77	100.07
32982A	Greywacke - Rakaia	1.89	4.06	2.51	0.15	1.53	100.28
32983A	Greywacke - Ashburton Cliffs	2.57	3.61	2.06	0.14	1.71	100.06
32984A	Greywacke - Kaitorete Barrier	2.52	3.38	1.79	0.13	1.44	100.14
34715A	Olivine (1)	0.25	<0.1	0.04	0.02	0.42	99.93
34938A	Magnetite - Barrytown	5.07	0.54	0.47	0.14	- 1.44	99.64
34939A	Dolomite	55.41	<0.1	<0.01	0.02	43.88	99.88
34941A	Olivine (2)	0.35	0.24	0.32	0.04	- 0.43	99.90
34943A	Calcite	55.47	<0.1	0.03	0.02	43.79	99.71

Appendix D – Producer Gas Composition Calculations

In some cases, producer gas samples from the gasifier are contaminated with outside air or from flue gas infiltrating into the gasification column. Additionally, nitrogen is used as a purge gas to exclude producer gas infiltration into the wood feed system. This nitrogen flows into the gasification column to some degree depending on the level of wood pellets in the feed hopper. Finally, the silica gel moisture trap absorbs differing amounts of the producer gas components depending on the sample number. In order to more accurately compare the results of different samples, the results are normalised to account for these impurities.

An Excel worksheet can be constructed to calculate accurate producer gas compositions based on the following procedures. The compositions of the producer gas and concurrent flue gas, including the helium tracer, are required.

1. Let the analysed composition be X0 = {xHe, xH_2, xO_2, xN_2, xCH_4, xCO, xCO_2, xC_2H_4, xC_2H_6}$_0$. From the analysed composition, exclude any oxygen present in the analysis by taking a basis of 100 moles, setting oxygen to 0 and totalling the remaining components, then normalising the proportions of the remaining components by multiplying by 100 over the total. Let this new composition be X1.

2. Apply the experimentally determined silica gel calibration values. For each of the components, add or subtract the proportions in Figure D.1 according to which number sample is being analysed for that run. Normalise the remaining values to the basis of 100 mol as in (1). Let this new composition be X2

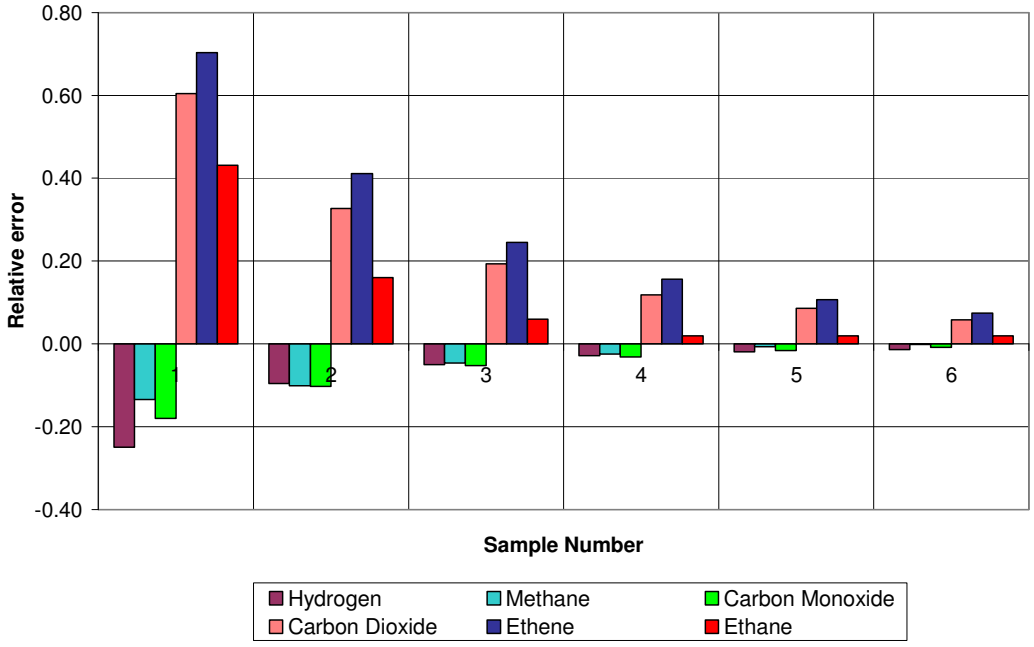

Figure D.1 – Silica gel calibration chart showing relative errors of the key producer gas components.

3. The common components of the producer gas and flue gas are nitrogen and carbon dioxide. From comparing these components to the flows of producer gas and flue gas, calculated according to helium composition, a simultaneous nitrogen and CO_2

balance can be constructed. First, label solver cells for flow of producer gas F_{pg}, flow of flue gas F_{fg} and ACTUAL producer gas CO_2 composition ξ_{CO2}. Then, construct the N_2 balance, CO_2 balance and mass balance equations below. y_a indicates a flue gas composition of component *a.*

$$\frac{y_{N_2}}{100}F_{fg} + 0.03F_{pg} = x_{N_2} \qquad (D.1)$$

$$\frac{y_{CO_2}}{100}F_{fg} + \xi_{CO_2}F_{pg} = x_{CO_2} \qquad (D.2)$$

$$F_{fg} + F_{pg} = 100 \qquad (D.3)$$

From these three equations, the actual composition of CO_2 in the producer gas and the actual producer gas flow (the basis for relative composition) can be determined. The equations assume an actual nitrogen composition of 3%, which is an average value as a result of flow from the wood feed system into the gasification column. Hence, compositions for He, H_2, CH_4, CO, CO_2, C_2H_4, C_2H_6 can be calculated by dividing X2 by F_{pg}. Nitrogen composition is calculated circularly by multiplying 3 by the sum of (X2/F_{fg})/100. Normalising to a 100 mol basis once again will give the actual producer gas composition Ξ.

Appendix E – Fluidisation Velocity Calculations

As described by Grace [Grace, 1997], minimum fluidisation velocity of different materials is dependent on four parameters: particle density, particle diameter, fluid density and fluid viscosity. The ratio of gas superficial velocity to particle minimum fluidisation velocity gives a simple description of how well fluidised is a bed of particles, especially in the bubbling bed régime as found in the gasification column of the gasifier. Additionally, calculation of terminal velocity gives the minimum superficial velocity of the gas stream in a circulating fluidised bed, as found in the combustion column. Superficial velocity determines column cross sectional area, hence is required for reactor sizing.

Archimedes Number is used to relate the particle and fluid properties:

$$Ar = \frac{\rho_f (\rho_s - \rho_f) d_p^3 g}{\mu^2} \qquad (E.1)$$

where particle density is found from considering the packing factor of the material, determined by the particle shape. For the materials tested in this research, greywacke, olivine and magnetite were assumed to be spherical particles with a packing factor of 0.74, while calcite and dolomite were irregular shaped particles and assumed to have a packing factor of 0.5. This was substantiated by comparison to known particle density ranges for these materials.

From Archimedes Number, Reynolds Number of a suspended particle in a fluid can be calculated:

$$\mathrm{Re} = \sqrt{27.2^2 + 0.0408 Ar} - 27.2 \qquad (E.2)$$

Minimum fluidisation velocity is then found from the definition of Reynolds Number:

$$U_{mf} = \frac{\mathrm{Re}.\mu}{d_p.\rho_f} \qquad (E.3)$$

Finally, superficial velocity U is defined as the gas velocity through an empty column. The ratio U/U_{mf} gives a simple indication of the degree of fluidisation. For a bubbling fluidised bed, U/U_{mf} is approximately equal to 6.

Particle terminal velocity U_t defines the negative minimum fluid velocity for pneumatic transport, required by a circulating fluidised bed. It is calculated according to *E*.4:

$$U_t = \sqrt{\frac{4 g d_p}{3 C_D} \frac{(\rho_s - \rho_f)}{\rho_f}} \qquad (E.4)$$

where C_D is the drag coefficient, in this case taken to be equal to 0.6.

Appendix F – Economic Analysis Cost Calculations

Scenario 1: Pure Hydrogen Production

Plant Item	Parameters			Unit Cost	IF	TOTAL	
Biomass dryer	Moisture removed	18	t/h	$ 6,650,000 NZD	1	$ 6,650,000	$ 6,650,000
Gasification column	Diameter	1.74	m	$ 123,568 NZD	6	$ 741,405	$ 741,000
	Height	17.4	m				
Combustion column	Diameter	0.67	m	$ 81,777 NZD	6	$ 490,661	$ 491,000
	Height	24.8	m				
Flue Gas Cyclone	flow	44.2	m^3/s	$ 73,736 NZD	2	$ 147,473	$ 147,000
Producer Gas Cyclone	flow	14.1	m^3/s	$ 26,108 NZD	2	$ 52,215	$ 52,000
Blower	flow	17.7	m^3/s	$ 16,083 NZD	3	$ 48,249	$ 48,000
Burners	number	4		$ 48,000 NZD	2	$ 96,000	$ 96,000
TOTAL - GASIFIER						$ 1,576,004	$ 1,575,000
Heat Recovery Steam Generator	Heating duty	20500	kW	$ 1,980,000 USD	1	$ 3,600,000	$ 3,600,000
Steam superheater HX	UA	8586	W/K				
	Area	151	m^2	$ 261,975 NZD	2	$ 523,949	$ 524,000
Air preheater HX	UA	25303	W/K				
	Area	445	m^2	$ 482,974 NZD	2	$ 965,947	$ 966,000
TOTAL - PLANT INTEGRATION						$ 1,489,896	$ 1,490,000
Flue Gas Bag Filter	Flow	21.6	m^3/s	$ 178,489 NZD	4	$ 713,955	$ 714,000
Producer Gas Bag Filter	Flow	6.94	m^3/s	$ 84,255 NZD	4	$ 337,021	$ 337,000
Biodiesel Scrubber (2 columns)	Flow	6.94	m^3/s	$ 141,244 NZD	6	$ 847,463	$ 847,000
TOTAL - GAS CLEANING						$ 1,898,440	$ 1,898,000
Reformer	Internal Volume	0.46	m^3	$ 150,000 USD	4	$ 1,090,909	$ 1,091,000
Reformer Furnace	Heating Duty	6800	kW	$ 1,297,800 USD	2	$ 4,719,273	$ 4,719,000
Reformer Compressor	Power (η = 0.75)	2123	kW	$ 2,568,588 NZD	6	$ 15,411,528	$ 15,412,000
TOTAL - REFORMER						$ 21,221,710	$ 21,222,000
High Temperature WGSR	Internal Volume	12.85	m^3	$ 240,000 USD	4	$ 1,745,455	$ 1,745,000
Low Temperature WGSR	Internal Volume	9.33	m^3	$ 150,000 USD	4	$ 1,090,909	$ 1,091,000
TOTAL - SHIFT REACTORS						$ 2,836,364	$ 2,836,000
Pressure Swing Adsorbers (2 columns)	Internal Volume	7.5	m^3	$ 270,000 USD	6	$ 2,945,455	$ 2,945,000
Compressor	Power (η = 0.75)	2788	kW	$ 3,373,480 NZD	6	$ 20,240,880	$ 20,241,000
Contingency and Fee				15%		$ 9,368,812	**$ 9,369,000**
Working Capital				1%		$ 624,587	**$ 625,000**
TOTAL						**$ 72,452,147**	**$ 72,452,000**

Operating Costs				Unit Cost	TOTAL	
Raw Materials	Wood	301.95	GJ/h	$2 /GJ	$ 4,831,200	$ 4,831,000
	Transport	33	t/h	$0 /t	$ -	$ -
Utilities	Electricity	41,250,720	kWh	0.1 /kWh	$ 4,125,072	$ 4,125,000
	Biodiesel	negligible				
Labour	Operators	16000	h/y	$20 /h	$ 320,000	$ 320,000
	Supervisors	15%	*Op Lab		$ 48,000	$ 48,000
	Admin & O/H	60%	*Lab + Maintenance		$ 1,090,226	$ 1,090,000
Other	Maintenance	2%	*Cap Cost		$ 1,449,043	$ 1,449,000
	Local Taxes	1%	*Cap Cost		$ 724,521	$ 725,000
	Insurance	1.5%	*Cap Cost		$ 1,086,782	$ 1,087,000
	Operating Supplies	15%	*Maintenance Cost		$ 217,356	$ 217,000
TOTAL					**$ 13,892,201**	**$ 13,892,000**

Revenue			Unit Cost	TOTAL	
Hydrogen Production	1463	kg/h	$1.73 /kg	$ 20,253,788	$ 20,254,000
Tax	0%	*revenue		$ -	
Depreciation	0%	*capital cost		$ -	
Tax refund	0%	*depreciation		$ -	
Net Revenue			**<10 years**	**$20,253,788**	**$ 20,254,000**
			>10 years	**$20,253,788**	**$ 20,254,000**

Scenario 2: Biomass Integrated Gasification – Fuel Cell

Plant Item	Parameters			Unit Cost		IF	Total	
Biomass dryer	Moisture removed	18	t/h	$ 6,650,000	NZD	1	$ 6,650,000	$ 6,650,000
Gasification column	Diameter	1.74	m	$ 148,281	NZD	6	$ 889,686	$ 890,000
	Height	17.4	m					
Combustion column	Diameter	0.67	m	$ 98,132	NZD	6	$ 588,793	$ 589,000
	Height	24.8	m					
Flue Gas Cyclone	flow	44.2	m³/s	$ 73,736	NZD	2	$ 147,473	$ 147,000
Producer Gas Cyclone	flow	14.1	m³/s	$ 26,108	NZD	2	$ 52,215	$ 52,000
Blower	flow	17.7	m³/s	$ 16,083	NZD	3	$ 48,249	$ 48,000
Burners	number	4		$ 48,000	NZD	2	$ 96,000	$ 96,000
TOTAL - GASIFIER							$ 1,822,417	$ 1,822,000
Tar Cracker column	Diameter	0.89	m	$ 44,860	NZD	6	$ 269,163	$ 269,000
	Height	8.9	m					
Tar Cracker cyclone	flow	6.4	m³/s	$ 12,629	NZD	2	$ 25,257	$ 25,000
PG candle filter	flow	6.4	m³/s	$ 90,000	USD	4	$ 654,545	$ 655,000
FG candle filter	flow	22.2	m³/s	$ 170,000	USD	4	$ 1,236,364	$ 1,236,000
TOTAL - GAS CLEANING							$ 2,185,329	$ 2,185,000
			Sensitivity factor	0%				
Molten Carbonate Fuel Cell		36	cells	$ 298,000	USD	6	$ 117,032,727	$ 117,033,000
Steam Turbine	shaft power	1693.2	kW	$ 290,000	USD	6	$ 3,163,636	$ 3,164,000
Air preheater HX	UA	7514	W/K					
	Area	132	m²	$ 242,924	NZD	2	$ 485,848	$ 486,000
Steam Generator	UA	32306	W/K					
	Area	412	m²	$ 461,795	NZD	2	$ 923,591	$ 924,000
Steam superheater	UA	9136	W/K					
	Area	161	m²	$ 271,343	NZD	2	$ 542,685	$ 543,000
TOTAL - HEAT INTEGRATION							$ 1,952,124	$ 1,952,000
Contingency and Fee				15%			$ 19,920,935	$ 19,921,000
Working Capital				1%			$ 1,328,062	$ 1,328,000
TOTAL CAPITAL COSTS							**$ 154,055,230**	**$ 154,055,000**

Item				Unit Cost			Total	
Raw Materials	Wood	301.95	GJ/h	$ 2.00	/GJ		$ 4,831,200	$ 4,831,000
	Transport	33	t/h	$ 10.00	/t		$ 2,640,000	$ 2,640,000
Utilities	Electricity	-	kWh	$ 0.10	/kWh		$ -	$ -
Labour	Operators	16000	h/y	$ 20.00	/h		$ 320,000	$ 320,000
	Supervisors	15%	*Op Lab				$ 48,000	$ 48,000
	Admin & O/H	60%	*Lab + Maintenance				$ 2,069,463	$ 2,069,000
Other	Maintenance	2%	*Cap Cost				$ 3,081,105	$ 3,081,000
	Local Taxes	1%	*Cap Cost				$ 1,540,552	$ 1,541,000
	Insurance	1.5%	*Cap Cost				$ 2,310,828	$ 2,311,000
	Operating Supplies	15%	*Maintenance Cost				$ 462,166	$ 462,000
TOTAL OPERATING COSTS							**$ 17,303,314**	**$ 17,303,000**

Revenue				Unit Value			Total	
Revenue	Electricity	47.5	MW	$ 0.1057	/kWh		$ 40,152,832	**$ 40,153,000**
Less Tax				-30%			-$ 12,045,850	**-$ 12,046,000**
Depreciation				10%			$ 13,280,623	
Tax refund				30%			$ 3,984,187	**$ 3,984,000**
TOTAL REVENUE						<10y	$ 32,091,170	**$ 32,091,000**
						>10y	$ 28,106,983	**$ 28,107,000**